2015

Solvento iron(IV) oxo complexes in catalytic oxidations and electron transfer reactions

Hajem Bataineh
Iowa State University

Solvento iron(IV) oxo complexes in catalytic oxidations and electron transfer reactions

by

Hajem Bataineh

A dissertation submitted to the graduate faculty

in partial fulfillment of the requirements for the degree of

DOCTOR OF PHILOSOPHY

Major: Inorganic Chemistry

Program of Study Committee:
Andreja Bakac, Co-Major Professor
Aaron Sadow, Co-Major Professor
William Jenks
Javier Vela
Keith Woo

Iowa State University

Ames, Iowa

2015

DEDICATION

To my parents, brothers and sisters:

Thank you for your endless support, encouragement and love.

TABLE OF CONTENTS

ACKNOWLEDGMENTS

I would like to thank my major professor, Dr. Andreja Bakac, for her guidance, encouragement, patience and friendship. I would also like to thank the other committee members for their comments and support.

In addition, I would also like to thank my friends, colleagues, the chemistry department faculty and staff for making my time at Iowa State University a wonderful experience.

I would especially like to thank my current and former fellow group members for their insightful discussions, and friendship.

Finally, thanks to my family for their encouragement and support throughout my life.

ABSTRACT

Iron(IV)-oxo species are powerful oxidants that are involved as intermediates in iron-catalyzed oxidations of organic substrates. This includes their role in enzymatic oxidations which provided strong incentive to generate, characterize and explore the chemistry of novel Fe(IV) compounds from the perspective or reactivity and mechanism. The simplest iron(IV) complexes that have been prepared in solution are aqueous Fe(IV)-oxo ions. Even though these species can be conveniently generated from Fe(II) precursors and oxygen atom donors, studies of the chemistry of aqueous iron(IV) are difficult because of their short lifetime, high reactivity, and sensitivity to the surroundings. Herein we describe how changes in the pH, coordinating ligands and solvent can lead to dramatic changes in the lifetime and chemistry of aqueous Fe(IV)-oxo complexes.

pH-Induced Mechanistic Changeover From Hydroxyl Radicals to Iron(IV) in the Fenton Reaction

A major pathway in the reaction between Fe(II) and H_2O_2 at pH 6-7 in non-coordinating buffers exhibits inverse kinetic dependence on $[H^+]$ and leads to oxidation of dimethyl sulfoxide (DMSO) to dimethyl sulfone ($DMSO_2$). This step regenerates Fe(II) and makes the oxidation of DMSO catalytic, a finding that strongly supports Fe(IV) as a Fenton intermediate at near-neutral pH. This Fe(IV) is a less efficient oxidant for DMSO at pH 6-7 than is $(H_2O)_5FeO^{2+}$, generated by ozone oxidation of $Fe(H_2O)_6^{2+}$, in acidic solutions. Large concentrations of DMSO are needed to achieve significant turnover numbers at pH≥6 owing to the rapid competing reaction between Fe(II) and Fe(IV) that leads to irreversible loss of the catalyst. At pH 6 and ≤0.02 mM Fe(II), the ratio of apparent rate constants for the reactions of Fe(IV) with DMSO and with Fe(II) is ~10^4. The results at pH 6-7 stand in stark

contrast with those reported previously in acidic solutions where Fenton reaction generates hydroxyl radicals. Under those conditions, DMSO is oxidized stoichiometrically to methylsulfinic acid and ethane. This path still plays a minor role (1-10%) at pH 6-7.

Fe(II) Catalysis in Oxidation of Hydrocarbons with Ozone in Acetonitrile

Oxidation of alcohols, ethers, and sulfoxides by ozone in acetonitrile is catalyzed by sub-millimolar concentrations of $Fe(CH_3CN)_6^{2+}$. The catalyst provides both rate acceleration and greater selectivity toward the less oxidized product. For example, $Fe(CH_3CN)_6^{2+}$-catalyzed oxidation of benzyl alcohol yields benzaldehyde almost exclusively (>95%) whereas uncatalyzed reaction generates a 1:1 mixture of benzaldehyde and benzoic acid. Similarly, aliphatic alcohols are oxidized to aldehydes/ketones, cyclobutanol to cyclobutanone, and diethyl ether to a 1:1 mixture of ethanol and acetaldehyde. The kinetics of oxidation of alcohols and diethyl ether are first order in $Fe(CH_3CN)_6^{2+}$ and ozone, and independent of [Substrate] at concentrations greater than ~5 mM. In this regime, the rate constant for all of the alcohols is approximately the same, $k_{cat} = (8\pm1) \times 10^4\ M^{-1}\ s^{-1}$, and that for $(C_2H_5)_2O$ is $(5\pm0.5) \times 10^4\ M^{-1}\ s^{-1}$. In the absence of substrate, $Fe(CH_3CN)_6^{2+}$ reacts with O_3 with $k_5 = (9.3\pm0.3) \times 10^4\ M^{-1}\ s^{-1}$. The similarity between the rate constants k_5 and k_{cat} strongly argues for $Fe(CH_3CN)_6^{2+}/O_3$ reaction as rate determining in catalytic oxidation. The active oxidant produced in $Fe(CH_3CN)_6^{2+}/O_3$ reaction is suggested to be an Fe(IV) species in analogy with a related intermediate in aqueous solutions. This assignment is supported by the similarity in kinetic isotope effects and relative reactivities of the two species toward substrates.

Electron Transfer Reactivity of Aqueous Iron(IV) oxo Complex

The reactivity of $Fe_{aq}^{IV}O^{2+}$, generated in the reaction of Fe_{aq}^{2+} and ozone at pH 1, toward various inorganic complexes and some organic substrates, including ferrocene derivatives, Ni(II) macrocyclic tetraamines complexes, polypyridyl complexes of Os(II), Fe(II) and Ru(II), phenothiazines, $HABTS^-$, Na_3IrCl_6, $Co^{II}(dmgBF_2)_2$ and $Ce(ClO_4)_3$ with reduction potentials ranging from 0.52 to 1.7 V has been studied at room temperature. All substrates have shown to react with $Fe_{aq}^{IV}O^{2+}$ quantitatively producing the 1e oxidation product except for the phenothiazines and polypyridyl complexes of Fe(II) and Ru(II). Phenothiazines reacted through oxygen atom transfer to produce sulfoxides while the reactions with polypyridyl complexes of Fe(II) and Ru(II) were complicated and showed no Fe(III) or Ru(III) formation. The obtained second order rate constants of these reactions are within $10^4 - 10^8$ M^{-1} s^{-1} with no straightforward relation to reduction potentials. Among all the substrates, $Os(phen)_3^{2+}$ seems to react through outer-sphere ET. In addition, the no dependence of $Os(phen)_3^{2+}$ reactivity on acid concentration (0.05 – 0.2 M) indicates no prior protonation of the $Fe_{aq}^{IV}O^{2+}$, which is consistent with stepwise electron-transfer followed by proton transfer. Our results suggest that the $Fe_{aq}^{IV}O^{2+}/Fe_{aq}^{III}O^{+}$ potential is not much lower than that for $Os(phen)_3^{3+}/ Os(phen)_3^{2+}$ couple (0.84 V vs. NHE).

GENERAL INTRODUCTION

Introduction

Iron(IV) species have attracted a considerable amount of attention in the past few years, especially after the discoveries of nonheme iron(IV) active site in several enzymatic systems[1-4] and the recent approaches to design a green synthetic catalyst,[5] considering their novel properties like oxidation power, selective reactivity and low environmental impact. Many researchers have focused on synthesis and characterization of iron(IV) complexes in attempts to mimic and understand the chemistry of both heme and nonheme enzymes utilizing iron centers. Such complexes have shown to be strong oxidants capable of abstracting hydrogen atom in C-H bond activation reactions.[6,7]

Mononuclear nonheme iron-oxo complexes

Mononuclear nonheme iron-oxo (Fe(IV)-oxo) complexes are of particular interest for catalytic applications in context of the metabolically vital oxidative transformations that nonheme iron enzymes generating iron(IV)-oxo intermediates can perform in nature, represented by their involvement in the catalytic cycle of dioxygen activation and the wide range of oxidation reactions they perform, including hydroxylation, halogenation, desaturation, epoxidation, cis-dihydroxylation, and aromatic ring cleavage reactions.[8,9] However, the successful synthesis and characterization of such complexes have been limited by their high reactivity and instability under ambient conditions.[6,10]

The first spectroscopic evidence for mononuclear nonheme iron(IV)-oxo species was reported in 2000 by Grapperhaus et al. in the ozonolysis of $[Fe^{III}(cyclam\text{-}acetato)(CF_3SO_3)]^+$ (cyclam-acetato = 1-(carboxymethyl)-1,4,8,11-tetraazacyclotetradecane) in acetone/water.[10] However, the breakthrough in the synthetic iron(IV)-oxo chemistry happened in 2003, when the

first crystal structure of a mononuclear nonheme iron(IV)-oxo complex bearing a macrocyclic supporting ligand, $[(TMC)Fe^{IV}(O)]^{2+}$ was obtained.[11] The remarkable stability of this complex provided the first well-characterized nonheme iron(IV)-oxo complex with a detailed spectroscopic analyses. Since then, a wide range of mononuclear nonheme iron(IV)-oxo complexes, stabilized by polyamine azamacrocycles or acyclic aminopyridine ligands (Fig. 1) have been synthesized and characterized by spectroscopic methods.[6,10-22] These iron(IV)-oxo complexes have been generated under various reaction conditions, at low or room temperatures and in different solvents by reacting an Fe(II)/Fe(III) precursor with oxygen atom donors such as iodosylbenzene (PhIO),[6,11,13-16] peracids,[16-19] hydroperoxides,[11,16,20] NaOX (X = Cl or Br),[21] potassium monopersulfate ($KHSO_5$)[16] or O_3.[10,22] Most of the synthetic iron(IV)-oxo complexes contain intermediate-spin (S = 1) ferryl center rather than the high-spin iron(IV)-oxo (S = 2) generally involved in natural nonheme enzymatic reactions. However, a number of high-spin iron(IV)-oxo species have been trapped and characterized by different spectroscopic methods.[7,22-26]

Reactivity of nonheme Fe(IV)-oxo complexes

The successful characterization of a wide range of mononuclear nonheme iron(IV)-oxo complexes provided researchers with enough spectroscopic data to identify such species, when generated as reaction intermediates and to study their reactivity in various reactions, such as aliphatic hydroxylation,[6,18] olefin epoxidation,[18,19] alcohol oxidation,[27,28] C−H bond activation of alkylaromatics,[29] N-dealkylation,[30] aromatic hydroxylation,[31] oxidation of sulfides and phosphines,[11,16,29,32,33] and electron- and hydride-transfer (Fig 2).[34,35] These studies reveal the high oxidation power of these synthetic Fe(IV)-oxo complexes and show their efficiency and selectivity in the catalytic oxidation of hydrocarbons, making them a useful enzymatic models.

For example, both $[(N4Py)Fe^{IV}=O]^{2+}$ and $[Me_3NTB)Fe^{IV}=O]^{2+}$ activate strong C–H bonds, such as in cyclohexane (99.3 kcal mol^{-1}), at room and low temperatures (-40 ^{o}C) respectively, and found to be more reactive than the Fe(IV)-oxo porphyrin π-cation radical in compound I of cytochrome p450. Compound I is a potent oxidant that can hydroxylate inert C-H bonds with bond dissociation energies exceeding 95 kcal/mol.[6,36,37] Adding to that, the reaction rates of C-H bond activation were found to correlate with bond dissociation energies (BDE) of the substrates with a large kinetic isotope effect (KIE ~ 30), similar to KIE for H-atom abstraction by nonheme iron enzymes.[38]

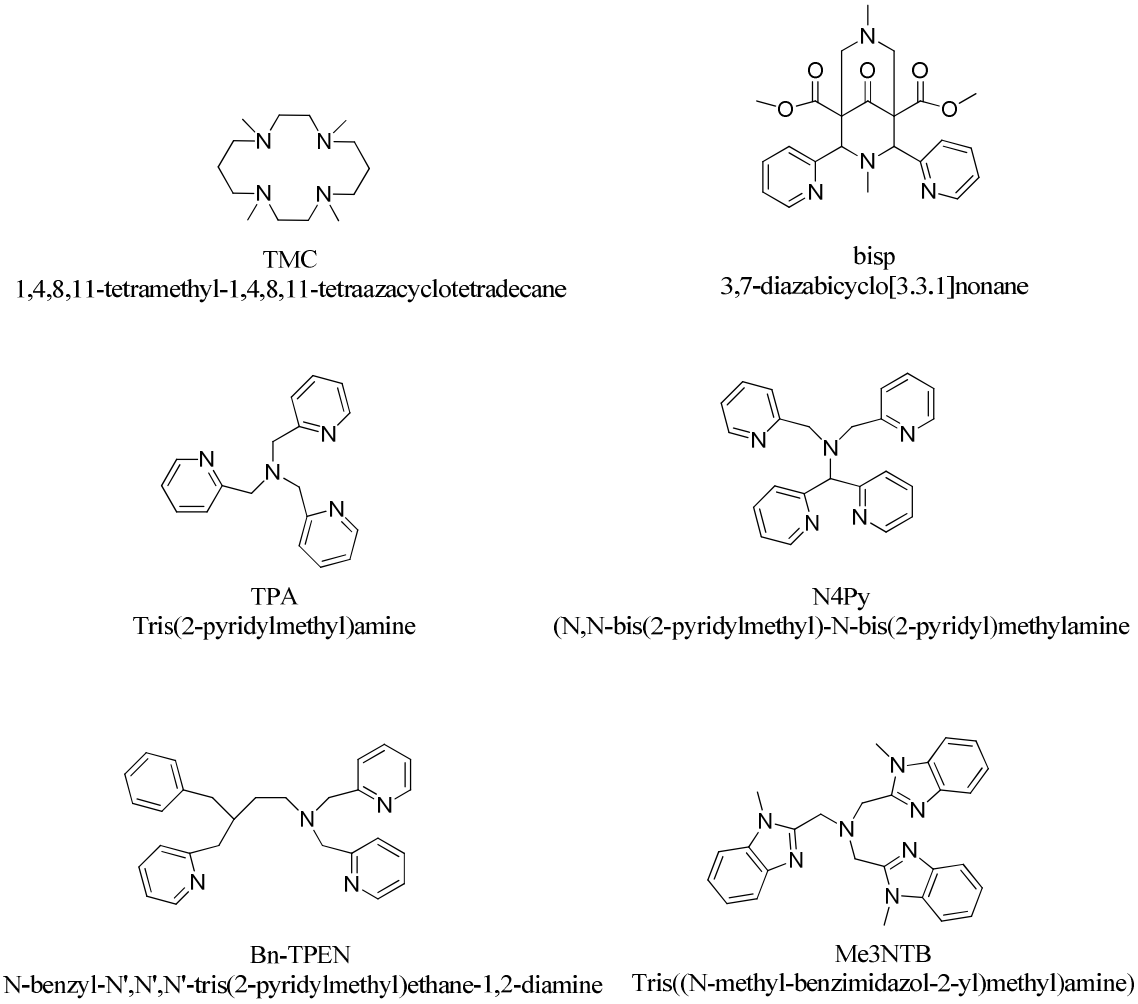

Figure 1. Some of the ligands used to generate nonheme iron(IV)-oxo complexes.

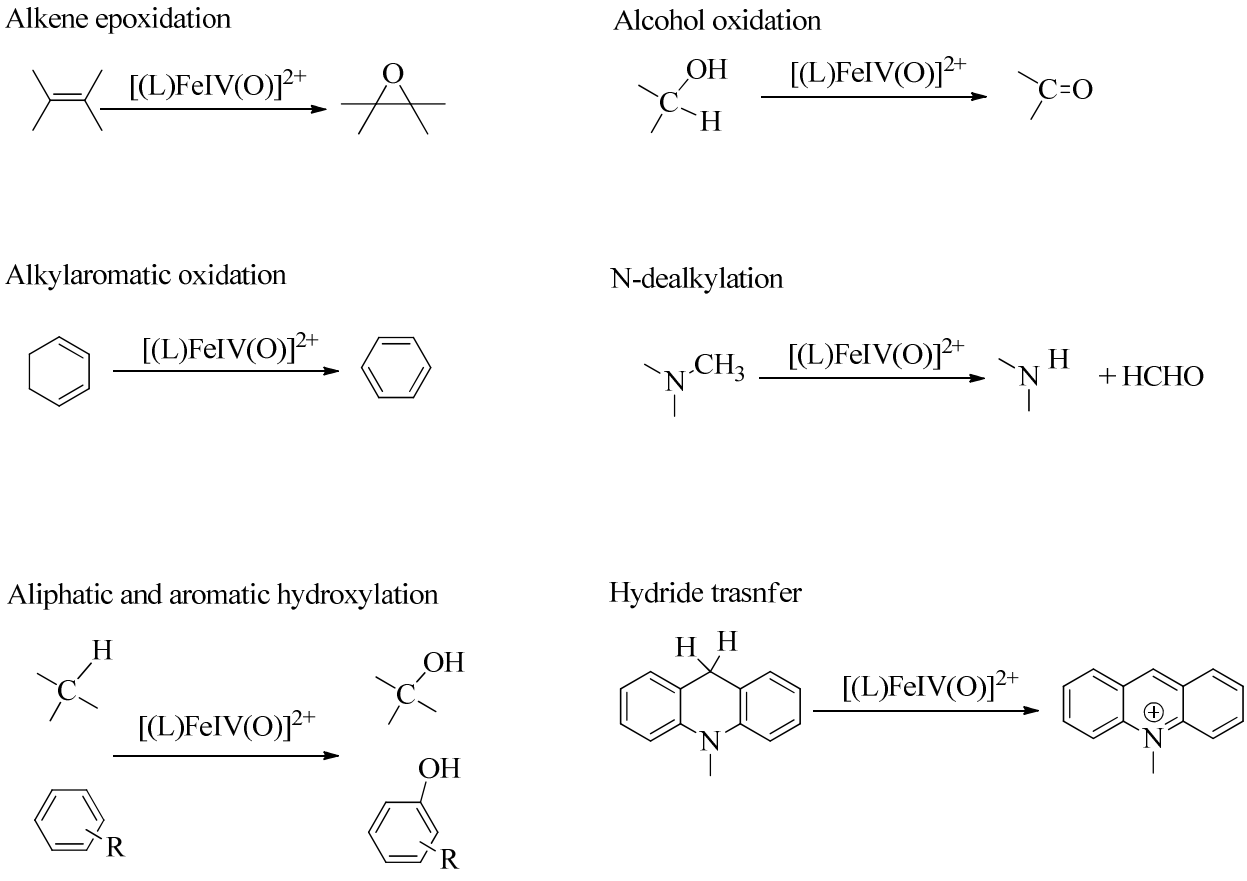

Figure 2. Examples of reactions of synthetic mononuclear nonheme iron(IV)-oxo complexes.

Factors affecting reactivity of nonheme Fe(IV)-oxo complexes

The effect of coordinating ligands, solvent, and pH have been studied in attempts to tune the reactivity and stability of such complexes. The identity of the axial ligands has been found to significantly change the reactivity of $[Fe^{IV}(O)(TMC)(X)]^{n+}$ complexes (**1**) (X = CH_3CN, CF_3COO^-, or N_3^-) toward oxo-transfer to PPh_3, and H-atom abstraction from phenol O-H and alkylaromatic C-H bonds. Replacement of CH_3CN with anionic axial ligand decreases the

electrophilicity of Fe(IV)–oxo unit lowering its reactivity The observed reactivity order in the oxidation of PPh_3 is **1**-$NCCH_3$ > **1**-$OOCCF_3$ > **1**-N_3. However, the reactivity order was the opposite in the oxidation of phenol O-H and alkylaromatic C-H bonds, i. e. **1**-N_3 > **1**-$OOCCF_3$ > **1**-$NCCH_3$.[29] Quantum mechanical calculations show a decrease in the gap between the ground and the excited states with the more electron-donating axial ligand, which enhances the overall reactivity in H-atom abstraction. Also, it was found that replacing the axial CH_3CN ligand in $[Fe^{IV}(O)(TMC)(NCCH_3)]^{2+}$ with anions would result in complexes with shorter lifetimes.[16,39]

A number of studies have focused on enhancing Fe(IV)-oxo stability and reactivity by changing the supporting ligands. $[Fe^{IV}(O)(TMC)]^{2+}$ has shown a low reactivity in hydrogen- and oxygen-atom transfer reactions (HAT and OAT. However, the synthesis of Fe(IV)-oxo complex bearing smaller TMC ring (13-TMC = 1,4,7,10-tetramethyl-1,4,7,10-tetraazacyclotridecane) resulted in a much more reactive Fe(IV)-oxo unit. The 13-TMC complex is ~3.0×10^3 times more reactive in HAT reactions and ~3.0×10^5 times more reactive in OAT reactions at -40 ºC, which is attributed to the 0.22 V increase in the $Fe^{IV/III}$ redox potential.[40] The effect of ligand topology on two Fe(IV)-oxo complexes, cis-α-$[Fe^{IV}(O)(BQCN)]^{2+}$ and cis-β-$[Fe^{IV}(O)(BQCN)]^{2+}$ (BQCN = N,N-dimethyl-N,N-bis(8-quinolyl)cyclohexanediamine), was examined and found that the cis-α-$[Fe^{IV}(O)(BQCN)]^{2+}$ complex is more reactive in C-H bond activation and sulfide oxidation reactions. Difference in reactivities was attributed to the higher 0.11 V $Fe^{IV/III}$ redox potential of the cis-α isomer.[41] On the other hand, the synthesis of high spin (S =2) Fe(IV)-oxo complexes was achieved by using tripodal tetradentate N4 ligands, such as TPA and Me_3NTB. Such complexes were found to be very strong oxidants.[19,37,42]

Solvent is an important factor in generating Fe(IV)-oxo species. For example, $[(TMC)Fe^{II}]^{2+}$ is stable in aerated or O_2-saturated CH_3CN at 25 ºC. However, when a solvent

mixture (1:1 v/v) of CH_3CN and ethanol, butyl ether, or THF was used, $[(TMC)Fe^{IV}(O)]^{2+}$ was formed from the reaction of $[(TMC)Fe^{II}]^{2+}$ and O_2.[32] Another example is the reaction of $[Fe^{II}(\beta\text{-BPMCN})]^{2+}$ (BPMCN = *N,N′*-bis(2-pyridylmethyl)-*N,N′*-dimethyl-*trans*-1,2-diaminocyclohexane) with *tert*-butyl hydroperoxide to generate Fe(IV)-oxo species. In CH_3CN at -40 °C $[FeIV(\beta\text{-BPMCN})(O)(NCMe)]^{2+}$ complex was formed, but in CH_2Cl_2 at -70 °C $[Fe^{IV}(\beta\text{-BPMCN})(OO^tBu)(OH)]^{2+}$ was formed.[43]

The pH of reaction solution could remarkably affect the stability of the Fe(IV)-oxo complex. The stability and reactivity of $[Fe^{IV}(N4Py)(O)]^{2+}$ was investigated in buffered solvent mixture (3:1 v/v) of H_2O and CH_3CN at 10 °C at pH 5-9. $[Fe^{IV}(N4Py)(O)]^2$ is stable at pH 5-6 but decays at a fast rate at higher pH, especially pH >7. The reactivity toward sulfide oxidation found to have very little dependence on the pH (pH 5-7) with only ~ 1.6-fold increases in the rate going from pH 5 to 7.[16] In addition, $[Fe(H_2O)_5(O)]^{2+}$ has been reported to be stable for several seconds at low pH 0-2, but decays faster at higher pH.[22,44]

Aqueous Fe(IV)-oxo

Aqueous Fe(IV) (Fe_{aq}^{IV}) has long been considered as intermediate in the oxidation of Fe^{II} by H_2O_2 in water (Fenton reaction).[45] However, the formation of Fe_{aq}^{IV} in Fenton reaction has always been debated and invoked as alternative oxidant to the hydroxyl radical.[45,46] The extremely short-life for such species and sensitivity to their chemical environment make it difficult to get solid evidence about their formation. Recently, we have provided evidence about the formation of Fe_{aq}^{IV} in Fenton reaction under certain conditions (see Chapter 1).[47] In addition, aqueous Fe(IV)-oxo ($Fe_{aq}^{IV}O^{2+}$) have been reported to form in the reaction of Fe_{aq}^{II} and oxygen-atom donors other than H_2O_2, such as O_3 and HOCl. The fair stability of the Fe(IV) species formed in the Fe_{aq}^{II} and ozone reaction in acidic solutions, life-time of 10 s at pH 1 at room

temperature, allowed their full characterization using various spectroscopic methods and confirmed to be $Fe_{aq}^{IV}O^{2+}$.[22]

Despite the high reactivity of the $Fe_{aq}^{IV}O^{2+}$ and the fact that it is the first synthetic complex with a high spin (S = 2) Fe(IV)-oxo unit, similar to intermediates involved in natural nonheme enzymatic reactions, the number of reports on its chemistry are limited.[22,28,33,44,48] It has been shown that $Fe_{aq}^{IV}O^{2+}$ is a highly reactive species capable of oxidizing a wide range of organic substrates, such as sulfoxides, alcohols, ethers, aldehydes, phenol, carboxylic acids, acetone, and acetonitrile, by various mechanisms including oxygen-, hydride- and H-atom transfer.[22,28,33,48] Noteworthy, reactions with alcohols, ethers and aldehydes proceed through two parallel 1-e (H-atom transfer) and 2-e (hydride transfer) pathways.[28] The hydride path is catalytic as it generates Fe_{aq}^{2+} which can be reoxidized to $Fe_{aq}O^{2+}$. However, the catalytic efficiency is poor because of the loss of the catalyst (Fe_{aq}^{2+}) as Fe_{aq}^{3+} in the 1-e path. In this current work we show that catalysis can be improved by changing the solvent to CH_3CN (see Chapter 2).

Electron transfer properties of nonheme Fe(IV)-oxo complexes

Many reports have been focused on the reactivities of synthetic Fe(IV)-oxo complexes with wide range of organic substrates. However, only few reports have investigated the fundamental electron-transfer (ET) properties of such complexes with different organometallic or inorganic substrates.[34,48-52] $[(TMC)Fe^{IV}(O)]^{2+}$ reacts with ferrocene (Fc) forming ferrocenium ion (Fc^+) and $[(TMC)Fe^{III}(O)]^+$. The ET process found to exhibit equilibrium and the one-electron reduction potentials (E_{red}) of $[(TMC)Fe^{IV}(O)]^{2+}$ was determined to be 0.39 V vs SCE.[34] The one-electron reduction potentials of other Fe(IV)-oxo complexes, $[(Bn\text{-}TPEN)Fe^{IV}(O)]^{2+}$ and $[(N4Py)Fe^{IV}(O)]^{2+}$ were determined the same way and found to be 0.49 V and 0.51 V vs. SCE respectively. The reactions of these complexes with Fc and some ferrocene derivatives found to

proceed through outer-sphere ET and their reactivities were recently[53] review by Fukuzumi and found to follow Marcus theory of electron transfer (eq. 1)[54] where Z is the collision frequency

$$k_{ET} = Z \exp\left(\frac{-\left(\frac{\lambda}{4}\right)\left(1+\frac{\Delta G_{ET}}{\lambda}\right)^2}{k_B T}\right) \quad (1)$$

($1\times10^{11}M^{-1}\ s^{-1}$), λ is the reorganization energy of electron transfer, k_B is the Boltzmann constant, T is the absolute temperature, and ΔG_{ET} is the free energy change of electron transfer (see Table 1).

Also, it was pointed out that the flexibility of the ligand would result in larger reorganization energy. For $[(bisp)Fe^{IV}(O)]^2$, which bears the more rigid bispidine ligand, the reorganization energy (2.05 eV) is significantly smaller compared to the other Fe(IV)-oxo complexes in Table 1. Also the reduction potential of $[(bisp)Fe^{IV}(O)]^{2+}$ (0.73 V vs. SCE) is one of the highest compared to other synthetic Fe(IV)-oxo complexes which is attributed to the rigid structure of the ligand that makes the Fe(IV) metal center more electron deficient.[49,53]

The protonation of the Fe(IV)-oxo unit by Brønsted acid or the binding of metal ions, acting as Lewis acid such as Sc^{3+}, to the Fe(IV)-oxo unit have shown to enhance the reduction potential and significantly promote the ET process.[51,52] For example, no ET was observed between $[(N4Py)Fe^{IV}(O)]^{2+}$ complex (E = 0.51 V vs. SCE) and $[Ru^{II}(Clphen)_3]^{2+}$ (Clphen = 5-chlorophenathrene) (E = 1.36 V vs. SCE) in CH_3CN at 25 ºC, as expected. However, ET occurred efficiently in the presence of $HClO_4$ by proton-coupled electron-transfer.[52]

Table 1. ET Rate Constants (k_{ET}), and Reorganization Energies (λ) of One-electron Reduction of some Nonheme Fe(IV)-oxo Complexes by Ferrocene Derivatives and the One-electron Reduction Potentials of the Fe(IV)-oxo Complexes (E_{FeO}) and the Ferrocene Derivatives (E_{Fc}).[a]

		k_{ET} (M^{-1} s^{-1})		
Electron donor	E_{Fc} (V vs. SCE)	$[(TMC)Fe^{IV}(O)]^{2+}$	$[(Bn\text{-}TPEN)Fe^{IV}(O)]^{2+}$	$[(N4Py)Fe^{IV}(O)]^{2+}$
Ferrocene (Fc)	0.37	14	24	5
n-Amyl-Fc	0.31	39	45	15
Dimethyl-Fc	0.26	1.0×10^2	1.0×10^2	24
Octamethyl-Fc	- 0.04	2.7×10^4	2.3×10^4	3.0×10^3
Decamethyl-Fc	- 0.08	6.3×10^4	4.3×10^4	7.0×10^3
E_{FeO} (V vs. SCE)		0.39	0.49	0.51
λ (eV)		2.37	2.55	2.74

[a] All data are adopted from ref. 34 and 53.
see Fig. 1 for ligands names abbreviations.

On the other hand, the electron transfer properties of the $Fe_{aq}^{IV}O^{2+}$ species are still unexplored and is the topic of Chapter 3 in this thesis. The only literature report related to this subject deals with the kinetics of oxidation of several inorganic substrates, i. e. HSO^{3-}, NO^{2-}, Mn^{2+} and Cl^-. Reactions were concluded to take place by electron transfer based on the linear relationship between log k and the standard one electron potential of the substrate.[48]

All previous reports have shown that synthetic mononuclear nonheme Fe(IV)-oxo complexes are very powerful oxidants, with similar to higher reactivities in contrast to the natural enzymatic systems, capable of reacting with wide range of organic and inorganic substrates through different mechanisms. In addition, reports have shown that these complexes

are sensitive to their chemical environment and a moderate change in the environment can dramatically alter their reactivities and stability. The current work focuses on the chemistry of aqueous Fe(IV)-oxo species and the factors that affect their reactivity and stability. Changes in the pH, coordinating ligands and solvent are found to have a dramatic effect on the life time and chemistry of Fe(IV) as described in this dissertation.

Dissertation Organization

This dissertation consists of three chapters. Chapter one has been published in *Chemical Science*. Chapter two corresponds to a manuscript ready to be submitted to *ACS Catalysis*. Chapter three corresponds to a manuscript in preparation. Each chapter is self-contained with its own equations, figures, tables, and references.

References

(1) Price, J. C.; Barr, E. W.; Tirupati, B.; Bollinger, J. M.; Krebs, C. *Biochemistry* **2003**, *42*, 7497.

(2) Liu, K. E.; Valentine, A. M.; Wang, D.; Huynh, B. H.; Edmondson, D. E.; Salifoglou, A.; Lippard, S. J. *Journal of the American Chemical Society* **1995**, *117*, 10174.

(3) Wallar, B. J.; Lipscomb, J. D. *Chemical Reviews* **1996**, *96*, 2625.

(4) Sturgeon, B. E.; Burdi, D.; Chen, S.; Huynh, B.-H.; Edmondson, D. E.; Stubbe, J.; Hoffman, B. M. *Journal of the American Chemical Society* **1996**, *118*, 7551.

(5) Ryabov, A. D. In *Advances in Inorganic Chemistry*; Rudi van, E., Colin, D. H., Eds.; Academic Press: 2013; Vol. Volume 65, p 117.

(6) Kaizer, J.; Klinker, E. J.; Oh, N. Y.; Rohde, J.-U.; Song, W. J.; Stubna, A.; Kim, J.; Münck, E.; Nam, W.; Que, L. *Journal of the American Chemical Society* **2003**, *126*, 472.

(7) Krebs, C.; Galonić Fujimori, D.; Walsh, C. T.; Bollinger, J. M. *Accounts of Chemical Research* **2007**, *40*, 484.

(8) Solomon, E. I.; Brunold, T. C.; Davis, M. I.; Kemsley, J. N.; Lee, S.-K.; Lehnert, N.; Neese, F.; Skulan, A. J.; Yang, Y.-S.; Zhou, J. *Chemical Reviews* **1999**, *100*, 235.

(9) Abu-Omar, M. M.; Loaiza, A.; Hontzeas, N. *Chemical Reviews* **2005**, *105*, 2227.

(10) Grapperhaus, C. A.; Mienert, B.; Bill, E.; Weyhermüller, T.; Wieghardt, K. *Inorganic Chemistry* **2000**, *39*, 5306.

(11) Rohde, J.-U.; In, J.-H.; Lim, M. H.; Brennessel, W. W.; Bukowski, M. R.; Stubna, A.; Münck, E.; Nam, W.; Que, L. *Science* **2003**, *299*, 1037.

(12) Que, L. *Accounts of Chemical Research* **2007**, *40*, 493.

(13) Suh, Y.; Seo, M. S.; Kim, K. M.; Kim, Y. S.; Jang, H. G.; Tosha, T.; Kitagawa, T.; Kim, J.; Nam, W. *Journal of Inorganic Biochemistry* **2006**, *100*, 627.

(14) Sastri, C. V.; Park, M. J.; Ohta, T.; Jackson, T. A.; Stubna, A.; Seo, M. S.; Lee, J.; Kim, J.; Kitagawa, T.; Münck, E.; Que, L.; Nam, W. *Journal of the American Chemical Society* **2005**, *127*, 12494.

(15) Bukowski, M. R.; Comba, P.; Lienke, A.; Limberg, C.; Lopez de Laorden, C.; Mas-Ballesté, R.; Merz, M.; Que, L. *Angewandte Chemie International Edition* **2006**, *45*, 3446.

(16) Sastri, C. V.; Sook Seo, M.; Joo Park, M.; Mook Kim, K.; Nam, W. *Chemical Communications* **2005**, 1405.

(17) Bukowski, M. R.; Koehntop, K. D.; Stubna, A.; Bominaar, E. L.; Halfen, J. A.; Münck, E.; Nam, W.; Que, L. *Science* **2005**, *310*, 1000.

(18) Martinho, M.; Banse, F.; Bartoli, J.-F.; Mattioli, T. A.; Battioni, P.; Horner, O.; Bourcier, S.; Girerd, J.-J. *Inorganic Chemistry* **2005**, *44*, 9592.

(19) Lim, M. H.; Rohde, J.-U.; Stubna, A.; Bukowski, M. R.; Costas, M.; Ho, R. Y. N.; Münck, E.; Nam, W.; Que, L. *Proceedings of the National Academy of Sciences* **2003**, *100*, 3665.

(20) Kaizer, J.; Costas, M.; Que, L. *Angewandte Chemie International Edition* **2003**, *42*, 3671.

(21) Balland, V.; Charlot, M.-F.; Banse, F.; Girerd, J.-J.; Mattioli, Tony A.; Bill, E.; Bartoli, J.-F.; Battioni, P.; Mansuy, D. *European Journal of Inorganic Chemistry* **2004**, *2004*, 301.

(22) Pestovsky, O.; Stoian, S.; Bominaar, E. L.; Shan, X.; Münck, E.; Que, L.; Bakac, A. *Angewandte Chemie International Edition* **2006**, *45*, 340.
(23) England, J.; Martinho, M.; Farquhar, E. R.; Frisch, J. R.; Bominaar, E. L.; Münck, E.; Que, L. *Angewandte Chemie International Edition* **2009**, *48*, 3622.

(24) Bautz, J.; Comba, P.; Lopez de Laorden, C.; Menzel, M.; Rajaraman, G. *Angewandte Chemie International Edition* **2007**, *46*, 8067.

(25) England, J.; Guo, Y.; Farquhar, E. R.; Young Jr, V. G.; Münck, E.; Que Jr, L. *Journal of the American Chemical Society* **2010**, *132*, 8635.

(26) Lacy, D. C.; Gupta, R.; Stone, K. L.; Greaves, J.; Ziller, J. W.; Hendrich, M. P.; Borovik, A. S. *Journal of the American Chemical Society* **2010**, *132*, 12188.

(27) Oh, N. Y.; Suh, Y.; Park, M. J.; Seo, M. S.; Kim, J.; Nam, W. *Angewandte Chemie International Edition* **2005**, *44*, 4235.

(28) Pestovsky, O.; Bakac, A. *Journal of the American Chemical Society* **2004**, *126*, 13757.

(29) Sastri, C. V.; Lee, J.; Oh, K.; Lee, Y. J.; Lee, J.; Jackson, T. A.; Ray, K.; Hirao, H.; Shin, W.; Halfen, J. A.; Kim, J.; Que, L.; Shaik, S.; Nam, W. *Proceedings of the National Academy of Sciences* **2007**, *104*, 19181.

(30) Nehru, K.; Seo, M. S.; Kim, J.; Nam, W. *Inorganic Chemistry* **2006**, *46*, 293.

(31) de Visser, S. P.; Oh, K.; Han, A.-R.; Nam, W. *Inorganic Chemistry* **2007**, *46*, 4632.

(32) Kim, S. O.; Sastri, C. V.; Seo, M. S.; Kim, J.; Nam, W. *Journal of the American Chemical Society* **2005**, *127*, 4178.

(33) Pestovsky, O.; Bakac, A. *Inorganic Chemistry* **2005**, *45*, 814.

(34) Lee, Y.-M.; Kotani, H.; Suenobu, T.; Nam, W.; Fukuzumi, S. *Journal of the American Chemical Society* **2007**, *130*, 434.

(35) Fukuzumi, S.; Kotani, H.; Lee, Y.-M.; Nam, W. *Journal of the American Chemical Society* **2008**, *130*, 15134.

(36) Kumar, D.; Hirao, H.; Que, L.; Shaik, S. *Journal of the American Chemical Society* **2005**, *127*, 8026.

(37) Seo, M. S.; Kim, N. H.; Cho, K.-B.; So, J. E.; Park, S. K.; Clemancey, M.; Garcia-Serres, R.; Latour, J.-M.; Shaik, S.; Nam, W. *Chemical Science* **2011**, *2*, 1039.

(38) Price, J. C.; Barr, E. W.; Glass, T. E.; Krebs, C.; Bollinger, J. M. *Journal of the American Chemical Society* **2003**, *125*, 13008.

(39) Rohde, J.-U.; Que, L. *Angewandte Chemie International Edition* **2005**, *44*, 2255.

(40) Hong, S.; So, H.; Yoon, H.; Cho, K.-B.; Lee, Y.-M.; Fukuzumi, S.; Nam, W. *Dalton Transactions* **2013**, *42*, 7842.

(41) Hong, S.; Lee, Y.-M.; Cho, K.-B.; Sundaravel, K.; Cho, J.; Kim, M. J.; Shin, W.; Nam, W. *Journal of the American Chemical Society* **2011**, *133*, 11876.

(42) Bigi, J. P.; Harman, W. H.; Lassalle-Kaiser, B.; Robles, D. M.; Stich, T. A.; Yano, J.; Britt, R. D.; Chang, C. J. *Journal of the American Chemical Society* **2012**, *134*, 1536.

(43) Fiedler, A. T.; Que, L. *Inorganic Chemistry* **2009**, *48*, 11038.

(44) Loegager, T.; Holcman, J.; Sehested, K.; Pedersen, T. *Inorganic Chemistry* **1992**, *31*, 3523.

(45) Bray, W. C.; Gorin, M. H. *Journal of the American Chemical Society* **1932**, *54*, 2124.

(46) Barb, W. G.; Baxendale, J. H.; George, P.; Hargrave, K. R. *Transactions of the Faraday Society* **1951**, *47*, 462.

(47) Bataineh, H.; Pestovsky, O.; Bakac, A. *Chemical Science* **2012**, *3*, 1594.

(48) Jacobsen, F.; Holcman, J.; Sehested, K. *International Journal of Chemical Kinetics* **1998**, *30*, 215.

(49) Comba, P.; Fukuzumi, S.; Kotani, H.; Wunderlich, S. *Angewandte Chemie International Edition* **2010**, *49*, 2622.

(50) Fukuzumi, S.; Kotani, H.; Suenobu, T.; Hong, S.; Lee, Y.-M.; Nam, W. *Chemistry – A European Journal* **2010**, *16*, 354.

(51) Morimoto, Y.; Kotani, H.; Park, J.; Lee, Y.-M.; Nam, W.; Fukuzumi, S. *Journal of the American Chemical Society* **2010**, *133*, 403.

(52) Park, J.; Morimoto, Y.; Lee, Y.-M.; Nam, W.; Fukuzumi, S. *Journal of the American Chemical Society* **2012**, *134*, 3903.

(53) Fukuzumi, S. *Coordination Chemistry Reviews* **2013**, *257*, 1564.

(54) Marcus, R. A. *Annual Review of Physical Chemistry* **1964**, *15*, 155.

CHAPTER 2

pH-INDUCED MECHANISTIC CHANGEOVER FROM HYDROXYL RADICALS TO IRON(IV) IN THE FENTON REACTION

A paper published in *Chemical Science*[*]

Abstract

A major pathway in the reaction between Fe(II) and H_2O_2 at pH 6-7 in non-coordinating buffers exhibits inverse kinetic dependence on $[H^+]$ and leads to oxidation of dimethyl sulfoxide (DMSO) to dimethyl sulfone ($DMSO_2$). This step regenerates Fe(II) and makes the oxidation of DMSO catalytic, a finding that strongly supports Fe(IV) as a Fenton intermediate at near-neutral pH. This Fe(IV) is a less efficient oxidant for DMSO at pH 6-7 than is $(H_2O)_5FeO^{2+}$, generated by ozone oxidation of $Fe(H_2O)_6^{2+}$, in acidic solutions. Large concentrations of DMSO are needed to achieve significant turnover numbers at pH≥6 owing to the rapid competing reaction between Fe(II) and Fe(IV) that leads to irreversible loss of the catalyst. At pH 6 and ≤0.02 mM Fe(II), the ratio of apparent rate constants for the reactions of Fe(IV) with DMSO and with Fe(II) is ~10^4. The results at pH 6-7 stand in stark contrast with those reported previously in acidic solutions where Fenton reaction generates hydroxyl radicals. Under those conditions, DMSO is oxidized stoichiometrically to methylsulfinic acid and ethane. This path still plays a minor role (1-10%) at pH 6-7.

[*] Bataineh, Hajem; Pestrovsky, Oleg; Bakac, Andreja *Chem. Sci.* **2012**, *3* 1594 - 1599

Introduction

The reaction between iron(II) and hydrogen peroxide (Fenton reaction)[1] is one of the best known and most widespread oxidation reactions. In addition to its natural occurrence in biology,[2-5] environment[6], and atmosphere,[7] this reaction is a key step in iron-based advanced oxidation processes (AOP)[8] for waste-water treatment and soil remediation.

The ubiquity and effectiveness of the Fenton reaction stems from the fact that two widely available and stable reagents generate an intermediate capable of oxidizing a wide variety of organic and inorganic substrates. The exact nature of the intermediate(s) has been debated for decades.[9-14] Most of the discussion focused on hydroxyl radicals[4,11,14] and an Fe(IV) species,[10] i.e. products generated by one-electron and two-electron transfers, respectively. Reaction products and kinetics of oxidation of various substrates strongly support $HO^{\bullet}$ in acidic solutions.[13] Mechanistic studies took advantage of the independently known chemistry[15,16] of $HO^{\bullet}$ and often utilized specific $HO^{\bullet}$ scavengers as diagnostic tools. None the less, the issue was not fully resolved until the ferryl(IV) ion, $(H_2O)_5Fe^{IV}O^{2+}$, was generated and characterized independently.[17-20] As expected, it was found that most substrates react with Fe(IV) and with $HO^{\bullet}$ to yield identical products, but several crucial exceptions exist. Most notably, dimethyl sulfoxide reacts with Fe(IV) by oxygen atom transfer and yields dimethyl sulfone, $(CH_3)_2SO_2$,[19] whereas hydroxyl radicals generate methyl sulfinic acid and ethane (via free methyl radicals), Scheme 1.[15,16] Methylsulfinic acid and ethane are also produced in the Fenton reaction.[21] These and related observations rule out $(H_2O)_5FeO^{2+}$ and establish $HO^{\bullet}$ as the Fenton intermediate at pH $\leq$3.[19]

Other studies, both experimental[22-26] and computational[27-29] suggest, however, that Fe(IV) may be involved in some cases. Most convincing evidence for Fe(IV) was obtained in studies at

higher, near-neutral pH. Hug *et al*[22,30,31] invoked an intermediate different from hydroxyl radicals, most likely an Fe(IV) species, to explain the failure of 2-propanol to quench the oxidation of As(III) with the Fenton reagent at neutral pH. This interpretation received support from several other groups,[32-35] but was questioned by Pang *et al* who proposed that surface interactions, and not Fe(IV), were responsible for the observed behavior in these inhomogeneous environments.[36,37]

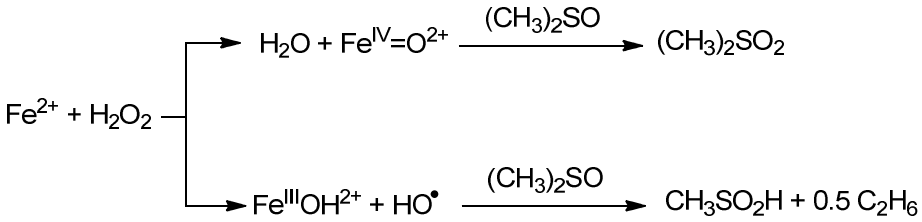

Scheme 1.

As part of our on-going interest in high-valent iron chemistry and the Fenton reaction, we conducted an in depth study of the kinetics and products of the reaction of $Fe(H_2O)_6^{2+}$ and H_2O_2 at $6 \leq pH \leq 7$ in the presence of non-coordinating buffers. Here we present our results. We also draw attention to a misstatement in our earlier publication[19] regarding the involvement of hydroxyl radicals in neutral solutions. That work was done at a natural pH in unbuffered solutions (initial pH ~7). We failed to take into account the increase in acid concentration by hydrolysis of Fe(III) produced in the course of the reaction. This lowering of the pH was the reason for the formation of hydroxyl radicals.

Experimental

Stock solutions of iron(II) perchlorate in H_2O or D_2O were prepared freshly before each set of experiments and standardized with phenanthroline. All of the solutions were handled anaerobically under argon. The solvent was H_2O for kinetic studies, and D_2O for NMR product

analysis. The pH (pD) was controlled with noncoordinating tertiary amine buffers[39] MES (pK_a 6.06), MOPS (pK_a 7.09), MOBS (pK_a 7.48) and PIPBS (pK_{a1} 4.29, pK_{a2} 8.55) or with phosphate buffers (pH 6-8). Buffer concentrations were typically 8-50 times greater than the concentration of the limiting reagents so as to hold the pH at the desired value without interfering with the NMR spectra or altering the chemistry. The pH decrease was less than 0.2 units in kinetics experiments, and 0.3-0.5 units in the NMR experiments.

The stoichiometry was determined from absorbance changes at 270 nm using $\Delta\varepsilon_{270}$ = 2650±50 M^{-1} cm^{-1} at pH 6-7. This value was obtained on solutions generated by mixing Fe(II) (0.01 - 0.02 mM) with excess H_2O_2 (0.1 - 1.5 mM) either in the stopped flow or in a conventional spectrophotometer as described in detail in SI. After Fe(III) was generated, the absorbance at 270 nm remained constant for at least five minutes, showing that the turbidity or precipitation of iron(III) did not affect absorbance readings. This point is also illustrated in the kinetic plots in Figures S6-S8, all of which exhibit the same $\Delta\varepsilon$, even though the reaction times vary by a factor of 14.

Results

Products and stoichiometry

The products of the Fe(II)/H_2O_2/$(CH_3)_2SO$ reaction in D_2O buffered with either phosphate or noncoordinating tertiary amine buffers (MES, MOPS or PIPBS) under air-free conditions were determined by ^1H NMR. In tertiary amine buffers the reaction generated $(CH_3)_2SO_2$ (6% yield at pH 6-7, $[(CH_3)_2SO]_0$ = 36 mM, [MES] = 10 mM), Figures 1 and S1. Increasing buffer concentration from 10 to 24 mM had no effect on the nature or yield of products, which rules out the involvement of buffer in the reaction. Additional comments on noninterference of buffers is provided in SI.

The yields of $(CH_3)_2SO_2$ in MES buffer under conditions in Figure 1 increased four-fold when Fe(II) was added slowly with a syringe pump. Also, as shown later, higher concentrations of dimethyl sulfoxide led to a systematic increase in the amount of $(CH_3)_2SO_2$ produced. These observations demonstrate a competition for the reactive intermediate between the sulfoxide to generate sulfone, and Fe(II) to generate Fe(III). The most reasonable candidate for this intermediate is an Fe(IV) species. Attempts to prepare Fe(IV) at pH 6 from Fe(II) and ozone[19] and to examine its chemistry directly were not successful owing to its rapid decomposition at this pH. However, the kinetic and product data described below provide overwhelming support for Fe(IV) as a key intermediate.

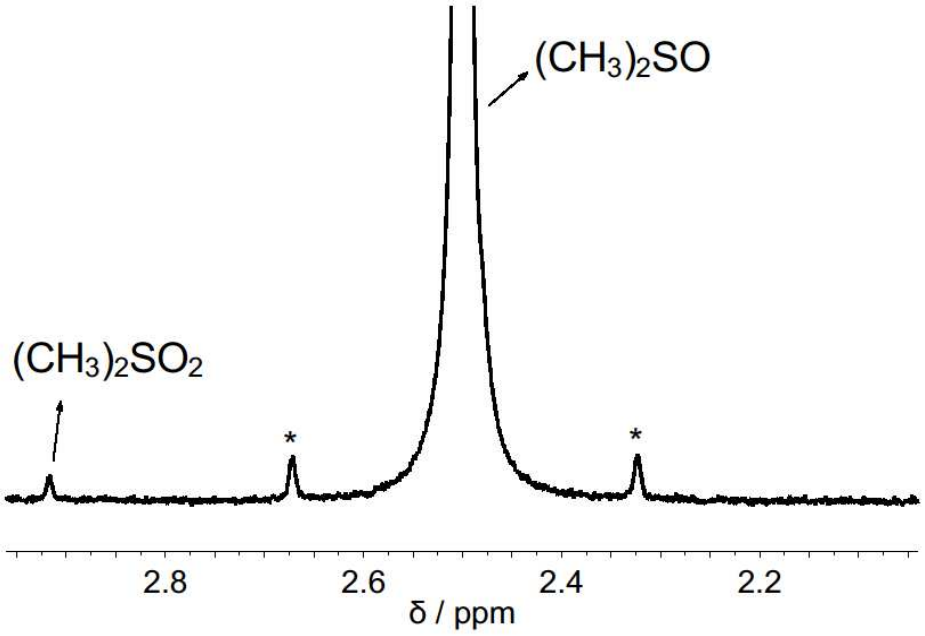

Figure 1. ^{1}H NMR spectrum of the products obtained in MES buffer (10 mM) at pD 6.8 and acidified to pD 1 after the reaction. Conditions: 1.2 mM $Fe(ClO_4)_2$, 1.1 mM H_2O_2 and 36 mM $(CH_3)_2SO$. ^{13}C satellite peaks are denoted with an asterisk.

Strikingly, when the Fe(II)/H_2O_2/$(CH_3)_2SO$ reaction was run in phosphate buffers, the

products changed to ethane (60% yield at pH 7) and methylsulfinate (25%), indicative of HO• radicals,[19] Figure 2 and Table 1. The yields of methylsulfinate are lower than expected for reasons that are not fully understood, but most likely some of the anion is complexed with the Fe(III) product and thus not detected by NMR. The yields of all of the products in both tertiary amines and phosphate buffers decreased significantly as the pH increased from 6 to 8, but the prevalence of •OH-derived products in phosphate and of 2-e products in noncoordinating buffers remained throughout, **Table 1.**

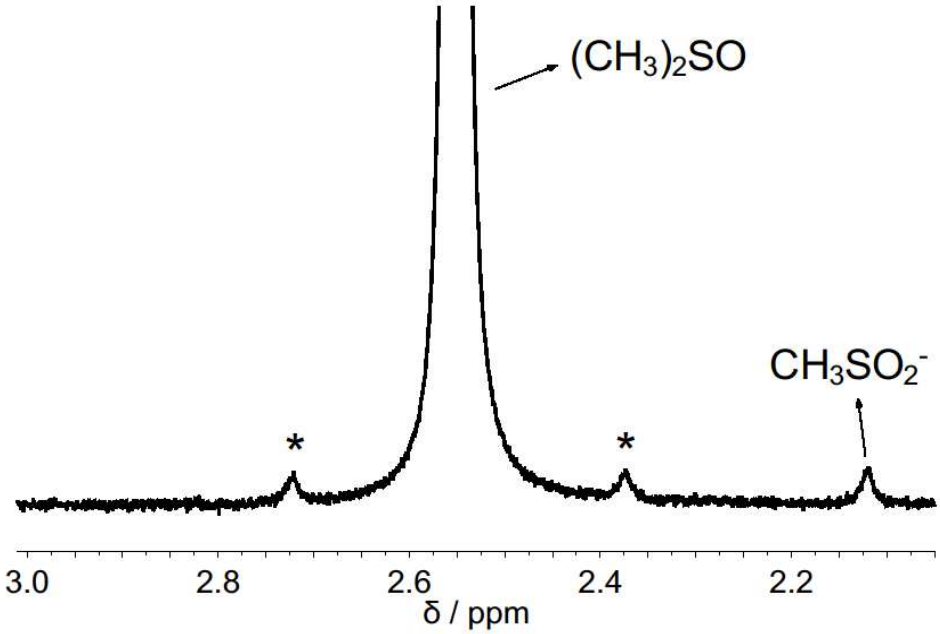

Figure 2. ^{1}H NMR spectrum of the products obtained in phosphate buffer (10 mM) at pD 7.6. Conditions: 1.0 mM $Fe(ClO_4)_2$, 1.0 mM H_2O_2, 15 mM $(CH_3)_2SO$.

Table 1. GC Peak Areas for Methane and Ethane Generated in the Fenton Reaction with $(CH_3)_2SO$[a]

Initial pH[b]	Buffer/(conc/mM)	Ethane[c]	Methane[c]
6.1	MES (16)	(1)	15
6.1	phosphate (19)	1200[d]	76
7.0	MOPS (15)	0.5	6
8.2	MOBS (19)	3	7
8.0[e]	phosphate (10)	65	17

[a] Obtained by injecting 80 μL of head gas into gas chromatograph. Reaction conditions: 0.93 ± 0.03 mM $Fe(ClO_4)_2$, 0.95 ± 0.03 mM H_2O_2, 66 mM DMSO. [b] pH decreased in the course of the run by 0.2 units. [c] Relative peak areas in gas chromatograms. [d] Absolute concentration = 0.27 mM (60% of theoretical yield). [e] $[Fe(ClO_4)_2]_0 = [H_2O_2]_0 = 0.40$ mM, [DMSO] = 39 mM.

para-Tolyl methyl sulfoxide, $(CH_3C_6H_4)S(O)CH_3$) (TMSO) in PIPBS buffer at pH 6-7 was oxidized to $TMSO_2$ (35 % yield, $[TMSO]_0$ = 30-50 mM, $[Fe(ClO_4)_2]_0$ = (1-2) mM, $[H_2O_2]_0$ = (1-2) mM), Figure S2. No products were observed in phosphate buffer, Figure S3, similar to our earlier results in acidic solutions in the absence of buffers where HO• radical was established as the reaction intermediate.[19]

In experiments with large concentrations of $(CH_3)_2SO$ and excess H_2O_2, **Table 2**, the oxidation of sulfoxides becomes catalytic in tertiary amine buffers but not in phosphate. In MES (Table 2, entries 1-3) the reaction of 0.2 mM H_2O_2 with 0.02 mM Fe(II) consumed 0.02 mM H_2O_2 in the absence of substrate, 0.08 mM H_2O_2 in the presence of 45 mM $(CH_3)_2SO$, and all of the H_2O_2 (0.2 mM) at 0.96 M $(CH_3)_2SO$, leading to an overall stoichiometry $\Delta[H_2O_2]/\Delta[Fe(II)]$ = 10 at the highest $[(CH_3)_2SO]$. Large, nonstoichiometric amounts of H_2O_2 were also consumed at pH 7 (entry 4).

Table 2. Effect of Buffers and Concentration of $(CH_3)_2SO$ on Yields of $(CH_3)_2SO_2$[a]

Entry	Buffer[b]	$[H_2O_2]_0$	$[Fe(II)]_0$	$[(CH_3)_2SO]$	$[H_2O_2]_\infty$	$Fe(II)_\infty$	$[(CH_3)_2SO_2]_\infty$	$\frac{\Delta[H_2O_2]}{\Delta[Fe(II)]}$
1	MES	0.20	0.020	0	0.18	0		~1
2	MES	0.20	0.020	45	0.12	0		4
3	MES	0.20	0.020	960	0	0		10
4	MOPS[c]	0.20	0.020	1090	0.06			7
5	MES [d,e]	0.49	0.49	190	0	0.18	0.26	1.6
6	MES[d,e]	0.49	0.49	950	0	0.36	0.48	3.8
7	phosphate	0.20	0.02	0	0.19		f	
8	phosphate	0.20	0.02	960	0.16		f	

[a] In H_2O, pH 6.1 - 6.3. All concentrations in mM. [b] [Buffer] = 1 mM. [c] pH 7.0 [d] [Buffer] = 10 mM. [e] In D_2O. [f] Products are ethane and $CH_3SO_2^-$, see text.

At the small concentrations of H_2O_2 and Fe(II) in the above experiments, the yields of organic products were too small to be quantified by NMR. In the next set, the concentrations of both H_2O_2 and Fe(II) were raised to 0.49 mM and the products were analyzed by NMR. After completion of the reaction in the presence of 190 mM $(CH_3)_2SO$, there remained 0.18 mM unreacted Fe(II) (entry 5). At 950 mM $(CH_3)_2SO$, 0.36 mM

Fe(II) was recovered (entry 6). Both experiments generated large amounts of dimethyl sulfone, 0.26 and 0.48 mM, respectively (Figures S4 and S5). The dependence of $(CH_3)_2SO_2$ yield on substrate concentration is evidence for the loss of oxidizing intermediate in competing side reaction(s) that do not involve substrate. The competition is less favorable at pH ≥7, where the product yields are even lower.

In contrast to these results, there was no indication of catalysis in phosphate buffers. The reaction consumed close to stoichiometric amounts of H_2O_2 even at 1 M $(CH_3)_2SO$, entries 7-8, and produced methylsulfinate and ethane.

Kinetics of Fe(II)-H_2O_2 reaction at pH 6-7.

The experiments were performed under pseudo-first order conditions using either reagent in excess. Kinetic traces (Figures S6-S8) were exponential and yielded pseudo-first order rate constants that exhibit linear dependence on the concentration of excess reagent, as shown in Figures S9-S11. After correction for the stoichiometric factor of 2 (eq 1-2) in experiments with excess H_2O_2, one obtains a second order rate constant k_{Fe} = 650 (± 20) $M^{-1}s^{-1}$ at pH 6, and 5.9 (± 0.2) × 10^3 $M^{-1}s^{-1}$ at pH 7. Data obtained with excess Fe(II) were somewhat more scattered (Figure S11) but yielded a comparable value, k_{Fe} = 670 (± 70) $M^{-1}s^{-1}$ at pH 6 consistent with the 2:1 [Fe(II)]/[H_2O_2] stoichiometry that was also obtained directly from the observed absorbance changes in these experiments. For comparison, the rate constant in acidic solutions, determined

in this and earlier work[40] is k_{Fe} = 58 $M^{-1}s^{-1}$, independent of pH in the range 3≥pH≥1. Similar values have been reported by other groups, as summarized in ref. 22. The kinetic data are summarized in **Table 3.** Assuming that the reaction at pH 6-7 takes place by two parallel pathways, one involving $Fe(H_2O)_6^{2+}$ and the other, $Fe(H_2O)_5OH^+$, see later, and taking pK_a = 9.5 for $Fe(H_2O)_6^{2+}$,[41] one calculates the rate constant k_{FeOH} = (1.8 ± 0.2) × 10^6 M^{-1} s^{-1} for the $Fe(H_2O)_5OH^+/H_2O_2$ reaction, in reasonable agreement with previous studies[22,42,43] which reported k_{FeOH} in the range (0.4 - 6) × 10^6 M^{-1} s^{-1}.

$$Fe(II) + H_2O_2 \xrightarrow{k_{Fe}} Int \xrightarrow{Fe(II),\ fast} 2\ Fe(III) \qquad (1)$$

$$-dFe(II)]/2\ dt = -d[H_2O_2]/dt = k_{Fe}[Fe(II)][H_2O_2] \qquad (2)$$

Table 3. Effect of pH on the Kinetics of Fenton Reaction[a]

pH	$k_{Fe}/M^{-1}\ s^{-1}$ [b]	Source
1-3	58	Ref. 40 and this work
6	650 ± 20	This work
6.2[c]	(1.7 ± 0.1) × 10^3	This work
7	(5.9 ± 0.2) × 10^3	This work

[a] 25.0 ± 0.1 ^{0}C. pH 6-7 maintained with non-coordinating buffers. [b] As defined in eq 2. [c] Phosphate buffer

The next set of kinetic runs was performed in the presence of $(CH_3)_2SO$ under catalytic conditions comparable to those in the top part of **Table 2.** The rate constant for the loss of Fe(II), i. e. the catalyst, in MES buffer decreased with increasing concentrations of $(CH_3)_2SO$, as shown in **Figure 3.** These kinetic data agree well with the increased stoichiometric ratios $\Delta[H_2O_2]/\Delta[Fe(II)]$ at higher $[(CH_3)_2SO]$ in **Table 2.** Iron(II) has the opposite effect as shown by

increased product yields when Fe(II) was added slowly with a syringe pump, and points to Fe(II) as the species involved in depletion of the active catalytic intermediate.

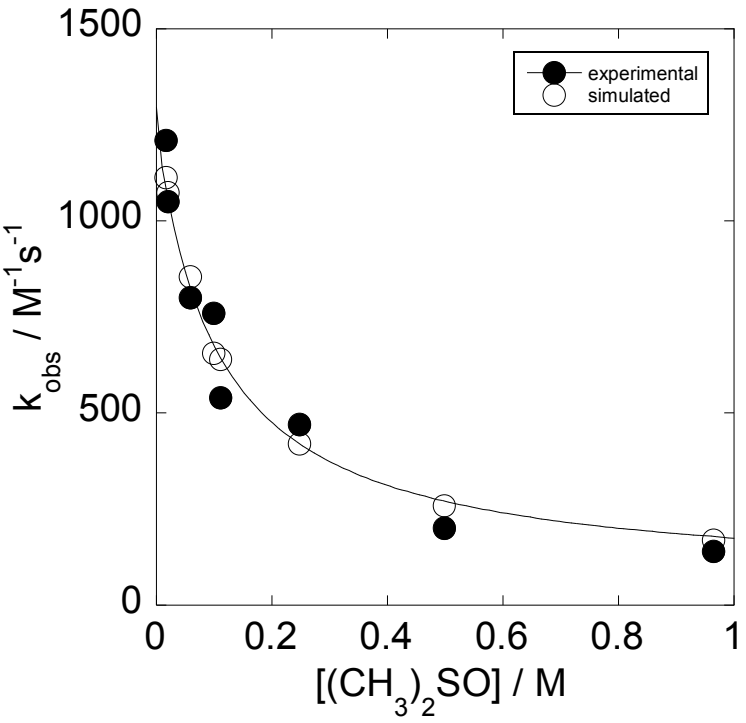

Figure 3. Plot of k_{obs} against $[(CH_3)_2SO]$ (filled circles), and fit to eq 8 for the reaction of 0.020 mM Fe(II) with excess H_2O_2, pH 6 (MES). Open circles show Kinsim-simulated data.

At pH 1, where the reaction involves •OH radicals and is not catalytic, the rate constant for the $Fe(H_2O)_6^{2+}/H_2O_2$ reaction, 58 M^{-1} s^{-1}, remains independent of $[(CH_3)_2SO]$. Similarly, the concentration of $(CH_3)_2SO$ plays a negligible role in phosphate buffer at pH 6 ($k = 1.5 \times 10^3$ M^{-1} s^{-1} in the absence of $(CH_3)_2SO$, Figures S12-S13, and 1.2×10^3 M^{-1} s^{-1} in 1 M $(CH_3)_2SO$) where the reaction is non-catalytic and appears to involve •OH radicals. The nature of the Fe(II) reactant in phosphate buffers is not known, but at the low concentrations of both Fe(II) (0.02 mM) and the buffer (<1 mM) the solutions appeared clear to the eye and exhibited no UV absorption that would indicate the presence of colloids. The reaction yielded smooth,

exponential kinetic traces leading us to conclude that the reacting species is a single iron(II) phosphate complex. Similar observations were reported earlier for the growth of ESR signal of trapped hydroxyl radicals in the Fenton reaction at pH 7.4 in 20 mM phosphate buffer, where k = 2×10^4 M^{-1} s^{-1}.[44]

The results presented above confirm that the dependence on $[(CH_3)_2SO]$ is an inherent feature of the catalytic reaction, and show that the rate effects in Figure 3 are not caused by the formation of less reactive sulfoxide complexes of Fe(II). Obviously, such complexes either do not form or do not significantly affect the reactivity of Fe(II) toward H_2O_2.

All of the data at pH ≤ 7 are fully explained by the mechanism in eq 3-9.

$$Fe(H_2O)_6^{2+} \rightleftharpoons (H_2O)_5Fe^{II}OH^+ + H^+ \qquad pK_a = 9.5^{41} \qquad (3)$$

$$Fe(H_2O)_6^{2+} + H_2O_2 \xrightarrow{-H_2O} (H_2O)_5Fe(H_2O_2)^{2+} \rightarrow (H_2O)_5Fe^{III}OH^{2+} + HO^{\bullet} \qquad (4)$$

$$HO^{\bullet} + (CH_3)_2SO \rightarrow CH_3SO_2H + 0.5\ C_2H_6 \text{ (via } CH_3^{\bullet}) \qquad (5)$$

$$HO^{\bullet} + Fe(H_2O)_6^{2+} \xrightarrow{-H_2O} (H_2O)_5Fe^{III}OH^{2+} \qquad (6)$$

$$(H_2O)_5Fe^{II}OH^+ + H_2O_2 \xrightarrow{-H_2O} (H_2O)_4Fe(OH)(H_2O_2)^+ \rightarrow (HO)Fe^{IV}O^n + H_2O \qquad (7)$$

$$Fe^{IV}O^n + (CH_3)_2SO \longrightarrow Fe(II) + (CH_3)_2SO_2 \qquad (8)$$

$$Fe^{IV}O^n + Fe(II) \longrightarrow 2Fe(III) \qquad (9)$$

Steps 3-6 describe the known reaction between $Fe(H_2O)_6^{2+}$ and H_2O_2 that involves $^{\bullet}OH$[19] and that continues to contribute at pH 6-7 where both reactants still exist predominantly in their acidic forms. In addition, the small fraction of iron(II) is present as $(H_2O)_5FeOH^+$ that reacts in a

new pathway in eq 7-8. Critical for the observed mechanistic change is the greatly increased rate of Fe(II)/H_2O_2 reaction at higher pH such that even at pH 6, >90% of the reaction proceeds through the inverse [H^+] path even though <0.1% of Fe(II) is present as $(H_2O)_5FeOH^+$. The value of k_7 used in calculations was obtained by subtracting k_4 (58 $M^{-1}s^{-1}$) from the measured value of k_{Fe}.

Based on eq 3-9, the kinetics of disappearance of Fe(II) can be approximated as a sum of two kinetic processes associated with pathways in eq 4-6 and 7-9, which leads to the rate law in eq 10. The fit in **Figure 3** was obtained by fixing k_4 (58 $M^{-1}s^{-1}$), k_5 (7×10^9),[15] k_6 (3.2×10^8)[15] and k_7 (592, see above) at their independently known values to obtain the ratio $k_8/k_9 = 9\ (\pm 2) \times 10^{-5}$ at pH 6. This ratio is one of the factors that determine the efficiency of the catalytic reaction. At higher substrate concentration, reaction 8 is favored over reaction 9, thereby slowing the loss of Fe(II) in reaction 9 and increasing the number of catalytic turnovers.

$$k_{obs} = k_4 \left(1 + \frac{k_6[Fe(II)]_{av}}{k_5[(CH_3)_2SO] + k_6[Fe(II)]_{av}}\right) + 2k_7 \frac{k_9[Fe(II)]_{av}}{k_8[(CH_3)_2SO] + k_9[Fe(II)]_{av}} \qquad (10)$$

Clearly, the derived value of the ratio k_8/k_9 is only an approximation because eq 10 treats Fe(II) as a constant, i. e. $[Fe(II)]_{av} = 0.5\ [Fe(II)]_0$, even though the actual concentration changes from (typically) 2×10^{-5} M to zero. This simplified treatment is justified by the growing importance of reaction 4 as [Fe(II)] decreases and reaction 9 slows down which makes the kinetic traces appear as single exponentials despite the more complicated dependence on Fe(II) in eq 10. The traces were simulated with Kinsim[45] on the basis of the mechanism in eq 3-9. The fits to exponential equation were excellent up to 5 half-lives and required $k_8/k_9 = 1.7 \times 10^{-4}$ to match the fitted data (open circles in Figure 3) with the experimental curve. The agreement

between the experimentally estimated and Kinsim-derived value of k_8/k_9 to within a factor of two is good, although the simulated value is probably more accurate because no approximations were used to obtain it.

Discussion

The change from pH ≤3 to pH≥6 has the following effect on the Fenton reaction: (1) At the higher pH the kinetics exhibit inverse acid-dependence and become much faster than those in the pH-independent regime in acidic solutions. (2) The products of sulfoxide oxidation change from those derived from hydroxyl radicals at acidic pH to sulfones at pH ≥6. (3) The reaction at higher pH becomes catalytic in Fe(II). (4) Catalysis is more efficient at high substrate and low Fe(II) concentrations.

All of these findings lead to the conclusion that the mechanism of peroxo O-O bond cleavage, as outlined in Scheme 2, changes from homolytic to heterolytic at higher pH. As a result of this mechanistic change, hydroxyl radicals are replaced by Fe(IV) as the Fenton intermediate, which is the key to the onset of catalysis at higher pH. Similar proposals have been made earlier,[22,30-32,34,35] but no evidence for Fe(IV) has been obtained until now.

The switch from homolytic to heterolytic O-O bond cleavage is believed to be related to the changed thermodynamics of Fe(II)/Fe(III)/Fe(IV) chemistry. Also, the removal of a proton from coordinated water and replacing $(H_2O)_5Fe(H_2O_2)^{2+}$ (eq 4) with $(H_2O)_4Fe(OH)(H_2O_2)^{+}$ (eq 7) may play a critical kinetic role and activate the push-pull mechanism[38] for the formation of an iron-oxo species, similar to the known heterolytic cleavage of metal hydroperoxo sites in enzymes,[46,47] model complexes,[48] and inorganic hydroperoxides[25] such as $(H_2O)_5CrOOH^{2+}$.[49]

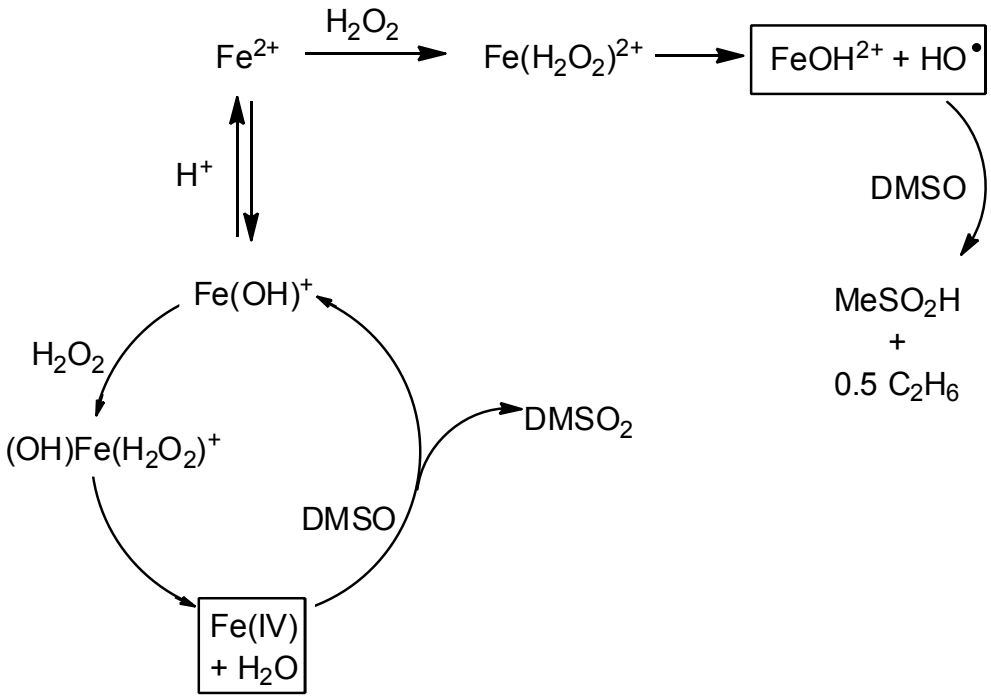

Scheme 2.

As we discussed earlier,[38] the hydroperoxo-to-metal oxo conversion can be accomplished by formal proton transfer from coordinated H_2O to -OOH, i. e. $(H_2O)M(OOH) \rightarrow (OH)M(OOH_2)$ (M = metal) in concert with two-electron intramolecular oxidation of the metal. In this picture, proton transfer is essential as it generates the hydroxo ligand to stabilize the emerging high oxidation state of the metal. Simultaneous protonation of the hydroperoxide facilitates the O-O bond cleavage and departure of a molecule of water.

All of the necessary elements for this mechanism[38] are available to $(H_2O)_4Fe(OH)(H_2O_2)^+$, which can be converted to Fe(IV) either directly as in eq 11, or via the isomeric hydroperoxide $(H_2O)_5FeOOH^+$. The ion $(H_2O)_5Fe(H_2O_2)^{2+}$, on the other hand, lacks the essential basic site.

$$(H_2O)_4Fe(OH)(H_2O_2)^+ \rightleftharpoons (H_2O)_4(HO)FeO^+ + H_2O \qquad (11)$$

Absolute values of k_8 and k_9 for the competing reactions of Fe(IV) cannot be obtained from experimental data, but the ratio, ~ 10^{-4}, is much smaller than that calculated for $(H_2O)_5FeO^{2+}$ in acidic solutions, i. e. 2.9.[50] Clearly, oxygen atom transfer is much less competitive at high pH, as one might expect for a strongly hydrolyzed oxidant. The low reactivity of Fe(IV) toward sulfoxides relative to the competing decay process(es) is responsible for low product yields, such as those in Figure 1. This finding may also explain the decrease in yields of oxidized products with increasing pH in related reactions involving iron and oxygen or hydrogen peroxide.[22,30-32,34-36] The competing reduction of Fe(IV) by Fe(II) in eq 9, on the other hand, remains fast owing to the increased reducing power of Fe(II) at higher pH. In contrast to these observations, the kinetics of oxidation of a nonheme Fe(II) complex with H_2O_2 to yield a persistent Fe(IV) oxo species are slower at higher pH but the yields of Fe(IV) are greater.[51]

The effect of phosphate is believed to reside in its affinity for Fe(II) and Fe(III). The nature of the Fe(II) reactant in phosphate buffers is not known, but our observations suggest that it is a single iron(II) phosphate complex. The change from $Fe^{II}(H_2O)_5OH^+$ to $Fe^{II}(H_2O)n(P)m$ (where P = $H_2PO_4^-$, HPO_4^{2-} or PO_4^{3-}) apparently shifts the energetics of electron transfer back to one-electron path by stabilizing the trivalent product over Fe(IV). Direct evidence for OH radicals were obtained by ESR in 20 mM phosphate buffer.[44]

Conclusion

The Fenton intermediate at near-neutral pH has now been identified as an Fe(IV) species that has the ability to oxidize $(CH_3)_2SO$ to $(CH_3)_2SO_2$. The species at pH 6-7 is shorter-lived and appears to be substantially less reactive as oxidant than is the previously characterized $(H_2O)_5FeO^{2+}$ at pH≤1.[20,52]

Acknowledgment

This manuscript has been authored under Contract No. DE-AC02-07CH11358 with the U.S. Department of Energy.

Supplemental Information

Figures S1-S13 and additional experimental detail are shown in Appendix A.

References

1. H. J. H. Fenton, *J. Chem. Soc.*, 1894, **65**, 899-910.

2. M. J. Burkitt, *Prog. React. Kinet. Mech.*, 2003, **28**, 75-103.

3. J. M. C. Gutteridge, T. Westermarck and B. Halliwell, *Mod. Aging Res.*, 1986, **8**, 99-139.

4. B. Halliwell and J. M. C. Gutteridge, *FEBS Lett.*, 1992, **307**, 108-112.

5. J. Prousek, *Pure Appl. Chem.*, 2007, **79**, 2325-2338.

6. J. J. Pignatello, E. Oliveros and A. MacKay, *Crit. Rev. Environ. Sci. Technol.*, 2006, **36**, 1-84.

7. Y. Zuo and J. Hoigne, *Science*, 1993, **260**, 71-73.

8.C. Sun, C. Chen, W. Ma and J. Zhao, *Phys. Chem. Chem. Phys.*, 2011, **13**, 1957-1969.

9. W. G. Barb, J. H. Baxendale, P. George and K. R. Hargrave, *Trans. Faraday Soc.*, 1951, **47**, 462-500.

10. W. C. Bray and M. H. Gorin, *J. Am. Chem. Soc.*, 1932, **54**, 2124-2125.

11. F. Haber and J. Weiss, *Proc. Royal Soc. London*, 1934, **147**, 332-351.

12. W. H. Koppenol, *Free Radical Biol. Med.*, 1993, **15**, 645-651.

13. C. Walling, *Acc. Chem. Res.*, 1975, **8**, 125-131.

14. C. Walling, *Acc. Chem. Res.*, 1998, **31**, 155-157.

15. G. V. Buxton, C. L. Greenstock, W. P. Helman and A. B. Ross, *J. Phys. Chem. Ref. Data*, 1988, **17**, 513-886.

16. B. C. Gilbert, R. O. C. Norman and R. C. Sealy, *J. Chem. Soc, Perkin II*, 1975, 303-308.

17. T. J. Conocchioli, E. J. Hamilton, Jr. and N. Sutin, *J. Am. Chem. Soc.*, 1965, **87**, 926-927.

18. T. Logager, J. Holcman, K. Sehested and T. Pedersen, *Inorg. Chem.*, 1992, **31**, 3523-3529.

19. O. Pestovsky, S. Stoian, E. L. Bominaar, X. Shan, E. Münck, L. J. Que and A. Bakac, *Angew. Chem., Int. Ed.*, 2005, **44**, 6871-6874.

20. O. Pestovsky and A. Bakac *J. Am. Chem. Soc.*, 2004, **126**, 13757-13764.

21. M. K. Eberhardt and R. Colina, *J. Org. Chem.*, 1988, **53**.

22. S. J. Hug and O. Leupin, *Environ. Sci. Technol.*, 2003, **37**, 2734-2742.

23. J. A. Imlay, S. M. Chin and S. Linn, *Science*, 1988, **240**, 640-642.

24. M. A. Sharpe, S. J. Robb and J. B. Clark, *J. Neurochem.*, 2003, **87**, 386-394.

25. J. T. Groves, *J. Inorg. Biochem.*, 2006, **100**, 434-447.

26. D. A. Wink, R. W. Nims, J. E. Saavedra, W. E. Utermahlen, Jr and P. C. Ford, *Proc. Natl. Acad. Sci. U.S.A.*, 1994, **91**, 6604-6608.

27. F. Buda, B. Ensing, M. C. M. Gribnau and E. J. Baerends, *Chem. Eur. J.*, 2001, **7**, 2775-2783.

28. B. Ensing, F. Buda, P. Blochl and E. J. Baerends, *Angew. Chem. Int. Ed.*, 2001, **40**, 2893.

29. B. Ensing, F. Buda, P. Blochl and E. J. Baerends, *Phys. Chem. Chem. Phys.*, 2002, **4**, 3619-3627.

30. I. A. Katsoyiannis, T. Ruettimann and S. J. Hug, *Environ. Sci. Technol.*, 2008, **42**, 7424-7430.

31. I. A. Katsoyiannis, T. Ruettimann and S. J. Hug, *Environ. Sci. Technol.*, 2009, **43**, 234.

32. C. R. Keenan and D. L. Sedlak, *Environ. Sci. Technol.*, 2008, **42**, 1262-1267.

33. C. Lee, C. R. Keenan and D. L. Sedlak, *Environ. Sci. Technol.*, 2008, **42**, 4921-4926.

34. J. I. Nieto-Juarez, K. Pierzchla, A. Sienkiewicz and T. Kohn, *Environ. Sci. Technol.*, 2010, **44**, 3351-3356.

35. C. R. Keenan, R. Goth-Goldstein, D. Lucas and D. L. Sedlak, *Environ. Sci. Technol.*, 2009, **43**, 4555-4560.

36. S.-Y. Pang, J. Jiang and J. Ma, *Environ. Sci. Technol.*, 2011, **45**, 307-312.

37. S.-Y. Pang, J. Jiang, J. Ma and F. Ouyang, *Environ. Sci. Technol.*, 2009, **43**, 3978-3979.

38. O. Pestovsky and A. Bakac, *Dalton Trans.*, 2005, 556-560.

39. A. Kandegedara and D. B. Rorabacher, *Anal Chem*, 1999, **71**, 3140-3144.

40. W.-D. Wang, A. Bakac and J. H. Espenson, *Inorg. Chem.*, 1993, **32**, 2005-2009.

41. D. T. Richens, *The Chemistry of Aqua Ions*, Wiley, Chichester, 1997.

42. F. J. Millero and S. Sotolongo, *Geochim. Cosmochim. Acta*, 1989, **53**, 1867-1873.

43. D. L. Sedlak and J. Hoigne, *Environ. Sci. Technol.*, 1994, **28**, 1898-1906.

44. I. Yamazaki and L. H. Piette, *J.Biol. Chem.*, 1990, **265**, 13589-13594.

45. B. A. Barshop, R. F. Wrenn and C. Frieden, *Anal. Biochem.*, 1983, **130**, 134 -145.

46. P. R. Ortiz De Montellano and J. J. De Voss, *Nat. Prod. Rep.*, 2002, **19**, 477-493.

47. J.-L. Primus, S. Grunenwald, P.-L. Hagedoorn, A.-M. Albrecht-Gary, D. Mandon and C. Veeger, *J. Am. Chem. Soc.*, 2002, **124**, 1214-1221.

48. N. Jin, D. E. Lahaye and J. T. Groves, *Inorg. Chem.*, 2010, **49**, 11516-11524.

49. J. M. Carraher and A. Bakac, *Chem. Res. Toxicol.*, 2010, **23**, 1735-1742.

50. O. Pestovsky and A. Bakac, *Inorg. Chem.*, 2006, **45**, 814-820.

51. J. Bautz, M. R. Bukowski, M.Kerscher, A. Stubna, P. Comba, A. Lienke, E. Munck and L. Que, Jr. Angew. Chem. Int. Ed. 2006, **45**, 5681-5684.

52. F. Jacobsen, J. Holcman and K. Sehested, *Int. J. Chem. Kin.*, 1998, **30**, 215-221.

CHAPTER 3

Fe(II) CATALYSIS IN OXIDATION OF HYDROCARBONS WITH OZONE IN ACETONITRILE

Will be submitted to *ACS catalysis* journal

Abstract

Oxidation of alcohols, ethers, and sulfoxides by ozone in acetonitrile is catalyzed by sub-millimolar concentrations of $Fe(CH_3CN)_6^{2+}$. The catalyst provides both rate acceleration and greater selectivity toward the less oxidized product. For example, $Fe(CH_3CN)_6^{2+}$-catalyzed oxidation of benzyl alcohol yields benzaldehyde almost exclusively (>95%) whereas the uncatalyzed reaction generates a 1:1 mixture of benzaldehyde and benzoic acid. Similarly, aliphatic alcohols are oxidized to aldehydes/ketones, cyclobutanol to cyclobutanone, and diethyl ether to a 1:1 mixture of ethanol and acetaldehyde. The kinetics of oxidation of alcohols and diethyl ether are first order in $Fe(CH_3CN)_6^{2+}$ and ozone, and independent of [Substrate] at concentrations greater than ~5 mM. In this regime, the rate constant for all of the alcohols is approximately the same, $k_{cat} = (8\pm1) \times 10^4\ M^{-1}\ s^{-1}$, and that for $(C_2H_5)_2O$ is $(5\pm0.5) \times 10^4\ M^{-1}\ s^{-1}$. In the absence of substrate, $Fe(CH_3CN)_6^{2+}$ reacts with O_3 with $k_5 = (9.3\pm0.3) \times 10^4\ M^{-1}\ s^{-1}$. The similarity between the rate constants k_5 and k_{cat} strongly argues for $Fe(CH_3CN)_6^{2+}/O_3$ reaction as rate determining in catalytic oxidation. The active oxidant produced in $Fe(CH_3CN)_6^{2+}/O_3$ reaction is suggested to be an Fe(IV) species in analogy with a related intermediate in aqueous solutions. This assignment is supported by the similarity in kinetic isotope effects and relative reactivities of the two species toward substrates.

Introduction

Previous studies from this group[1,2] and others[3,4] have established that the reaction of $Fe(H_2O)_6^{2+}$ with ozone generates an iron(IV) species best described as $Fe^{IV}(H_2O)_5O^{2+}$ (hereafter $Fe_{aq}O^{2+}$) on the basis of spectroscopic evidence, chemical reactivity and DFT calculations.[1,2,5] Oxidations with $Fe_{aq}O^{2+}$ take place by oxygen atom transfer to e. g. sulfoxides and phosphines, and by hydride and hydrogen atom abstraction from C-H bonds.[1] In reactions with alcohols, aldehydes and ethers the latter two mechanisms operate in parallel, Scheme 1. The hydride path is catalytic as it generates $Fe(H_2O)_6^{2+}$ which can be reoxidized to $Fe_{aq}O^{2+}$. Overall, however, the catalytic efficiency is poor because of the loss of iron as $Fe(H_2O)_6^{3+}$ in the parallel one-electron (hydrogen atom transfer) path.

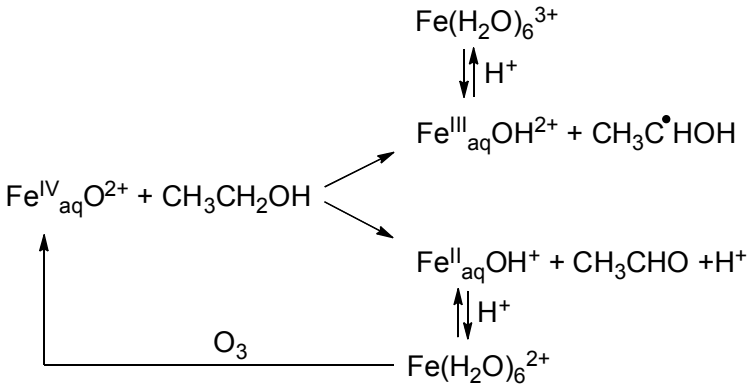

Scheme 1

In the reaction between $Fe(H_2O)_6^{2+}$ and H_2O_2 (Fenton reaction) the reactive intermediate changes from hydroxyl radicals in acidic solutions to an iron(IV) species at near neutral pH.[6] Such a major mechanistic change caused by a modest change in reaction conditions led us to consider the effect of other parameters, including solvent, on reactions involving solvento iron species in oxidation states 2+ to 4+. Specifically, the much higher reduction potential of the Fe(III)/Fe(II) couple in acetonitrile[7,8] as compared to that in water suggests that the preference

for two-electron pathways of a hypothetical iron(IV) species might be greater in acetonitrile. To explore this possibility and its potential consequences for iron-catalyzed oxidations, we initiated a study of the reaction of $Fe(CH_3CN)_6^{2+}$ with O_3 in acetonitrile in the presence of oxidizable substrates.[9] The results are described herein.

Experimental

The following chemicals were obtained commercially and used as received: iron(II) perchlorate hydrate $Fe(ClO_4)_2.xH_2O$ (98%), deuterium oxide D_2O (99.9 atom %D), 1,10-phenanthroline (99+ %), benzyl alcohol anhydrous (99.8%), cyclobutanol (99+%) (all Aldrich), dimethyl sulfoxide (≥ 99.9%, A.C.S spectrophotometric grade) and cyclopentanol (99%) (both Sigma-Aldrich), 2-propanol (99.9% certified ACS), tetrahydrofuran (99.9% HPLC grade), and ethyl ether anhydrous (99.9% certified ACS) (all Fisher scientific), acetonitrile-d3 (99.8 atom % D) (Cambridge Isotope Laboratories, Inc), acetonitrile (low water content (~10 ppm) for HPLC, GC and spectrophotometry, Honeywell - Burdick & Jackson), 2-propanol-2-d1 (99.8 atom % D) and 2-propanol-d8 (99.9 atom % D) (both CDN Isotopes), benzyl-α,α-d2 alcohol (98 atom % D, ISOTEC). Iron(II) bis(acetonitrile)bis(triflate) $Fe(OTf)_2(CH_3CN)_2$ was synthesized according to a literature procedure.[10]

In experiments designed to explore the effect of water on products and kinetics, anhydrous iron(II) triflate was used instead of hydrated iron(II) perchlorate. Deuterated acetonitrile was dried over 4A molecular sieves until the HDO/H_2O signal disappeared in the ^1H NMR spectrum.

UV-Vis absorbance measurements and kinetic studies used a Shimadzu UV-3101 PC spectrophotometer and Olis RSM-1000 stopped-flow at 24.9 ± 0.1 °C. ^1H NMR spectra were recorded with a 400 MHz Bruker DRX-400 or 600 MHz Bruker Avance III spectrometer at room temperature. Waters GCT accurate mass time-of-flight mass spectrometer in positive EI mode

(70 EV) with a scan rate of 0.3 seconds per scan and a mass range of 10–200 Daltons was used to qualitatively detect some of the products. Waters MassLynx 4.0 software was used to acquire and process GC-MS data. Ozone was generated in an Ozonology L-100 ozone generator. Oxygen concentration was measured using Hanna Edge dissolved oxygen meter.

Procedures

Stock solutions of iron(II) perchlorate in CH_3CN or CD_3CN were prepared fresh before each set of experiments and standardized with phenanthroline after dilution with H_2O and using $\varepsilon = 1.14 \times 10^4\ M^{-1}\ cm^{-1}$ for $Fe(phen)_3^{2+}$ at 510 nm. A correction was applied for the absorbance of iron(III)-phenanthroline as previously described.[1] Ozone solutions were prepared by continuous bubbling of ozone through CH_3CN or CD_3CN for >5 min at room temperature and diluted to the desired concentration. The concentration of ozone in stock solutions was typically 5.6±0.1 mM as determined spectrophotometrically at 260 nm, $\varepsilon_{260} = 3350\ M^{-1}\ cm^{-1}$. These solutions always contained residual oxygen, typically about 5.9 mM, as described below.

To determine the amount of oxygen generated in the $Fe(CH_3CN)_6^{2+}/O_3$ reaction in the presence and absence of substrates, the reactants were mixed rapidly in an air-free, tightly sealed vial, leaving only minimal head space to avoid equilibration between the solution and gas phases. A sample (0.5-1.0 mL) was withdrawn and injected into another sealed vial containing a dissolved oxygen electrode immersed in 18 mL of air-free water. The measurement was completed in about 40 seconds after injection. The measured value was corrected for the concentration of residual oxygen, typically around 5.9 mM in ozone stock solutions as determined after removal of O_3 with excess fumaric or maleic acid.[11] The same procedure was used to determine the concentration of O_2 in O_2- saturated acetonitrile. The value obtained, 11.3 mM, is in acceptable agreement with the value reported for air-saturated acetonitrile, 2.42 mM.[12]

Except in experiments specifically designed to explore the effect of O_2 on kinetics and products, solutions of iron(II) and substrates were prepared and handled anaerobically. However, since some O_2 was present in stock solutions of ozone, see above, and since the $Fe(CH_3CN)_6^{2+}$ /O_3 reaction itself produces O_2, none of the reaction solutions were completely O_2-free.

Competition experiments

A solution containing known concentrations of Fe(II) and two or three substrates were mixed with ozone in a UV cell. After the disappearance of ozone at 260 nm, the products were quantified by ^{1}H NMR. In all of the experiments the substrate concentrations were sufficiently large to make the kinetics of each individual reaction fall into the plateau region of Figure 4. Product yields for benzyl alcohol, which absorbs too strongly in the UV for direct kinetic measurements, were shown independently to remain unchanged at $[PhCH_2OH]_0 \geq 4$ mM. Similar experiments were conducted on mixtures of protiated and fully or partially deuterated substrates to determine kinetic isotope effects. Product yields derived from fully deuterated substrates (diethyl ether-d10 and 2-propanol-d8) were estimated as a difference between the total amount of products for the same competition observed with protiated compounds and the amount of product derived from the competing protiated substrate.

Kinetic data were obtained by monitoring the disappearance of ozone at 260 nm (Shimadzu) or in the 260-280 nm spectral range (Olis RSM-1000 Rapid Scan). In stopped flow experiments, a mixture of $Fe(CH_3CN)_6^{2+}$ and substrate was placed in one syringe, and ozone solution in the other. Experiments designed to study the effect of [substrate] used 0.06-0.15 mM ozone, 0.025 mM $Fe(CH_3CN)_6^{2+}$ and 1-50 mM substrate. The effect of $[Fe(CH_3CN)_6^{2+}]$ was explored at 0.08-0.12 mM ozone, 0.005-0.1 mM $Fe(CH_3CN)_6^{2+}$ and 2-50 mM substrate.

Kinetic traces were fitted to an expression for first order kinetics with Kaleidagraph v4.0 or with OLIS Global-Works v2.0.190. ^{1}H NMR and GC-MS analyses were initiated within 5-15 min after the completion of the reaction. 10% D_2O (v/v) was added to some NMR solutions to shift the interfering water peak.

Results

The UV spectrum after completion of the reaction between 1.1 mM benzyl alcohol and 0.22 mM ozone in acetonitrile exhibits a double feature in the 230-250 nm range, Figure 1, consistent with a mixture of benzaldehyde (λ_{max} 244 nm) and benzoic acid (λ_{max} 227 nm). The individual spectra are shown in Fig S1. This assignment was confirmed by ^{1}H NMR, Figure S2. The reaction with ozone also produced hydrogen peroxide, as shown by ^{1}H NMR signal at 8.56 ppm.

When the same reaction was conducted in the presence of 0.011 mM $Fe(CH_3CN)_6^{2+}$, benzaldehyde was the major product detected by UV (Fig 1), ^{1}H NMR (Fig 2), and GC-MS. Small amounts of benzoic acid (~10%) were also observed, some of it possibly generated by oxidation of benzaldehyde with O_2 during sample manipulation. The combined yield of PhCHO and PhCOOH, based on the initial ozone concentration, was 85%.

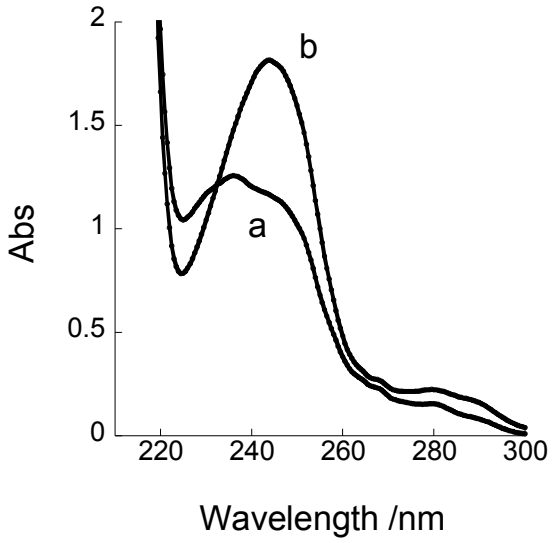

Figure 1. UV spectra of the products of the reaction between (a) 1.1 mM $PhCH_2OH$ and 0.22 mM O_3, and (b) 1.1 mM $PhCH_2OH$ and 0.3 mM O_3/0.011 mM $Fe(CH_3CN)_6^{2+}$.

$Fe(CH_3CN)_6^{2+}$-catalyzed oxidation of cyclobutanol by O_3 (1.8 mM) produced 1.55 mM cyclobutanone, Figure S3. No ring-opened products were observed by either ^1H NMR or GC-MS, ruling out a significant contribution from a path involving cyclobutanol radicals.[1] The latter are subject to rapid ring opening that ultimately yields an aldehyde(s). At the end of the reaction, about 80% of iron was still present as Fe(II).

Similarly, ethanol was oxidized to acetaldehyde, Figure S4, 2-propanol to acetone, and cyclopentanol to cyclopentanone. The results are summarized in Table 1. Product yields varied from 70% (acetaldehyde) to 85% (cyclopentanone). ^1H NMR of the products of ethanol oxidation exhibits additional signals at 8.03 and 4.64 ppm, consistent with small amounts of formic acid and acetal which are common overoxidation products of ethanol.[13] The yields of these products increase somewhat with increasing $[O_3]/[EtOH]$ ratio.

Table 1. Product Yields in $Fe(CH_3CN)_6^{2+}$-Catalyzed Oxidation of Alcohols, DMSO and Et_2O by Ozone

Substrate (mM)	$[O_3]$/mM	$[Fe(CH_3CN)_6^{2+}]$/mM	Major Product	% Yield
dimethyl sulfoxide (9.6)	1.9	0.028	dimethyl sulfone	100
diethyl ether (8.5)	1.2	0.052	(ethanol + acetaldehyde)	100
cyclopentanol (9.8)	1.4	0.024	cyclopentanone	85
cyclobutanol (9.6)	1.8	0.025	cyclobutanone	85
2-propanol (32)	0.1	0.025	acetone	80
ethanol (21.1)	0.83	0.055	acetaldehyde	70
benzyl alcohol (10)	1.8	0.048	benzaldehyde	70

The reaction with diethyl ether produced a 1:1 mixture of C_2H_5OH and CH_3CHO in 100% yield, Figure S5. Dimethyl sulfoxide (DMSO) was oxidized to the sulfone, also in 100% yield, Figure S6. At an initial $Fe(CH_3CN)_6^{2+}$ concentration of >0.020 mM, the majority (70-90%) of iron was still present as Fe(II) at the end of the reactions listed in Table 1 provided the concentration of substrate exceeded ~5 mM. At much lower initial concentrations of $Fe(CH_3CN)_6^{2+}$ and substrate, up to 40-60 % of $Fe(CH_3CN)_6^{2+}$ was oxidized to Fe(III).

$Fe(CH_3CN)_6^{2+}$-catalyzed oxidation of THF by O_3 yielded several products as shown by GC-MS and ^{1}H NMR, Figures 2 and S7. On the basis of mass spectra, the GC peak at 4.42 min is assigned to an equilibrated mixture[14] of 2-hydroxytetrahydrofuran (2-OH-THF) and 4-hydroxybutanal, and that at 6.18 min to γ-butyrolactone. All three species were clearly identified and quantified by ^{1}H NMR, Figure S7. The combined yield is 75% (in 4:2:1 ratio, respectively). Also observed in the ^{1}H NMR are small amounts of formic acid, similar to previous studies of THF oxidation.[15] Several other small peaks were not identified. The products eluting at 9-10 min in Figure 2 are attributed to THF dimers and condensation products as deduced from mass

spectral data. These products are also formed upon electrochemical oxidation of THF in aqueous sulfuric acid.[15]

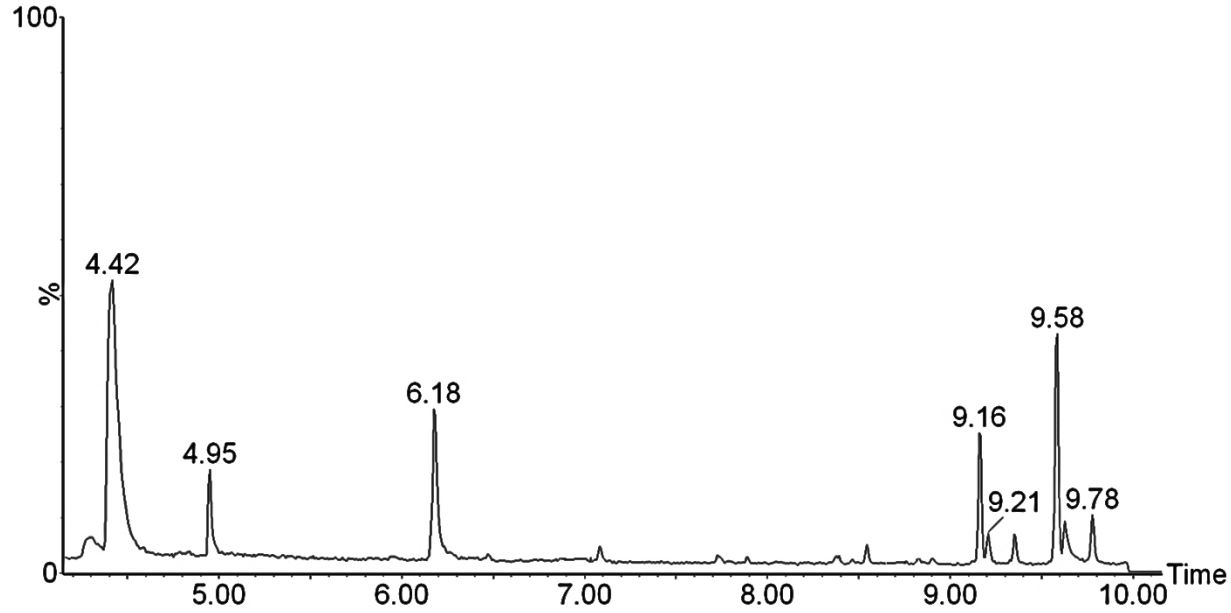

Figure 2. Gas chromatogram of products obtained by oxidation of 5.6 mM THF by 1.35 mM O_3/0.1 mM Fe(II).

The overall picture of THF oxidation changes dramatically when an alcohol is added as co-substrate. As shown on the example of THF/ benzyl alcohol mixture, Figures S8-S10, the products (>90%) are the acetal 2-OR-THF and aldehyde/ketone derived from the alcohol. THF oxidation products, i.e. hydroxytetrahydrofuran/4-hydroxybutanal and γ-butyrolactone accounted for only 5% of products.

In search of the source of 2-OR-THF we considered the known reaction[16] between alcohols and 4-hydroxybutanal, the latter being one of THF oxidation products. This reaction generates 2-OR-THF in the presence of an acid catalyst at 20-100° C,[16] but is extremely slow (about 17 hours) under our experimental conditions. Also, no new products were generated upon mixing alcohols with product solutions of $Fe(CH_3CN)_6^{2+}/O_3$/THF reaction. A slow overnight

reaction between alcohols and THF in the presence of $Fe(CH_3CN)_6^{2+}$ (0.5 mM) did produce 2-OR-THF when the concentrations of alcohols (60 mM) and THF (80 mM) were about ten-fold higher than is typical in our work. Clearly, the rapid (several seconds) formation of 2-OR-THF under our standard catalytic conditions utilizes a different path and must involve an intermediate(s) generated in the course of the $Fe(CH_3CN)_6^{2+}/O_3$ oxidation of THF and/or alcohol. Since close to 100% of iron was still present as Fe(II) at the end of the $Fe(CH_3CN)_6^{2+}$ $/O_3$/ THF/alcohol it is clear that the products were either formed in a series of 2-e steps or that Fe(III), if involved, was re-reduced to Fe(II) by reaction intermediate(s).

Kinetics

Substrates (5-50 mM) were used in large excess over ozone (0.06-0.15 mM) and $Fe(CH_3CN)_6^{2+}$. The loss of ozone was monitored at 260 nm. Kinetic traces in the plateau region, see below, were exponential and yielded pseudo-first-order rate constants k_{obs}.

Ozone oxidation of organic substrates used in this work is slow but not negligible in comparison with the $Fe(CH_3CN)_6^{2+}$-catalyzed reaction. The rate law for the disappearance of ozone is thus given by eq 1, where k_{cat} represents the rate constant for the catalytic reaction of eq 2, k_{O3} is the independently-determined rate constant for the direct O_3/substrate reaction, Table S1, and S is substrate. The contribution from the direct reaction to k_{obs} was typically <10%, but increased as substrate concentrations increased and Fe(II) concentrations decreased. In the least favorable case (50 mM 2-PrOH at 0.025 mM Fe(II)), this contribution was 20%. The use of higher concentrations of the catalyst, which would benefit the catalytic reaction, was not feasible because the reaction became too fast and signal-to-noise ratio poor.

$$-d[O_3]/dt = k_{O3}[O_3][S] + k_{cat}[O_3]\,[Fe(CH_3CN)_6^{2+}]^m\,[S]^n = k_{obs}\,[O_3] \qquad (1)$$

$$O_3 + S \xrightarrow{[Fe(II)} \text{Products} \qquad k_{cat} \qquad (2)$$

The experimentally determined k_{obs} was corrected for the direct path to give k_{corr}, eq 3.

$$k_{corr} = k_{obs} - k_{O3}[S] = k_{cat}\,[Fe(CH_3CN)_6^{2+}]^m\,[S]^n \qquad (3)$$

The reaction is first order in $[Fe(CH_3CN)_6^{2+}]$ (m = 1) as shown by linear dependence of k_{corr} on $[Fe(CH_3CN)_6^{2+}]$ at two different concentrations of 2-PrOH in Figure 3. First order dependence on $[Fe(CH_3CN)_6^{2+}]$ holds for all of the substrates examined.

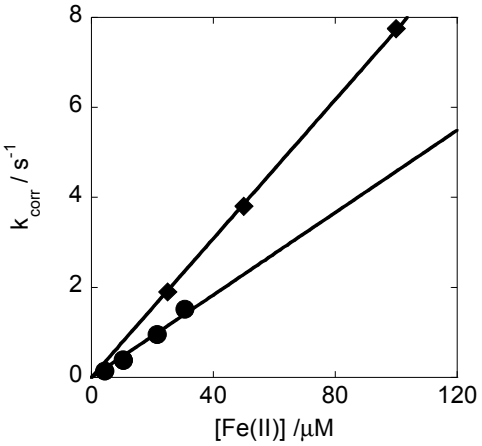

Figure 3. Plot of k_{corr} vs concentration of $Fe(CH_3CN)_6^{2+}$ for the catalytic oxidation of 2-PrOH with ozone (0.08-0.12 mM.). Concentrations of 2-PrOH are 2 mM (circles) and 50 mM (squares).

The dependence on [2-PrOH], on the other hand, is quite modest as shown by the small difference in slopes of the two lines in Figure 3, i. e. $3.6 \times 10^4\ M^{-1}s^{-1}$ and 7.7×10^4 at [2-PrOH] = 2 mM and 50 mM, respectively. This general picture holds for other substrates as well as shown in Table S2 and illustrated by the plot of k_{corr} *vs* [Substrate] in Figure **4**.

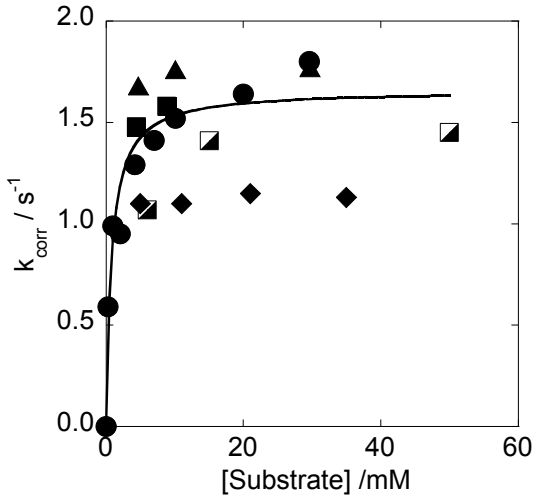

Figure 4. Plot of k_{corr} against substrate concentration for $Fe(CH_3CN)_6^{2+}$-catalyzed oxidations with ozone of 2-propanol (circles), ethanol (half-filled squares), THF (squares), cyclobutanol (triangles) and diethyl ether (diamonds). All experiments have $[Fe(CH_3CN)_6^{2+}]_0$ = 0.025 mM, $[O_3]$ = 0.06-0.15 mM.

After the sharp initial rise, the rate constants in Figure 4 reach an approximately constant value of 1.5 ± 0.2 s^{-1} for most substrates, and 1.1 s^{-1} for diethyl ether. The initial concentration of $Fe(CH_3CN)_6^{2+}$ in these experiments was approximately constant at 0.025 ± 0.002 mM. After the reaction, ~80% of $Fe(CH_3CN)_6^{2+}$ was recovered in the plateau region in Figure 4, but only about 50% in the rising portion at low substrate concentrations. Also, the fit to exponential kinetics at low [substrate] was poor, and only the initial 50% of reaction was used to evaluate the rate constants.

In the plateau region the reaction is clearly catalytic in $Fe(CH_3CN)_6^{2+}$ and the rate law is reasonably well approximated by eq 4 (i.e. *n* of eq 3 is zero), yielding $k_{cat} = k_{corr}/[Fe(CH_3CN)_6^{2+}]$ = (5±0.5) × 10^4 M^{-1} s^{-1} for Et_2O and (8±1) × 10^4 M^{-1} s^{-1} for the remaining substrates.

$$-d[O_3]/dt = d[Product]/dt = k_{cat}[Fe(CH_3CN)_6^{2+}][O_3] = k_{corr}\,[O_3] \qquad (4)$$

The kinetic behavior of DMSO is qualitatively similar to that of alcohols and ethers, but the rate constant is much larger, reaching a saturation value of 39 ± 1 s^{-1} at 0.025 mM Fe(II),

Figure 5. This result implies much greater reactivity of $Fe(DMSO)_n(CH_3CN)_{6-n}^{2+}$ complex(es)[17,18] compared to $Fe(CH_3CN)_6^{2+}$. The support for $Fe(DMSO)_n(CH_3CN)_{6-n}^{2+}$ in this work comes from the observation of broadened ^1H NMR methyl resonances of DMSO in CD_3CN in the presence of Fe(II), consistent with an exchange between free and complexed DMSO. As expected, the signal sharpens upon addition of D_2O (15%, v/v) which leads to dissociation of DMSO.

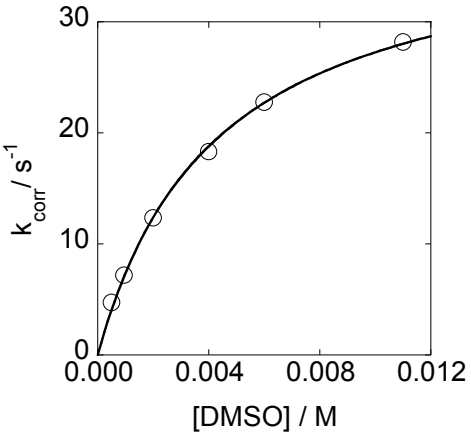

Figure 5. Plot of k_{obs} vs [DMSO] for the reaction with O_3 (0.1 mM) / $Fe(CH_3CN)_6^{2+}$ (0.025 mM).

Kinetic measurements for the $Fe(CH_3CN)_6^{2+}/O_3$ reaction in the absence of substrates and with $Fe(CH_3CN)_6^{2+}$ in large excess yielded $k_{obs} = 20\ s^{-1}$ at $[Fe(CH_3CN)_6^{2+}]_0 = 0.21$ mM, and $29\ s^{-1}$ at $[Fe(CH_3CN)_6^{2+}]_0 = 0.30$ mM, which results in $k_{Fe} = (9.3\pm0.3) \times 10^4\ M^{-1}\ s^{-1}$, eq 5. The similarity between the rate constants k_5 and k_{cat} strongly argues that they apply to the same reaction, i. e. formation of an intermediate, presumably $Fe^{IV}(CH_3CN)_5O^{2+}$ (hereafter $Fe^{IV}_{AN}O^{2+}$), see later, or a related species in analogy with $Fe^{IV}_{aq}O^{2+}$ that is produced in $Fe(H_2O)_6^{2+}/O_3$ reaction in acidic aqueous solutions. [1] In this scenario, $Fe^{IV}_{AN}O^{2+}$ rapidly oxidizes substrates as in eq 6, thereby regenerating $Fe(CH_3CN)_6^{2+}$ which re-enters eq 5.

$$Fe(CH_3CN)_6^{2+} + O_3 \rightarrow Fe^{IV}(CH_3CN)_5O^{2+} + O_2 + CH_3CN \qquad k_{Fe} \qquad (5)$$

$$Fe^{IV}(CH_3CN)_5O^{2+} + (C_2H_5)_2O \xrightarrow{CH_3CN,\ fast} Fe(CH_3CN)_6^{2+} + \{C_2H_5OH + CH_3CHO\} \quad (6)$$

Runs with excess ozone exhibited a rapid initial step followed by slower disappearance of large, nonstoichiometric amounts of ozone in a reaction apparently catalyzed by iron. The fast initial step took place on a time scale appropriate for k_{Fe} that was determined with excess $Fe(CH_3CN)_6^{2+}$, but a reliable rate constant could not be extracted under these conditions.

In several experiments the concentration of O_2 was determined at the end of reaction with use of a dissolved oxygen electrode as described in Experimental. Under standard catalytic conditions (0.050 mM $Fe(CH_3CN)_6^{2+}$, 0.8 mM O_3, 20 mM substrate), the reactions with DMSO and with $(C_2H_5)_2O$ generated 0.9 equivalents of O_2 per O_3, Table S3. This result, combined with quantitative product yields in Table 1, leads to the approximate stoichiometry in eq 7.

$$O_3 + (C_2H_5)_2O \text{ (or } Me_2SO) \xrightarrow{Fe(II)} \{CH_3CHO + C_2H_5OH\} \text{ (or } Me_2SO_2) + O_2 \qquad (7)$$

For the remaining substrates in Table 1, the net increase in O_2 content was lower, typically 0.6 equivalents per O_3, suggesting some O_2 consumption in parallel 1-e processes, see later. When no substrates were added, the increase in O_2 was only about 0.2 equivalents per mole of O_3 regardless of whether $Fe(CH_3CN)_6^{2+}$ was used in catalytic amounts or in concentrations comparable to those of O_3 (~ 0.8 mM). In both cases ozone was consumed completely, although at low iron concentrations the reaction took about 15 minutes, much longer than in the presence of added substrates. Given that O_3 persists in acetonitrile for hours in the absence of $Fe(CH_3CN)_6^{2+}$, it is clear that $Fe(CH_3CN)_6^{2+}$/acetonitrile combination leads to catalytic O_3 consumption. Clearly, acetonitrile is less reactive than the substrates in Table 1. Moreover, small amounts of $Fe(CH_3CN)_6^{2+}$ remained after completion of the reaction even when ozone was used in excess. In experiments with equimolar amounts of $Fe(CH_3CN)_6^{2+}$ and O_3, about 60% of

Fe(II) remained after completion of the reaction in CH_3CN, but only traces (<5%) in CD_3CN demonstrating a large solvent kie. Unfortunately, no oxidation products of CH_3CN could be detected by ^1H NMR or GC-MS owing to the interference by the large solvent peaks. No formaldehyde was detected with chromotropic acid.

Effect of Fe(III), O_2 and water

There is a mild increase in product yields under oxygen-rich conditions, as shown for ethanol in Table 2. At approximately constant concentrations of $Fe(CH_3CN)_6^{2+}$, O_3, and EtOH, an increase in oxygen concentration from 1 mM to 7 mM led to an increase in acetaldehyde yield from 82% to 94%, and an increase in the recovery of $Fe(CH_3CN)_6^{2+}$ from 91% to 98%. Oxygen also appears to have a mild inhibiting effect on the kinetics. The rate constant in the presence of excess O_2 (≥1.3 mM) is about 15% smaller than that obtained in the experiments that had only a small background concentration of O_2 (ca 0.2 mM, comparable to that of ozone).

Externally added $Fe(ClO_4)_3$ also improved product yields. As shown in the last entry in Table 2, the yields of acetaldehyde become quantitative in the presence of 0.24 mM Fe(III).

Up to 100 mM of added water has no effect on product yields or catalyst recovery as shown for ethanol and 2-propanol in Table 3, but the rate constant shows a small systematic increase with increasing $[H_2O]$. At larger concentrations of H_2O, product yields and catalyst recovery both decrease and the rate constant increases. All catalytic activity ceases when water content reaches 3% (~1.5 M). The presence of water in the coordination sphere of iron and in the solvent apparently changes the Fe(III)/Fe(II) potentials to an extent sufficient to restore the chemistry to that characteristic of aqueous solution.[1]

Table 2. Effect of Fe(III) and O_2 on Ethanol Oxidation[a]

$[O_2]$/ mM	$[Fe(III)]_0$ /mM	$\%[CH_3CHO]_\infty$[b]	% $[Fe(II)]_\infty$[c]
1		82	91
1[d]		82	93
7		94	98
1	0.052	85	105
1	0.24	100	130

[a] $[Fe(CH_3CN)_6^{2+}]_0$ = 0.047-0.060 mM, $[O_3]$ = 0.93-1.0 mM, $[C_2H_5OH]$ = 43-55 mM. [b] Percent yield of CH_3CHO. [c] Percent of Fe(II) recovered at the end of reaction. [d] Added $[H_2O]$ = 56 mM.

Table 3. Effect of H_2O on the Kinetics and Catalyst Recovery[a]

$[O_3]$/ mM	Substrate	Added $[H_2O]$/ mM	k_{corr}/s^{-1}	% $[Fe(II)]_\infty$[b]
0.054	2-propanol	0	1.7	96
0.064	2-propanol	50	2.0	92
0.056	2-propanol	99	2.6	96
0.050	2-propanol	198	3.0	80
0.072	ethanol	0	1.4	92
0.063	ethanol	149	2.3	76
0.060	ethanol	489	4.4	64

[a] Conditions: [Substrate] = 20 mM, $[Fe(CH_3CN)_6^{2+}]_0$ = 0.025 mM.

Competition Experiments.

To gain some insight into the reactivity of the catalytic intermediate, presumed to be $Fe^{IV}_{AN}O^{2+}$, competition experiments were performed with several substrates, see *Experimental.* The results (Figures S11-S16) are summarized in Table 4. The ratios of rate constants k_1/k_2 for

various substrates were calculated from the expression $k_1/k_2 = [P_1][S_2]/[P_2][S_1]$, where S_1 and S_2 are two competing substrates, and P_1 and P_2 their respective products. In the experiment with three competing substrates the listed ratios are $[P_1][S_2]/[P_2][S_1]$ and $[P_2][S_3]/[P_3][S_2]$, where S_3 and P_3 stand for $(CH_3)_2CHOH$ and $(CH_3)_2CO$, respectively,.

Table 4. Results of Competition Experiments[a]

O_3 /mM	Substrate (mM)	Product (mM)	k_1/k_2 [b]
0.66	benzyl alcohol (4.9) + ethanol (19)	benzaldehyde (0.27) + acetaldehyde (0.25)	4.2
0.73	benzyl alcohol (4.9) + cyclobutanol (10)	benzaldehyde (0.29) + cyclobutanone (0.31)	1.9
1.7	cyclobutanol (10) + ethanol (30)	cyclobutanone (0.62) + acetaldehyde (0.76)	2.4
0.86	cyclobutanol (10) + 2-propanol (11)	cyclobutanone (0.40) + acetone (0.34)	1.3
1.0	benzyl alcohol (4.7) + ethanol (10) + 2-propanol (9.6)	benzaldehyde (0.32) + acetaldehyde (0.18) + acetone (0.32)	3.8, 0.54[c]
1.1	benzyl alcohol (4.8) + diethyl ether (4.7)	benzaldehyde (0.49) + acetaldehyde / ethanol (0.37)	1.3

[a] $[Fe(CH_3CN)_6] = 0.05 – 0.06$ mM. [b] Ratio of rate constants for competing substrates S_1 and S_2 in the order listed in each set. [c] Ratio of rate constants for ethanol and 2-propanol.

All of the rate constants were normalized to $k_{EtOH} = 1.0$ in Table 5. Similar experiments with deuterated substrates (Figures S17-S21) yielded the results in Table 6 from which kinetic isotope effects in Table 7 were calculated.

Table 5. Relative Rate Constants for Oxidations with $Fe^{IV}_{AN}O^{2+}$

Substrate	Average k_{rel}	$k_{H2O}/M^{-1}s^{-1}$[a]
ethanol	[1.0]	2.51×10^3
2-propanol	2.0	3.22×10^3
cyclobutanol	2.2	3.13×10^3
diethyl ether	3.1	4.74×10^3
benzyl alcohol	4.0	14.2×10^3

[a] Directly measured rate constants for reactions of $Fe(H_2O)_5O^{2+}$ in 0.1 M aqueous $HClO_4$

Table 6. Products Obtained in Competition Between Protiated and Deuterated Substrates[a]

O_3 /mM	Substrate (mM)	Product (mM)
1.15	diethyl ether-d10 (5.6)	acetaldehyde / ethanol (0.20)[b]
	benzyl alcohol (4.8)	benzaldehyde (0.66)
1.1	ethanol (16.6)	acetaldehyde (0.53)
	benzyl alcohol-d2 (4.7)	benzaldehyde (0.18)
0.85	2-propanol-d1 (10.1)	acetone (0.19)
	benzyl alcohol (4.8)	benzaldehyde (0.46)
1.39	cyclobutanol (9.7)	cyclobutanone (0.81)
	benzyl alcohol-d2 (9.1)	benzaldehyde (0.34)
1	2-propanol-d8 (10.3)	acetone (0.22)[b]
	benzyl alcohol (4.8)	benzaldehyde (0.54)

[a] By ^1H NMR. [b] Estimated from experimentally determined amount of PhCHO and assuming a 75% cumulative yield of all products (as found with protiated substrates).

Table 7. Kinetic Isotope Effects for Reactions of $Fe^{IV}_{AN}O^{2+}$

Substrate	k_H/k_D
diethyl ether (d_{10})	2.3
benzyl alcohol (d_2)	3.8
2-propanol (d_1, d_8)	2.5

Discussion

The oxidation of alcohols, ethers and sulfoxides by ozone in acetonitrile is catalyzed by $Fe(CH_3CN)_6^{2+}$. The concentrations of $Fe(CH_3CN)_6^{2+}$ as low as 0.02 mM are sufficient for the catalytic reaction to dominate over the uncatalyzed O_3/substrate reaction at substrate concentrations lower than about 50 mM. The catalyst not only provides rate acceleration, but also increases the selectivity toward the less oxidized product. This is illustrated in Figure 1 and Figure S2 on the example of benzyl alcohol which is oxidized to benzaldehyde in the $Fe(CH_3CN)_6^{2+}$-catalyzed path, and to a 1:1 mixture of benzaldehyde and benzoic acid in direct oxidation with ozone.

Saturation kinetics are observed at [substrate] >5 mM (Figure 4). The rate constants reach an approximate limit of $k_{cat} = (8\pm1) \times 10^4$ M^{-1} s^{-1} for all of the substrates except diethyl ether which reacts somewhat more slowly, $k_{cat} = (5\pm0.5) \times 10^4$ M^{-1} s^{-1}. The observed variations in k_{cat} can be rationalized by variations in Fe(II)-substrate binding constants and perhaps different contributions from 1-e and 2-e paths, see later. The role of substrate binding is clearly seen in the reaction with DMSO which interacts strongly with $Fe(CH_3CN)_6^{2+}$ and reaches $k_{cat} = 1.5 \times 10^6$ M^{-1} s^{-1}, Figure 5.

As the concentration of substrate drops below 5 mM, the rate constant decreases sharply, Figure 4. In this regime up to 50% of iron is oxidized to Fe(III) in the course of the reaction resulting in slower kinetics. Side reactions of Fe(IV) with $Fe(CH_3CN)_6^{2+}$ and with the solvent, see later, are also most severe at low substrate concentrations, which further reduces the efficiency of the catalytic reaction. The remainder of the discussion will focus on the saturation regime.

Most efficient are the oxidations of diethyl ether and dimethyl sulfoxide. Both generate quantitative yields of 2-electron oxidation products, Figures S5 and S6, with only small losses (≤20%) of the catalyst over 20-70 catalytic cycles, Table 1. These data are most easily explained by a single-step two-electron oxidation of substrates by $Fe^{IV}_{AN}O^{2+}$, eq 6, followed by regeneration of $Fe^{IV}_{AN}O^{2+}$ in reaction 5.

Product yields are somewhat lower, 70-85%, in the reactions with alcohols, Table 1. We attribute these results to a contribution from a one-electron path of eq 7 which leads to oxygen radicals ($HO^{\bullet}/O^{\bullet-}$, $O_3^{\bullet-}$, $O_2^{\bullet-}$ and others) known to be involved in chain decomposition of O_3 in aqueous solutions.[19-24] Some of the key reactions believed responsible for the loss of O_3 in this work are shown in eq 8 - 18, written in analogy with the chemistry in aqueous solutions and in the gas phase and supported by the limited information on the reactivity of ozone and oxygen radicals in non-aqueous solvents.[25-30]

$$Fe^{IV}_{AN}O^{2+} + RCH_2OH \rightarrow Fe(III) + RC^{\bullet}HOH \quad (7)$$

$$RC^{\bullet}HOH + O_2 \rightarrow RCH(OH)OO^{\bullet} \quad (8)$$

$$RCH(OH)OO^{\bullet} \rightarrow RCHO + HO_2^{\bullet}/O_2^{\bullet-} \quad (9)$$

$$2RCH(OH)OO^{\bullet} \rightarrow\rightarrow 2\ RCHO + O_2 + H_2O_2 \xrightarrow{Fe(IV)} HO_2^{\bullet} + Fe(III) \quad (10)$$

$$RC^{\bullet}HOH + O_3 \rightarrow \rightarrow RC(O)OH + HO_2^{\bullet}/O_2^{\bullet-} \quad (11)$$

$$HO_2^{\bullet} \rightleftharpoons O_2^{\bullet-} + H^+ \quad (12)$$

$$O_2^{\bullet-} + Fe(III) \rightarrow O_2 + Fe(II) \quad (13)$$

$$O_2^{\bullet-} + O_3 \rightarrow O_2 + O_3^{\bullet-} \quad (14)$$

$$O_3^{\bullet-} \rightleftharpoons O^{\bullet-} + O_2 \quad (15)$$

$$O^{\bullet-} + H^+ \rightleftharpoons HO^{\bullet} \quad (16)$$

$$(HO^{\bullet}, O_3^{\bullet-}, O^{\bullet-}) + CH_3CN\ (+ O_2, O_3) \rightarrow \text{Products} \quad (17)$$

$$(HO^{\bullet}, O_3^{\bullet-}, O^{\bullet-}) + RCH_2OH \rightarrow RCH^{\bullet}OH + (O_2, H_2O, HO^-) \quad (18)$$

Hydroxyalkyl radicals generated in eq 7 react with both O_2 (eq 8) and O_3 (eq 11) and produce superoxide, a powerful reductant and nucleophile in acetonitrile.[30] The reduction of Fe(III) by $O_2^{\bullet-}$,[24] eq 13, is the key step that regenerates Fe(II). The competing reaction between O_3 and $O_2^{\bullet-}$,[31] the latter a well recognized chain carrier in the decomposition of ozone,[23,32] generates $O_3^{\bullet-}$ followed by dissociation[33] to give $O^{\bullet-}$, eq 14-15. The latter may be protonated (pK_a of $HO^{\bullet}$ in H_2O = 11.9)[34] if sufficient amount of water is present in the solvent, but protonation is not required for the next step since both $HO^{\bullet}$ and $O^{\bullet-}$ will oxidize the solvent and/or substrate by hydrogen atom abstraction,[33] eq 17 and 18. Even though the rate constant for the reaction of $HO^{\bullet}$ with acetonitrile is smaller ($k = 1.0 \times 10^6\ M^{-1}\ s^{-1}$ in acetonitrile)[35] than the rate constants for the reactions with alcohols (e. g. $k_{EtOH} = 8.3 \times 10^7\ M^{-1}\ s^{-1}$),[26] the concentration advantage makes the reaction with CH_3CN about 5-10 fold faster at 20-50 mM ethanol that is typical in this work. Presumably, other radicals in eq 17-18 exhibit similar reactivity pattern and together with $HO^{\bullet}$

lead to a loss of oxidizing equivalents and less than quantitative yields of substrate-derived products. Reaction 18 regenerates RC•HOH which reenters the scheme.

According to the above mechanism, the beneficial effect of added Fe(III) arises mainly from its efficient scavenging of $O_2^{\bullet-}$ in eq 13.[24] This step both regenerates the catalyst and minimizes the importance of reactions 14-17 which lead to the loss of O_3.

Increased product yields and somewhat slower kinetics of O_3 loss under O_2-rich conditions are also consistent with known reactivity of radicals with O_3 and O_2. At high [O_2], most of the radicals react with O_2 as in eq 8, followed by reactions 9-10 and 12-18. In the absence of externally added O_2, the concentrations of O_2 and O_3 are comparable (see Experimental), and reaction 11 becomes competitive with reaction 8 which increases the rate of ozone consumption and the yields of doubly oxidized products.[36] Moreover, alkylperoxyl radicals produced in eq 8 also react with O_3 to generate alkoxyl radicals RCH(OH)O•, eq 19, followed by rearrangement and/or further reactions with O_2, O_3 and substrates.[37,38]

$$RCH(OH)OO^{\bullet} + O_3 \xrightarrow{-O_2} RCH(OH)O^{\bullet} \xrightarrow{O_2, O_3, \text{substrate}} \text{products} \qquad (19)$$

In agreement with the above scheme, the concentration of O_2 found after completion of the reactions with alcohols is significantly smaller than one would calculate by adding the amount produced from ozone in reaction 5 to the [O_2] initially present. Clearly, some O_2 is consumed in the course of alcohol oxidation. On the other hand, the concentration of O_2 found after the oxidation of DMSO and $(C_2H_5)_2O$ is close to that calculated, supporting the notion that 1-e oxidation of these substrates is negligible. DMSO is probably oxidized by OAT, similar to the reaction in water.[1] Quantitative product yields and measurable hydrogen kie for diethyl ether suggests hydride transfer.[1]

The induction period observed in the O_3/substrate reaction when iron is initially present as Fe(III) is most easily explained by the need to reduce Fe(III) to Fe(II), presumably through a scheme involving one-electron reduction of O_3 by the substrate[19,39] followed by eq 15-18. The complex, multistep chemistry in eq 17-18 is envisioned to generate some $O_2^{\bullet-}$ which reduces Fe(III) to Fe(II) and thus leads to the production of $Fe^{IV}_{AN}O^{2+}$ via reaction 5.

The disappearance of ozone in the presence of catalytic amounts of $Fe(CH_3CN)_6^{2+}$ in acetonitrile even in the absence of more reducing substrates shows that the solvent itself can be catalytically oxidized. It is not clear whether $Fe^{IV}_{AN}O^{2+}$ oxidizes CH_3CN in 1-e or 2-e steps. Measurable amounts of $Fe(CH_3CN)_6^{2+}$ found in such solutions after all of O_3 disappeared support a 2-e catalytic reaction that might take place by oxygen atom transfer or hydride transfer. On the other hand, as shown above in the reaction with alcohols, 1-e chemistry can also bring about the disappearance of ozone and formation of $Fe(CH_3CN)_6^{2+}$. In support of the one-electron route we note that aqueous ferryl(IV) reacts with CH_3CN by hydrogen abstraction and does not regenerate Fe_{aq}^{2+}.[1] Also, the much smaller amount of recovered Fe(II) after completion of Fe(II)/O_3 reaction in CD_3CN indicates a large solvent isotope effect, again consistent with HAT, although hydride abstraction cannot be entirely ruled out.

Throughout this discussion it has been assumed that the reaction intermediate is an Fe(IV) species, $Fe^{IV}_{AN}O^{2+}$, although so far we have not been able to observe or characterize it spectroscopically. The relative reactivity toward the substrates in Table 5 appears consistent with this assignment in that the trend in acetonitrile follows closely that observed for $Fe_{aq}O^{2+}$ in aqueous solutions. In that work it was possible to carry out direct kinetic measurements of substrate oxidation by pre-formed $Fe_{aq}O^{2+}$. As shown in Table 5, benzyl alcohol is the most reactive among alcohols in both solvents, but the yield of 2-e oxidation product in acetonitrile is

among the lowest. This result may suggest a significant contribution from the 1-e path. Alternatively, the reaction may involve an attack by $Fe^{IV}_{AN}O^{2+}$ at the benzene ring to generate multiple products, similar to the reaction of O_3 with $PhCH_2OH$,[40] or reactions of other Fe(IV)-oxo complexes with aromatic compounds.[41,42]

The kinetic isotope effect for the reaction with 2-propanol is also similar in the two solvents. The value of k_H/k_D for the methine C-H is 2.5 in acetonitrile (Table 7) and 2.1 in H_2O,[1] consistent with hydride transfer proposed previously. These results however do not rigorously rule out other potential oxidizing intermediates, such as an ozonide or Fe(III)-(CH_2CN) radical that may also react by hydride or hydrogen atom transfer.

Conclusions

Perchlorate and trifluoromethane sulfonate salts of iron(II) efficiently catalyze oxidation of alcohols and ethers with ozone in acetonitrile. This result stands in stark contrast with that obtained in acidic aqueous solutions where, under comparable conditions, all of $Fe(H_2O)_6^{2+}$ is quickly oxidized to the unreactive $Fe(H_2O)_6^{3+}$. The difference between the two solvents can be rationalized by changes in redox thermodynamics of iron and acid-base chemistry of superoxide radical, $HO_2^{\bullet}/O_2^{\bullet-}$.

In both solvents the reaction between the substrate and active oxidant, an iron(IV) species, takes place in parallel one-electron (hydrogen-atom abstraction) and two-electron (hydride transfer) paths. The two-electron path is much more prominent in acetonitrile, presumably because it avoids the strongly oxidizing Fe(III) (E = 1.6 V vs. NHE).[8] This path regenerates the active catalyst, $Fe(CH_3CN)_6^{2+}$, directly. The parallel hydrogen atom transfer produces carbon radicals and Fe(III). The ensuing chemistry in the presence of O_2 generates superoxide $O_2^{\bullet-}$ (E^0 ($O_2/O_2^{\bullet-}$) = -0.80 V vs. NHE)[30] which rapidly reduces Fe(III) to Fe(II). This

step both regenerates the catalyst and removes $O_2^{\bullet-}$, the key intermediate involved in chain decomposition of ozone.

The two paths are of comparable importance in acidic aqueous solutions[1] so that a substantial portion of $Fe(H_2O)_6^{2+}$ is oxidized to $Fe(H_2O)_6^{3+}$ in a single cycle. Similar to the reaction in acetonitrile, the follow-up chemistry generates superoxide. However, under acidic conditions the superoxide is protonated (pK_a ($HO_2^{\bullet}$/ $O_2^{\bullet-}$) = 4.69)[30] and incapable of reducing $Fe(H_2O)_6^{3+}$. One-electron path in aqueous solution thus leads to irreversible removal of the catalyst.

Acknowledgment

We are grateful to Dr. Jana for help with the synthesis of iron(II) bis(acetonitrile) complex. This research is supported by the U.S. Department of Energy, Office of Science, Basic Energy Sciences, Division of Chemical Sciences, Geosciences, and Biosciences through the Ames Laboratory. The Ames Laboratory is operated for the U.S. Department of Energy by Iowa State University under Contract DE-AC02-07CH11358.

Supplemental Information

Figures S1-S21 and Tables S1-S3 are shown in Appendix B.

References

(1) Pestovsky, O.; Bakac, A. *J. Am. Chem. Soc.* **2004**, *126*, 13757-13764.

(2) Pestovsky, O.; Stoian, S.; Bominaar, E. L.; Shan, X.; Münck, E.; Que, L. J.; Bakac, A. *Angew. Chem., Int. Ed.* **2005**, *44*, 6871-6874.

(3) Jacobsen, F.; Holcman, J.; Sehested, K. *Int. J. Chem. Kin.* **1998**, *30*, 215-221.

(4) Logager, T.; Holcman, J.; Sehested, K.; Pedersen, T. *Inorg. Chem.* **1992**, *31*, 3523-3529.

(5) Pestovsky, O.; Bakac, A. *Inorg. Chem.* **2006**, *45*, 814-820.

(6) Bataineh, H.; Pestovsky, O.; Bakac, A. *Chem. Sci.* **2012**, *3*, 1594-1599.

(7) Kratochvil, B.; Long, R. *Analytical Chemistry* **1970**, *42*, 43-46.

(8) Sugimoto, H.; Sawyer, D. T. *J. Am. Chem. Soc.* **1985**, *107*, 5712-5716.

(9) Bakac, A.; Pestovsky, O.; Vol. U.S. Patent 8507730 (2013).

(10) Hagen, K. S. *Inorganic Chemistry* **2000**, *39*, 5867-5869.

(11) Leitzke, A.; von Sonntag, C. *Ozone: Sci. Eng.* **2009**, *31*, 301-308.

(12) Franco, C.; Olmsted Iii, J. *Talanta* **1990**, *37*, 905-909.

(13) Nimlos, M. R.; Wolfrum, E. J.; Brewer, M. L.; Fennell, J. A.; Bintner, G. *Environmental Science & Technology* **1996**, *30*, 3102-3110.

(14) Hay, M. T.; Geib, S. J.; Pettner, D. A. *Polyhedron* **2009**, *28*, 2183-2186.

(15) Avgousti, C.; Georgolios, N.; Kyriacou, G.; Ritzoulis, G. *Electrochimica Acta* **1999**, *44*, 3295-3301.

(16) Klang, J. A.; Lawson, A. P.; ARCO Chemical Technology, L.P.: United States, 1993; Vol. US005254702A, p 1-4.

(17) Suárez, A. R.; Rossi, L. I.; Martín, S. E. *Tetrahedron Letters* **1995**, *36*, 1201-1204.

(18) Kirchner, K.; Kirchner, R.; Jedlicka, R.; Schmid *Monatshefte für Chemie* **1992**, *123*, 203-209.

(19) Flyunt, R.; Leitzke, A.; Mark, G.; Mvula, E.; Reisz, E.; Schick, R.; von Sonntag, C. *The Journal of Physical Chemistry B* **2003**, *107*, 7242-7253.

(20) Langlais, B.; Reckhow, D. A.; Brink, D. R. In *Am Water Works Res*; CRC press: 1991.

(21) Gonzalez, M. C.; Mártire, D. O. *International Journal of Chemical Kinetics* **1997**, *29*, 589-597.

(22) Gonzalez, M. C.; Mártire, D. O. *Water Science and Technology* **1997**, *35*, 49-55.

(23) Naumov, S.; von Sonntag, C. *Environmental Science & Technology* **2011**, *45*, 9195-9204.

(24) Rush, J. D.; Bielski, B. H. J. *The Journal of Physical Chemistry* **1985**, *89*, 5062-5066.

(25) Nakano, Y.; Okawa, K.; Nishijima, W.; Okada, M. *Water Research* **2003**, *37*, 2595-2598.

(26) Mitroka, S.; Zimmeck, S.; Troya, D.; Tanko, J. M. *Journal of the American Chemical Society* **2010**, *132*, 2907-2913.

(27) Afanas'ev, I. B.; Kuprianova, N. S. *Journal of the Chemical Society, Perkin Transactions 2* **1985**, 1361-1364.

(28) Singh, P. S.; Evans, D. H. *The Journal of Physical Chemistry B* **2005**, *110*, 637-644.

(29) McCandlish, E.; Miksztal, A. R.; Nappa, M.; Sprenger, A. Q.; Valentine, J. S.; Stong, J. D.; Spiro, T. G. *Journal of the American Chemical Society* **1980**, *102*, 4268-4271.

(30) Sawyer, D. T.; Valentine, J. S. *Accounts of Chemical Research* **1981**, *14*, 393-400.

(31) Bielski, B. H. J.; Cabelli, D. E.; Arudi, R. L.; Ross, A. B. *J. Phys. Chem. Ref. Data* **1985**, *14*, 1041-1100.

(32) Lind, J.; Merenyi, G.; Johansson, E.; Brinck, T. *J. Phys. Chem. A* **2003**, *107*, 676-681.

(33) Gall, B. L.; Dorfman, L. M. *J. Amer. Chem. Soc.* **1969**, *91*, 2199-2204.

(34) Buxton, G. V.; Greenstock, C. L.; Helman, W. P.; Ross, A. B. *J. Phys. Chem. Ref. Data* **1988**, *17*, 513-886.

(35) DeMatteo, M. P.; Poole, J. S.; Shi, X.; Sachdeva, R.; Hatcher, P. G.; Hadad, C. M.; Platz, M. S. *J. Am. Chem. Soc.* **2005**, *127*, 7094-7109.

(36) Sehested, K.; Holcman, J.; Bjergbakke, E.; Hart, E. J. *J. Phys. Chem.* **1987**, *91*, 2359-2361.

(37) Batt, L. *Int. Rev. Phys. Chem.* **1987**, *6*, 53-90.

(38) Kirillov, A. I. *Zh. Obshch. Khim.* **1966**, *2*, 1048-1052.

(39) Martín, S. E.; Suárez, D. o. F. *Tetrahedron Letters* **2002**, *43*, 4475-4479.

(40) Potapenko, E. V.; Andreev, P. Y. *Russian Journal of Applied Chemistry* **2010**, *83*, 1243-1247.

(41) Fitzpatrick, P. F. *Biochemistry* **2003**, *42*, 14083-14091.

(42) de Visser, S. P.; Oh, K.; Han, A.-R.; Nam, W. *Inorganic Chemistry* **2007**, *46*, 4632-4641.

CHAPTER 4

ELECTRON TRANSFER REACTIVITY OF AQUEOUS IRON(IV) OXO COMPLEX

A manuscript in preparation

Abstract

The reactivity of $Fe_{aq}^{IV}O^{2+}$, generated in the reaction of Fe_{aq}^{2+} and ozone at pH 1, toward various inorganic complexes and some organic substrates, including ferrocene derivatives, Ni(II) macrocyclic tetraamines complexes, polypyridyl complexes of Os(II), Fe(II) and Ru(II), phenothiazines, $HABTS^{-}$, Na_3IrCl_6, $Co^{II}(dmgBF_2)_2$ and $Ce(ClO_4)_3$ with reduction potentials ranging from 0.52 to 1.7 V has been studied at room temperature. All substrates have shown to react with $Fe_{aq}^{IV}O^{2+}$ quantitatively producing the 1e oxidation product except for the phenothiazines and polypyridyl complexes of Fe(II) and Ru(II). Phenothiazines reacted through oxygen atom transfer to produce sulfoxides while the reactions with polypyridyl complexes of Fe(II) and Ru(II) were complicated and showed no Fe(III) or Ru(III) formation. The obtained second order rate constants of these reactions are within $10^4 - 10^8$ M^{-1} s^{-1} with no straightforward relation to reduction potentials. Among all the substrates, $Os(phen)_3^{2+}$ seems to react through outer-sphere ET. In addition, the no dependence of $Os(phen)_3^{2+}$ reactivity on acid concentration (0.05 – 0.2 M) indicates no prior protonation of the $Fe_{aq}^{IV}O^{2+}$, which is consistent with stepwise electron-transfer followed by proton transfer. Our results suggest that the $Fe_{aq}^{IV}O^{2+}/Fe_{aq}^{III}O^{+}$ potential is not much lower than that for $Os(phen)_3^{3+}/ Os(phen)_3^{2+}$ couple (0.84 V vs. NHE).

Introduction

In the last few years, the chemistry of high-valent iron oxo complexes have attracted considerable attention and many efforts have been made to understand their role in several enzymatic systems by carrying out oxidation reactions with wide range of organic substrates.[1-5] A number of iron(IV) complexes bearing stabilizing ligands have been synthesized and characterized by various spectroscopic methods and X-ray crystallography in attempts to unravel and mimic the chemistry of both heme and non-heme iron centers in enzyme active sites.[6-10] Many reports have shown how powerful oxidants are these iron(IV) oxo model complexes and how efficiently and selectively they can catalytically oxidize C-H bonds of many organic substrates.[8,10-17] In addition, the electron-transfer properties of some high-valent metal oxo complexes, including iron(IV), have been studied with some inorganic electron donors in attempts to give more insight about their reactions mechanism and oxidation power.[18-21] The one-electron reduction potential for some of the synthesized Fe(IV)-oxo complexes have been examined and reported to have values ranging from ~0.2 to 1.0 V vs. NHE.[19,22]

On the other hand, aqua iron(IV)-oxo complexes are generated in the reaction between aqueous Fe(II) and oxygen-atom donors, such as H_2O_2 and O_3.[23] However, their fast decay and sensitivity to the chemical environment make it hard to fully explore their chemistry. For example, an iron(IV) aqua complex was previously reported as one of the active intermediates, along with OH radical, in Fenton reaction (reaction of Fe_{aq}^{2+} and H_2O_2), and recently we have shown that the reactive intermediate changes from hydroxyl radicals in acidic solutions to an iron(IV) species at near neutral pH.[24] However, the generation of Fe(IV) species at near neutral pH was sensitive to the presence of coordinating ligands such as phosphate. In addition, the fast decay of Fe(IV) and the rapid reaction with Fe(II) at neutral pH made it hard to fully characterize

this species or study its reactivity, since this would require the use of very reactive substrates or high substrate concentrations which would interfere with the chemistry producing Fe(IV) and our ability to detect it.

The Fe(IV)-oxo complex formed in the reaction between Fe_{aq}^{2+} and ozone has been reported to have a lifetime of 10 seconds at pH 1 at room temperature, which provided a window to characterize and study the reactivity of this iron(IV) species.[25-27] A few reports have shown that the aqueous iron(IV) is capable of oxidizing a wide range of organic substrates effectively and selectively.[26,28,29] However, the redox-chemistry of the aqueous Fe(IV) species and its electron-transfer properties remain largely unexplored with only very few reports about its reaction with inorganic substrates. One of the reports has shown that Fe(IV) generated in Fenton reaction can oxidize As(III) to As(IV).[30] In addition, Jacobson et al have examined the reactivity of the aqueous Fe(IV)-oxo species with few inorganic substrates and reported a lower limit for the standard one electron reduction potential for the $Fe_{aq}O^{2+}$ / Fe_{aq}^{3+} couple of $E^o(Fe_{aq}O^{2+}$ / $Fe_{aq}^{3+}) \geq 0.87$ V vs. NHE.[26] The one-electron reduction potential for $Fe_{aq}^{IV/III}$ is still unavailable and the fact that the aqueous $Fe_{aq}O^{2+}$ can react in two parallel 1e and 2-e pathways[28] or the possibility that it might attack the coordinated ligands, when reacting with metal complexes, instead of the metal would make it very difficult to get a precise value on the one-electron potential for $Fe_{aq}^{IV/III}$. In addition, the $Fe_{aq}O^{2+}$ decays within 10 seconds at pH 1 through oxidizing water, which would make it difficult to establish steady equilibrium between the $Fe_{aq}O^{2+}$ / Fe_{aq}^{3+} couple and electron donors.

More to add, previous reports have shown that the oxidation power of synthesized Fe(IV)-oxo complexes enhanced in the presence of Lewis or BrØnsted acids, especially in organic solvents like acetonitrile, and an increase up to ~0.8 V in the reduction potential was

observed for some synthetic Fe(IV)-oxo complexes bearing tetradentate N4 ligands.[16,31-33] The protonation of or the binding of a metal ion Lewis acid like Sc^{3+} to the Fe(IV)-oxo unit has shown to cause weakening or elongation of the Fe^{IV}=O bond lowering the reorganization energy which would remarkably enhance the electron-transfer reactivity of the Fe(IV)-oxo complexes.[19] Aqueous $Fe_{aq}{}^{IV}O^{2+}$ is expected to behave similarly and to proceed through proton-coupled electron-transfer (PCET)[34,35] rather than simple electron-transfer (ET) since the latter would form $Fe_{aq}{}^{III}O^{+}$ complex rather than the stable hydroxyl-Fe(III) (see Scheme 1).

1) $Fe_{aq}O^{2+} \xrightarrow{e^-,\ H^+} Fe_{aq}OH^{2+}$ Proton-coupled electron-transfer

2) $Fe_{aq}O^{2+} \xrightarrow{e^-} Fe_{aq}O^{+} \underset{}{\overset{H^+}{\rightleftharpoons}} Fe_{aq}OH^{2+}$ Electron-transfer

Scheme 1. Proton-coupled electron-transfer (PCET) path vs. electron-transfer (ET).

In this work, we further explore the chemistry of $Fe_{aq}O^{2+}$, reporting its reactivity with various inorganic complexes, in attempts to give more insight about its electron-transfer characteristics and oxidation power.

Experimental

Materials

Most of the chemicals used were of analytical or reagent grade and were used as received from the suppliers. Iron(II) perchlorate hydrate ($Fe(ClO_4)_2.xH_2O$) (98%), ferrocenecarboxylic acid ($Fe(Cp)(C_5H_4COOH)$) (97%), 2,2'-azino-bis(3-ethylbenzothiazoline-6-sulphonic acid) diammonium salt (ABTS) $C_{18}H_{18}N_4O_6S_4.2NH_4$ (~98%), sodium hexachloroiridate(III) hydrate ($Na_3IrCl_6.xH_2O$), trifluoperazine dihydrochloride (TFP) $C_{21}H_{24}F_3N_3S.2HCl$ >99% and tris(2,2′-

bipyridyl)dichlororuthenium(II) hexahydrate ($Ru(bpy)_3Cl_2.6H_2O$) (Sigma-Aldrich), perchloric acid ($HClO_4$) (70 wt%) (Fisher), 1,1'- ferrocenedicarboxylic acid ($Fe(C_5H_4COOH)_2$) (98%) (Alfa Aesar), hydroxymethyl ferrocene ($Fe(Cp)(C_5H_4CH_2OH)$) (99%) and cerium(III) perchlorate hexahydrate ($Ce(ClO_4)_3.6H_2O$) (Strem), chlorpromazine hydrochloride (CPZ) $C_{17}H_{19}ClN_2S.HCl$ (99.9%) (Fluka). Tris(1,10-phenanthroline)osmium(II) triflate ($Os(phen)_3(CF_3SO_3)_2$) was a gift from Dr. Stanbury. The compounds bis(dimethylglyoximato)cobalt(II) ($(H_2O)_2Co(dmgBF_2)_2$)[36], Nickel(II) cyclam[37] ($Ni(cyclam)(ClO_4)_2$) (cyclam = 1,4,8,11-tetraazacyclotetradecane), ($Ni(hmc)(ClO_4)_2$)[38] (hmc = 5,7,7,12,14,14-hexamethyl-1,4,8,11-tetraazacyclotetradecane), tris*(*5,6-dimethyl-1,10-phenanthroline*)*ruthenium(II) chloride[39] ($Ru(5,6\text{-}Me_2phen)_3Cl_2$), and tris*(*4,7-dimethyl-1,10-phenanthroline*)*ruthenium(II) perchlorate[39] ($Ru(4,7\text{-}Me_2phen)_3(ClO_4)_2$) were prepared according to literature procedures. Solutions of *tris*(*1,10-phenanthroline*)iron(II) perchlorate ($Fe(phen)_3(ClO4_2)$) were prepared by mixing aqueous solutions of iron(II) perchlorate with three equivalents of 1,10-phenanthroline. Ozone was generated with Ozonology L-100 ozone generator. Water was purified by passage through a Barnstead Easy Pure II -UV/UF ultrapure water purification system.

UV-Vis spectra and kinetic studies were carried out with a Shimadzu UV-3101 PC spectrophotometer and Applied Photophysics (APP) sequential stopped-flow DX-18MV at 25.0 ± 0.2^0 C. Kinetic traces were fitted with Kaleidagraph 4.0 software.

Procedures

In most of the experiments, reaction solutions were open to air while handling. Oxygen sensitive ferrocenes were purged with argon before mixing. Light sensitive complexes, including ferrocenes and complexes of osmium and cobalt were handled in subdued light. Most of the reactions were studied in 0.1 M $HClO_4$. The reaction with Ce(III) was examined in 1.0 M

$HClO_4$. Owing to the low solubility of polypyridine ruthenium perchlorates, the solutions were prepared in 1 mM $HClO_4$ and mixed in the stopped-flow with Fe(II)/O_3 solutions in 0.1 M $HClO_4$, resulting in reaction $[H^+]$ = 0.05 M.

Molar extinction coefficients of ferrocenes were determined by dissolving the solid in 7:3 acetonitrile : water (v/v) and diluting the solution with a 10-fold volume of 0.1 M $HClO_4$ prior to recording the UV-Vis spectrum. The extinction coefficient of the ferrocenium derivatives was obtained by oxidizing a measured concentration of the corresponding ferrocene derivative with excess iron(III) perchlorate in 7:3 acetonitrile : water and recording the spectrum. Concentrations of iron(II) were determined with phenanthroline (ε_{510} = 1.14 x 10^4 M^{-1} cm^{-1}) after a correction for the absorption by iron(III)-phenanthroline complex, as previously described.[29] Ozone concentration was obtained from the absorbance at 260 nm using ε_{260} = 3300 M^{-1} cm^{-1}.[40] Substrate concentrations were determined spectrophotometrically using the molar absorptivities in Table 1.

Kinetics were measured with an APP sequential stopped-flow instrument by monitoring either the disappearance of the reactants or formation of products, as appropriate. Fe(II) and ozone solutions were mixed in the pre-mix drive and aged for five half-lives ($k_{Fe(II)/O3}$ = 8.3 x 10^5 M^{-1} s^{-1})[2], to ensure complete formation of Fe(IV), which was then mixed with the substrate solution in the flush drive. An acid range of 0.05 – 0.2 M $HClO_4$ was used in experiments designed to study the acid effect on the rate constants for the oxidation of Na_3IrCl_6 and $Os(phen)_3^{2+}$.

Table 1. Spectral Properties of Substrates.

Substrate	λ_{max} /nm (ε /M^{-1} cm^{-1})	Source
$Fe(Cp)(C_5H_4COOH)$	444 (324)	This study
$Fe(C_5H_4COOH)_2$	448 (324)	This study
$Fe(Cp)(C_5H_4CH_2OH)$	435 (100)	Ref. 41
$HABTS^-$	310 (3.66×10^4)	Ref. 42
TFP	255.5 (33400), 306 (3870)	This study
CPZ	254.5 (35900), 306 (4500)	This study
Na_3IrCl_6	415 (76)	Ref. 43
$Ce(ClO_4)_3$	253 (760)	Ref. 44
$Os(phen)_3(CF_3SO_3)_2$	430 (1.9×10^4)	Ref. 45
$(H_2O)_2Co(dmgBF_2)_2$	456 (4.06×10^3)	Ref. 36
$Ni(cyclam)^{2+}$	451 (47)	Ref. 37
$Ni(hmc)^{2+}$	463 (73)	This study
$Ru(5,6\text{-}Me_2phen)_3^{2+}$	453 (2.04×10^4)	Ref. 39
$Ru(4,7\text{-}Me_2phen)_3^{2+}$	445 (2.53×10^4)	Ref. 39
$Ru(bpy)_3^{2+}$	452 (1.46×10^4)	Ref. 39
$Fe(phen)_3^{2+}$	510 (1.14×10^4)	Ref. 29

TFP = trifluoperazine, CPZ = chlorpromazine, $HABTS^-$ = 2,2'-azino-bis(3-ethylbenzothiazoline-6-sulphonic acid), Cp = cyclopentadienyl, cyclam = 1,4,8,11-tetraazacyclotetradecane, hmc = 5,7,7,12,14,14-hexamethyl-1,4,8,11-tetraazacyclotetradecane.

Results

Due to the very fast reaction rates observed for most of the used substrates (rate constants of 10^6-10^8 M^{-1} s^{-1}), instrumental detection limit and low solubility of some of the metal complexes in acidic aqueous solutions, most of the kinetic studies were performed under second order conditions in a limited range of concentrations. The reported second order rate constants are averages of 2-3 experiments at different concentrations. Pseudo first order conditions were used with Na_3IrCl_6, $Os(phen)_3^{2+}$ and $Ce(ClO_4)_3$ which react more slowly.

The low extinction coefficients of the ferrocenes combined with large rate constants allowed us to observe and fit only the last 15-50% of the kinetic traces depending on the concentrations used. The traces were collected at the spectral maxima of substrates or products, Tables 1 and 2.

Polypyridyl Complexes of Fe(II), Ru(II) and Os(II)

Among all the used polypyridine complexes only $Os(phen)_3^{2+}$ produced the one electron oxidation product $Os(phen)_3^{3+}$. Polypyridyl complexes of Fe(II) and Ru(II) kinetics showed complicated multi-step reactions. No increase in absorbance was observed in the 600 – 700 nm range, in the case of $Fe(phen)_3^{2+}$ and $Ru(bpy)_3^{2+}$ reactions, ruling out the formation of $Fe(phen)_3^{3+}$ and $Ru(bpy)_3^{3+}$.[48,49] In the case of $Ru(4,7\text{-}Me_2phen)_3^{2+}$ and $Ru(5,6\text{-}Me_2phen)_3^{2+}$ an increase in absorbance was observed in the 600 – 650 nm where Ru(III) is expected to absorb,[47] however the change in absorbance was higher than the expected for such Ru(III) complexes ruling out the formation of Ru(III) complex or, if formed, will be as by-product along with other products. These observations suggest that $Fe_{aq}^{IV}O^{2+}$ is reacting with the ligand instead of the metal center forming some stable radicals intermediates that later will decay forming various products or give back the starting complex.

Table 2. Spectral Properties of Oxidation Products.

Product	λ /nm (ε /M^{-1} cm^{-1})	Source
$Ir^{IV}Cl_6^{2-}$	490 (3920)	Ref. 43
$Fe(Cp)(C_5H_4CH_2OH)^+$	629 (400)	Ref. 41
$Fe(Cp)(C_5H_4COOH)^+$	628 (410)	This study
$Fe(C_5H_4COOH)_2^+$	628 (400)	This study
$ABTS^{\cdot-}$	645 (1.35 x 10^4)	Ref. 42
$Ni(cyclam)^{3+}$	308 (1.1 x 10^4)	Ref. 46
$Ni(hmc)^{3+}$	400 (5.7 x 10^3)	This study
$Ru(4,7\text{-}Me_2phen)_3^{3+}$	630 (1.6 x 10^3)	Ref. 47
$Ru(bpy)_3^{3+}$	675 (476)	Ref. 48
$Fe(phen)_3^{2+}$	600 (830)	Ref. 49
$Ce(ClO_4)_4$	1380 [a]	This study
CPZ=O	235 (33000), 295 (4200)	Ref. 50

[a] This value was measured under our reaction conditions (~0.1 M $Ce(ClO_4)_4$, 1.0 M $HClO_4$) and will be different at different cerium and acid concentrations.
CPZ=O = chlorpromazine sulfoxide, ABTS = 2,2'-azino-bis(3-ethylbenzothiazoline-6-sulphonic acid), Cp = cyclopentadienyl, cyclam = 1,4,8,11-tetraazacyclotetradecane, hmc = 5,7,7,12,14,14-hexamethyl-1,4,8,11-tetraazacyclotetradecane.

Phenothiazines (CPZ and TFP)

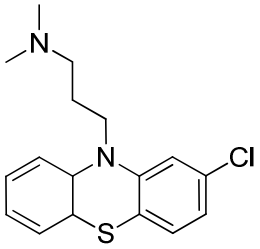

CPZ

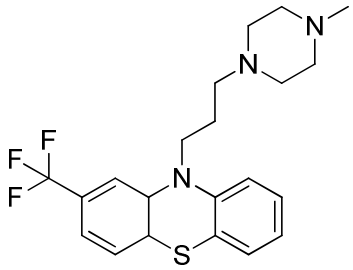

TFP

Many reports[51-53] have shown that CPZ and TFP undergo one electron transfer reaction to produce stable colored radical cations, $CPZ^{\bullet+}$ and $TFP^{\bullet+}$ respectively, which can be monitored spectrophotometrically. On the other hand, other reports showed that phenothiazines can be oxidized to their corresponding sulfoxide either directly via oxygen atom transfer or by the further oxidation of the radical cation.[52-55]

$Fe_{aq}^{IV}O^{2+}$ reaction with the phenothiazines, CPZ and TFP, produced the corresponding sufloxides directly through oxygen atom transfer. This was confirmed by the immediate formation of the sulfoxides at their maxima (see Table 2) with no formation of the radical cations during the reactions. Some of the radical cation was slowly formed after the reaction and was surprisingly stable. Further investigation showed that the formed Fe(III) reacts with phenothiazines, through a slow equilibrium, to produce the radical cation.

HABTS$^-$

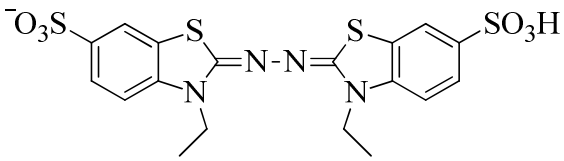

HABTS$^-$

50-60% of the $Fe_{aq}^{IV}O^{2+}$ reaction with $HABTS^-$ produced the stable radical anion $ABTS^{\bullet-}$. No $ABTS^0$, the 2-electron product, was formed during the reaction and the amount of $HABTS^-$ remained after the reaction does not account for the other 40-50%. This result suggests that part of the reaction took place by an attack at one or more reactive sites in the molecule leading to oxidative decomposition of $HABTS^-$.

Other Substrates

All the other substrates react with $Fe_{aq}^{IV}O^{2+}$ quantitatively forming their corresponding one electron oxidation product.

The reactions of $Fe_{aq}^{IV}O^{2+}$ with Na_3IrCl_6 and $Os(phen)_3^{2+}$ were carried under acid concentrations of 0.05 to 0.2 M $HClO_4$ and no change in the rate constants was observed.

Table 3 summarizes all the rate constants (k_{Fe}) determined in this work. Kinetic traces and conditions are shown in Table S1 and Figures S1-S12.

Table 3. Summary of Rate Constants for Oxidations with $Fe_{aq}O^{2+}$, and Reduction Potentials and Self-exchange Rate Constants of Reductants.*

Substrate	Product Observed	$k_{Fe}/M^{-1}\ s^{-1}$ [h]	E^o (V, NHE) (Electrochemical Conditions at 25 °C)	$k_{11}/M^{-1}\ s^{-1}$	Source [g]
$Fe(Cp)(C_5H_4CH_2OH)$	$Fe(Cp)(C_5H_4CH_2OH)^+$	6.4×10^7	**0.52** (n-PrOH-H_2O (1:1 v/v), 0.050 M $Ba(ClO_4)_2$)	4.2×10^6	Ref. 56
$Fe(Cp)(C_5H_4COOH)$	$Fe(Cp)(C_5H_4COOH)^+$	1.2×10^7	**0.70** (pH 1, 0.1 M LiCl, 1:1 (v/v) aqueous methanol	4.2×10^6 [a]	Ref. 57
$Fe(C_5H_4COOH)_2$	$Fe(C_5H_4COOH)_2^+$	1.0×10^6	**0.86** (pH 1, 0.1 M NaCl)	4.2×10^6 [a]	Ref. 58
Na_3IrCl_6	Na_2IrCl_6	1.3×10^6 [f]	**0.892** (0.1 M $NaClO_4$)	2.3×10^5	Ref. 59, 60
$Os(phen)_3^{2+}$	$Os(phen)_3^{3+}$	2.5×10^5 [f]	**0.84**	2×10^9	Ref. 61, 45

			(0.95 M NaCl, 0.05 M HCl)		
$Ni(cyclam)^{2+}$	$Ni(cyclam)^{3+}$	4.9×10^7	**0.95** (pH 1.6, 0.3 M $NaClO_4$)	2.0×10^3 1×10^3	Ref. 62, 63, 64
$Ni(hmc)^{2+}$	$Ni(hmc)^{3+}$	1.2×10^7	**1.19** (pH 2, 0.5 M $NaClO_4$)	1×10^3 [b]	Ref. 65
$Ce(ClO_4)_3$	$Ce(ClO_4)_4$	1.5×10^4	**1.7** (1 M $HClO_4$)	NA	Ref. 66
$Co(dmgBF_2)_2$	$Co(dmgBF_2)_2^+$	2.2×10^6	**0.65** (0.1 M $HClO_4$)	1.7×10^{-4} – 8.7×10^{-3}	Ref. 36,67
$Ru(4,7\text{-}Me_2phen)_3^{3+}$	Not identified	Multi-step	**1.09** (1 M H_2SO_4)	1.2×10^9 [c]	Ref. 39
$Ru(5,6\text{-}Me_2phen)_3^{2+}$	Not identified	Multi-step	**1.20** (1 M H_2SO_4)	1.2×10^9 [c]	Ref. 39
$Ru(bpy)_3^{3+}$	Not identified	Multi-step	**1.26** (1 M H_2SO_4)	1.2×10^9	Ref. 39,68
$Fe(phen)_3^{2+}$	Not identified	Multi-step	**1.06** (1 M H_2SO_4)	1.3×10^7 [e]	Ref. 69,70

CPZ	CPZ=O	1.2×10^7	**0.799** [d] (0.25 M H_2SO_4)		Ref. 71
TFP	TFP=O	5.3×10^6	**0.89** [d] (0.25 M H_2SO_4)		Ref. 71
$HABTS^-$	$ABTS^{\bullet-}$ + other not identified products	4.6×10^6	**0.81** (1.5 M $HClO_4$)	4×10^7	Ref. 42

* see Tables 1 and 2 footnotes for list of abbreviations.
[a] assumed to be the same as $Fe(Cp)(C_5H_4CH_2OH)$
[b] assumed to be the same as $Ni(cyclam)^{3+/2+}$
[c] assumed to be the same as $Ru(bpy)_3^{2+}$
[d] oxidation potentials of direct oxidation of CPZ and TFP to the corresponding sulfoxides are 0.95 and 1.0 V respectively in 0.5 M H_2SO_4.[71]
[e] measured at 3 °C.
[f] same rate constant was measured at 0.05 – 0.20 M $HClO_4$.
[g] references are for reduction potential and self-exchange rate constant of reductant respectively.
[h] all rate constants are measured in 0.1 M $HClO_4$ except for $Ce(ClO_4)_3$ which was measured in 1.0 M $HClO_4$

Discussion

This work focuses on electron transfer reactivity of $Fe_{aq}^{IV}O^{2+}$. Various metal complexes with different ligands were chosen to cover a wide range of potentials and to explore different mechanistic possibilities. For example, polypyridyl complexes of Os(II), Fe(II) and Ru(II) have a moderate to high reduction potentials and known to react through outer-sphere ET mechanism providing their near-diffusion self-exchange rate constants.[45,61,72] Ferrocenes, on the other hand, have low to moderate reduction potentials and have been reported to react with some Fe(IV)-oxo complexes through outer-sphere ET mechanism.[19,20] However, ferrocene derivatives having –COOH or $–CH_2OH$ groups on the cyclopentadienyl ring might also bind to the $Fe_{aq}^{IV}O^{2+}$ and react through inner-sphere ET as expected with other substrates like Na_3IrCl_6 which might bind to the $Fe_{aq}^{IV}O^{2+}$ though a chloride bridge during the ET process. $Co(II)(dmgBF_2)_2$ is known to react through inner-sphere ET mechanism as previously reported.[36] In addition, both Na_3IrCl_6 and $Os(phen)_3^{2+}$ were chosen to study the acid effect on reactivity since their reduction potentials do not have acid dependence as other substrates, which would make it possible to test the acid effect on $Fe_{aq}^{IV}O^{2+}$ reactivity.

Results show that the ET second order rate constants have no straightforward dependence on the reduction potentials (see Table 3). This would suggest that different substrates react through different ET mechanisms. However, $Os(phen)_3^{2+}$ seems to react through outer-sphere ET due to the following: i) $Fe_{aq}^{IV}O^{2+}$ failed to oxidize Fe(II) and Ru(II) metal centers of other polypyridine complexes, however, it was able to oxidize metal complexes with about similar or higher reduction potentials, such as Ni(II) macrocyclic compounds and $Ce(ClO_4)_3$, suggesting that the latter react by different mechanism. This would also suggest that $Fe_{aq}^{IV}O^{2+}$ does not have enough power to oxidize the metal center in these polypyridyl complexes through outer-sphere

ET path and thus, probably, attacking at the ligand. ii) Substrates with higher reduction potentials have shown higher ET rate constants compared to $Os(phen)_3^{2+}$ indicating that these substrates do not utilize an outer-sphere path as $Os(phen)_3^{2+}$.

The outer-sphere ET characteristics of $Os(phen)_3^{2+}$ reaction make it possible to examine its reaction with $Fe_{aq}^{IV}O^{2+}$ in light of Marcus theory of outer-sphere ET using the simplified equation (Eq. 1)[73], where $k_{ET} = k_{Fe}$ (Table 3) is the electron-transfer rate constant, K_{12} is the equilibrium constant, k_{11} and k_{22} are the electron self-exchange rate constants

$$k_{ET} = (k_{11}.k_{22}.K_{12})^{1/2} \quad \text{..... (1)}$$

for the substrate and $Fe^{(IV)/(III)}$ respectively. The full equation has additional terms (w and *f*) but in the present case these will not greatly change the outcome. Using Nernest equation (Eq. 2), where n is the number of electrons transferred =1, and $E^o = E^o_{FeIV/III} - E^o_{substrate}$ is the reaction standard potential, one can derive Eq. 3 and get an estimate of ($\log k_{22} + 16.9\ E^o_{FeIV/III}$) which should represent a constant value (see Table 4).

$$\log K_{12} = \frac{n}{0.05916} E^o \quad \text{..... (2)}$$

$$(\log k_{22} + 16.903\ E^o_{FeIV/III}) = 2 \log k_{ET} - \log k_{11} + 16.903\ E^o_{substrate} \quad \text{..... (3)}$$

Table 4 shows that no value was similar to the $Os(phen)_3^{2+}$, indicating that these substrates might not react through outer-sphere ET and suggesting inner-sphere path or other types of interactions. However, Na_3IrCl_6 reaction showed that $IrCl_6^{2-}$ is formed as the main product and no $Ir(OH_2)Cl_5^-$ was formed, since both have different spectral characteristics,[74] indicating no chloride transfer. This might also be consistent with outer-sphere mechanism, providing the small difference in the reduction potential and the ET rate constant compared to $Os(phen)_3^{2+}$ and the fact that the work term, principally electrostatic, in Marcus equation was not

taken into consideration. The work required to bring the two oppositely charged complexes $IrCl_6^{3-}$ and $Fe_{aq}^{IV}O^{2+}$ is expected to be lower compared to the $Os(phen)_3^{2+}$ reaction which have two complexes of the same +2 charge, which would suggest higher rate in $IrCl_6^{3-}$ case. Also, ferrocenes did not produce the same value (Table 4) compared to each other or compared to $Os(phen)_3^{2+}$, however, their values were the closest to $Os(phen)_3^{2+}$ which might suggest some outer-sphere characteristics. The scatter in the ferrocenes results could be attributed to the estimated self-exchange rate constants, the lack of the precise reduction potential for $Fe(Cp)(C_5H_4CH_2OH)$ under our reaction conditions and (or), again, neglecting the work term in Marcus equation, which is expected to be lower for the ferrocenes.

Table 4. Calculated (log k_{22} + 16.9 $E^o_{FeIV/III}$) for Some of the Substrates Using Eq. 3.

Substrate	$K_{Fe}/M^{-1}\ s^{-1}$	E^o (V, NHE)[a]	$k_{11}\ /M^{-1}\ s^{-1}$ [a]	$\log(k_{22})+16.9\ E^o_{FeIV/III}$
$Fe(Cp)(C_5H_4CH_2OH)$	6.4×10^7	0.52	4.2×10^6	17.8
$Fe(Cp)(C_5H_4COOH)$	1.2×10^7	0.70	4.2×10^6	19.4
$Os(phen)_3^{2+}$	2.5×10^5	0.84	2×10^9	15.7
Na_3IrCl_6	1.3×10^6	0.892	2.3×10^5	21.9
$Ni(cyclam)^{2+}$	4.9×10^7	0.95	2.0×10^3	28.1
$Fe(C_5H_4COOH)_2$	1.0×10^6	0.86	4.2×10^6	19.9
$Ni(hmc)^{2+}$	1.2×10^7	1.19	1×10^3	31.3
$HABTS^-$	4.6×10^6	0.81	4×10^7	19.4

* see Tables 1 and 2 footnotes for list of abbreviations.
[a] see table 3 for references and electrochemical conditions.

On the other hand, there is no dependence of the ET reactivity on acid concentration within acid range of 0.05 – 0.2 M and using Na_3IrCl_6 and $Os(phen)_3^{2+}$ as substrates, indicating that there is no prior protonation of $Fe_{aq}^{IV}O^{2+}$ and that the reactions proceed by electron transfer, forming $Fe_{aq}^{III}O^{+}$, followed by rapid protonation to form $Fe_{aq}^{III}OH^{2+}$ (equation 2, Scheme 1).

The findings that $Os(phen)_3^{2+}$ reacts through outer-sphere mechanism and shows no reactivity dependence on acid concentration suggest that the $Fe_{aq}^{IV}O^{2+}/Fe_{aq}^{III}O^{+}$ potential cannot be much lower than that for $Os(phen)_3^{3+}$/ $Os(phen)_3^{2+}$ couple (0.84 V vs. NHE), since the reaction equilibrium is always driven in the forward direction by the immediate protonation of the $Fe_{aq}^{III}O^{+}$.

In a previously study,[19] the reactions of some synthetic Fe(IV)-oxo complexes, bearing tetradentate N4 ligands, and ferrocenes as electron donor (see Table 5) have been reported to proceed by outer-sphere ET mechanism. In addition, the reactivities of the synthetic Fe(IV)-oxo complexes were compared to horseradish peroxidase (HRP) compound I and compound II (compound I contains a ferryl iron weakly spin-coupled to a porphyrin π-radical cation and compound II has ferryl iron center) and it was found that HRP-I has the highest reactivity due to the lowest reorganization energy and high reduction potential (see Table 5). A comparison for the reactivity of $Fe_{aq}^{IV}O^{2+}$ versus HRP with the ferrocenes used in this study is shown in Table 5. Compound I reacts 100-times faster than compound II which control the rate limiting step in HRP reactions.

Table 5 shows that $Fe_{aq}^{IV}O^{2+}$ rate constants are the highest among the other studied synthetic and enzymatic Fe(IV)-oxo complexes with ~10-times faster than the highly reactive HRP compound I. In addition, the ferrocenes used with the synthetic Fe(IV)-oxo complexes utilize lower reduction potential range than the ferrocenes used in this study, and the HRP

reactions were studied at ~ pH 6 where $Fe(Cp)(C_5H_4COOH)$ and $Fe(C_5H_4COOH)_2$ have shown to have lower reduction potential due to the deprotonation of the COOH group at higher pH,[57,58] which might suggest even lower rate constants of the other Fe(IV)-oxo complexes reactions under our conditions.

Despite the difficulties to study the redox chemistry of $Fe_{aq}^{IV}O^{2+}$ and the insufficient information about its precise ET properties, $Fe_{aq}^{IV}O^{2+}$ species are shown to be highly reactive and capable of oxidizing wide range of substrates including Ce^{3+} ($E^{o}_{Ce4+/3+}$ = 1.7 V) with ~ 10^4 M^{-1} s^{-1} ET rate constant.

Table 5. Rate Constants for Ferrocenes Reactions with Tetradentate N4-Fe(IV)-oxo Complexes, HRP and $Fe_{aq}^{IV}O^{2+}$. [a]

Electron donor	E_{ox} (V)	k_{ET} (M^{-1} s^{-1})						
		1 [b] E = 0.63 V	**2** [b] E = 0.73 V	**3** [b] E = 0.75 V	**4** [c] E = 0.97 V	HRP [d] steady state	HRP-I [d] E = ~ 0.9 V	$Fe_{aq}^{IV}O^{2+}$
Ferrocene	0.61	14	24	5	4.9×10^3	1.9×10^5	-	-
Dimethylferrocene	0.50	1.0×10^2	1.0×10^2	24	-	-	-	-
Decamethylferrocene	0.16	6.3×10^4	4.3×10^4	7.0×10^3	-	-	-	-
$Fe(Cp)(C_5H_4CH_2OH)$	0.52	-	-	-	-	3.56×10^4	-	6.4×10^7
$Fe(Cp)(C_5H_4COOH)$	0.70	-	-	-	-	8.9×10^3	1×10^6	1.2×10^7
$Fe(C_5H_4COOH)_2$	0.86	-	-	-	-	7.3×10^3	-	1.0×10^6

1 = $(TMC)Fe^{IV}(O)(NCCH_3)^{2+}$,[75] **2** = $(Bn\text{-}TPEN)Fe^{IV}(O)^{2+}$,[18] **3** = $(N4Py)Fe^{IV}(O)^{2+}$ [18] and **4** = $(bisp)Fe^{IV}(O)(NCCH_3)^{2+}$ [20], where TMC = 1,4,8,11-tetra-methyl-1,4,8,11-tetraazacyclotetradecane; Bn-TPEN = N-benzyl-N,N′,N′-tris(2-pyridylmethyl)ethane-1,2-diamine; N4Py = N,N-bis(2-pyridylmethyl)-N-bis(2-pyridyl)methylamine; bisp = 3,7-diazabicyclo[3.3.1]nonane.

[a] all reported potentials are vs. NHE.

[b] measured in deaerated acetonitrile at 298K. [18,19,75]

[c] measured in deaerated acetonitrile at 238K. [20]

[d] measured at ~ pH 6 at 298 K. [76-79]

Conclusions

Electron transfer properties of $Fe_{aq}^{IV}O^{2+}$ have been investigated with variuos inorganic electron donors. The large measured ET rate constants ~ 10^4 - 10^8 M^{-1} s^{-1} shows how reactive the $Fe_{aq}^{IV}O^{2+}$ species are, toward electron donors. However, substrates reactivities show no straightforward dependence on the reduction potentials indicating a non outer-sphere ET behavior.

The fact that $Os(phen)_3^{2+}$ rate constant was smaller than other substrates utilizing greater reduction potentials, such as Na_3IrCl_6 and Ni(II) macrocyclic tetraamines complexes, and that $Fe_{aq}^{IV}O^{2+}$ failed to oxidize the metal center in other polypyridine complexes having reduction potentials greater than $Os(phen)_3^{2+}$ complex, strongly argues that $Os(phen)_3^{2+}$ reacts by outer-sphere ET mechanism. In addition, changing acid concentration from 0.05 to 0.2 M showed no change in the measured rate constants for $Os(phen)_3^{2+}$ reaction, indicating that there is no prior protonation of $Fe_{aq}^{IV}O^{2+}$ and that $Fe_{aq}^{III}O^{+}$ is formed in the ET step followed by proton transfer to form $Fe_{aq}^{III}OH^{2+}$. In other words, the one electron reduction potential for the $Fe_{aq}O^{2+}$ / $Fe_{aq}O^{+}$ couple cannot be much lower than that for $Os(phen)_3^{3+}$/ $Os(phen)_3^{2+}$ couple (0.84 V vs. NHE).

The reactivity of $Fe_{aq}^{IV}O^{2+}$ toward ferrocenes as electron donors was viewed in comparison to HRP enzyme and other synthtic tetradentate-N4 Fe(IV)-oxo complexes, having reduction potentials up to 0.97 V vs. NHE, and found that $Fe_{aq}^{IV}O^{2+}$ has the highest reactivity. The lack of electron donating coordinating ligands in $Fe_{aq}^{IV}O^{2+}$ provides an electron deficient metal center that exhibits high reactivity toward various electron donors.

Acknowledgment

This research is supported by the U.S. Department of Energy, Office of Science, Basic Energy Sciences, Division of Chemical Sciences, Geosciences, and Biosciences through the Ames Laboratory. The Ames Laboratory is operated for the U.S. Department of Energy by Iowa State University under Contract DE-AC02-07CH11358.

Supplemental Information

Figures S1-S12 and Table S1 are shown in Appendix C.

References

(1) Abu-Omar, M. M.; Loaiza, A.; Hontzeas, N. *Chemical Reviews* **2005**, *105*, 2227.

(2) Costas, M.; Mehn, M. P.; Jensen, M. P.; Que, L. *Chemical Reviews* **2004**, *104*, 939.

(3) Tshuva, E. Y.; Lippard, S. J. *Chemical Reviews* **2004**, *104*, 987.

(4) Shaik, S.; Lai, W.; Chen, H.; Wang, Y. *Accounts of Chemical Research* **2010**, *43*, 1154.

(5) Zhang, R.; Newcomb, M. *Accounts of Chemical Research* **2008**, *41*, 468.

(6) Rohde, J.-U.; In, J.-H.; Lim, M. H.; Brennessel, W. W.; Bukowski, M. R.; Stubna, A.; Münck, E.; Nam, W.; Que, L. *Science* **2003**, *299*, 1037.

(7) Ray, K.; England, J.; Fiedler, A. T.; Martinho, M.; Münck, E.; Que, L. *Angewandte Chemie International Edition* **2008**, *47*, 8068.

(8) Wang, D.; Ray, K.; Collins, M. J.; Farquhar, E. R.; Frisch, J. R.; Gomez, L.; Jackson, T. A.; Kerscher, M.; Waleska, A.; Comba, P.; Costas, M.; Que, L. *Chemical Science* **2013**, *4*, 282.

(9) Kostka, K. L.; Fox, B. G.; Hendrich, M. P.; Collins, T. J.; Rickard, C. E. F.; Wright, L. J.; Munck, E. *Journal of the American Chemical Society* **1993**, *115*, 6746.

(10) Que, L. *Accounts of Chemical Research* **2007**, *40*, 493.

(11) Nam, W. *Accounts of Chemical Research* **2007**, *40*, 522.

(12) Kaizer, J.; Klinker, E. J.; Oh, N. Y.; Rohde, J.-U.; Song, W. J.; Stubna, A.; Kim, J.; Münck, E.; Nam, W.; Que, L. *Journal of the American Chemical Society* **2003**, *126*, 472.

(13) Lim, M. H.; Rohde, J.-U.; Stubna, A.; Bukowski, M. R.; Costas, M.; Ho, R. Y. N.; Münck, E.; Nam, W.; Que, L. *Proceedings of the National Academy of Sciences* **2003**, *100*, 3665.
(14) Oh, N. Y.; Suh, Y.; Park, M. J.; Seo, M. S.; Kim, J.; Nam, W. *Angewandte Chemie International Edition* **2005**, *44*, 4235.

(15) Park, M. J.; Lee, J.; Suh, Y.; Kim, J.; Nam, W. *Journal of the American Chemical Society* **2006**, *128*, 2630.

(16) Nam, W.; Lee, Y.-M.; Fukuzumi, S. *Accounts of Chemical Research* **2014**, *47*, 1146.

(17) Hong, S.; Lee, Y.-M.; Cho, K.-B.; Sundaravel, K.; Cho, J.; Kim, M. J.; Shin, W.; Nam, W. *Journal of the American Chemical Society* **2011**, *133*, 11876.

(18) Lee, Y.-M.; Kotani, H.; Suenobu, T.; Nam, W.; Fukuzumi, S. *Journal of the American Chemical Society* **2007**, *130*, 434.

(19) Fukuzumi, S. *Coordination Chemistry Reviews* **2013**, *257*, 1564.

(20) Comba, P.; Fukuzumi, S.; Kotani, H.; Wunderlich, S. *Angewandte Chemie International Edition* **2010**, *49*, 2622.

(21) Melton, J. D.; Bielski, B. H. J. *International Journal of Radiation Applications and Instrumentation. Part C. Radiation Physics and Chemistry* **1990**, *36*, 725.

(22) Wang, D.; Zhang, M.; Bühlmann, P.; Que, L. *Journal of the American Chemical Society* **2010**, *132*, 7638.

(23) Conocchioli, T. J.; Hamilton, E. J.; Sutin, N. *Journal of the American Chemical Society* **1965**, *87*, 926.

(24) Bataineh, H.; Pestovsky, O.; Bakac, A. *Chemical Science* **2012**, *3*, 1594.

(25) Pestovsky, O.; Stoian, S.; Bominaar, E. L.; Shan, X.; Münck, E.; Que, L.; Bakac, A. *Angewandte Chemie International Edition* **2005**, *44*, 6871.

(26) Jacobsen, F.; Holcman, J.; Sehested, K. *International Journal of Chemical Kinetics* **1998**, *30*, 215.

(27) Loegager, T.; Holcman, J.; Sehested, K.; Pedersen, T. *Inorganic Chemistry* **1992**, *31*, 3523.

(28) Pestovsky, O.; Bakac, A. *Journal of the American Chemical Society* **2004**, *126*, 13757.

(29) Pestovsky, O.; Bakac, A. *Inorganic Chemistry* **2005**, *45*, 814.

(30) Hug, S. J.; Leupin, O. *Environmental Science & Technology* **2003**, *37*, 2734.

(31) Park, J.; Morimoto, Y.; Lee, Y.-M.; Nam, W.; Fukuzumi, S. *Journal of the American Chemical Society* **2012**, *134*, 3903.
(32) Park, J.; Morimoto, Y.; Lee, Y.-M.; Nam, W.; Fukuzumi, S. *Journal of the American Chemical Society* **2011**, *133*, 5236.

(33) Park, J.; Morimoto, Y.; Lee, Y.-M.; You, Y.; Nam, W.; Fukuzumi, S. *Inorganic Chemistry* **2011**, *50*, 11612.

(34) Huynh, M. H. V.; Meyer, T. J. *Chemical Reviews* **2007**, *107*, 5004.

(35) Weinberg, D. R.; Gagliardi, C. J.; Hull, J. F.; Murphy, C. F.; Kent, C. A.; Westlake, B. C.; Paul, A.; Ess, D. H.; McCafferty, D. G.; Meyer, T. J. *Chemical Reviews* **2012**, *112*, 4016.

(36) Bakac, A.; Brynildson, M. E.; Espenson, J. H. *Inorganic Chemistry* **1986**, *25*, 4108.

(37) Bosnich, B.; Tobe, M. L.; Webb, G. A. *Inorganic Chemistry* **1965**, *4*, 1109.

(38) Warner, L. G.; Busch, D. H. *Journal of the American Chemical Society* **1969**, *91*, 4092.

(39) Lin, C. T.; Boettcher, W.; Chou, M.; Creutz, C.; Sutin, N. *Journal of the American Chemical Society* **1976**, *98*, 6536.

(40) Hart, E. J.; Sehested, K.; Holoman, J. *Analytical Chemistry* **1983**, *55*, 46.

(41) Lee, S.; Bakac, A.; Espenson, J. H. *Inorganic Chemistry* **1989**, *28*, 1367.

(42) Scott, S. L.; Chen, W. J.; Bakac, A.; Espenson, J. H. *The Journal of Physical Chemistry* **1993**, *97*, 6710.

(43) Hurwitz, P.; Kustin, K. *Inorganic Chemistry* **1964**, *3*, 823.

(44) Heidt, L. J.; Smith, M. E. *Journal of the American Chemical Society* **1948**, *70*, 2476.

(45) Sarala, R.; Rabin, S. B.; Stanbury, D. M. *Inorganic Chemistry* **1991**, *30*, 3999.

(46) Haines, R. I.; McAuley, A. *Inorganic Chemistry* **1980**, *19*, 719.

(47) Kato, S.; Jung, J.; Suenobu, T.; Fukuzumi, S. *Energy & Environmental Science* **2013**, *6*, 3756.

(48) Creutz, C.; Sutin, N. *Proceedings of the National Academy of Sciences* **1975**, *72*, 2858.

(49) Schmid, R.; Kirchner, K.; Dickert, F. L. *Inorganic Chemistry* **1988**, *27*, 1530.

(50) Puzanowska-Tarasiewicz, H.; Grudniewska, A.; Tarasiewicz, M. *Analytica Chimica Acta* **1977**, *94*, 435.

(51) Bahnemann, D.; Asmus, K.-D.; Willson, R. L. *Journal of the Chemical Society, Perkin Transactions 2* **1983**, 1661.

(52) Tomiyasu, T.; Sakamoto, H.; Yonehara, N. *Analytica Chimica Acta* **1996**, *320*, 217.

(53) Madej, E.; Wardman, P. *Radiation Physics and Chemistry* **2006**, *75*, 990.

(54) Borg, D. C.; Cotzias, G. C. *Proc Natl Acad Sci U S A* **1962**, *48*, 623.

(55) Cavanaugh, D. J. *Science* **1957**, *125*, 1040.

(56) Pladziewicz, J. R.; Espenson, J. H. *Journal of the American Chemical Society* **1973**, *95*, 56.

(57) Kutner, W.; Doblhofer, K. *Journal of Electroanalytical Chemistry* **1992**, *326*, 139.

(58) Faraggi, M.; Weinraub, D.; Broitman, F.; DeFelippis, M. R.; Klapper, M. H. *International Journal of Radiation Applications and Instrumentation. Part C. Radiation Physics and Chemistry* **1988**, *32*, 293.

(59) Margerum, D. W.; Chellappa, K. L.; Bossu, F. P.; Burce, G. L. *Journal of the American Chemical Society* **1975**, *97*, 6894.

(60) Hurwitz, P.; Kustin, K. *Transactions of the Faraday Society* **1966**, *62*, 427.

(61) Nord, G.; Pedersen, B.; Farver, O. *Inorganic Chemistry* **1978**, *17*, 2233.

(62) Zeigerson, E.; Ginzburg, G.; Meyerstein, D.; Kirschenbaum, L. J. *Journal of the Chemical Society, Dalton Transactions* **1980**, 1243.

(63) Anuradha, S.; Vijayaraghavan, V. *Journal of Chemical Sciences* **2013**, *125*, 1123.

(64) McAuley, A.; Macartney, D. H.; Oswald, T. *Journal of the Chemical Society, Chemical Communications* **1982**, 274.

(65) Zeigerson, E.; Bar, I.; Bernstein, J.; Kirschenbaum, L. J.; Meyerstein, D. *Inorganic Chemistry* **1982**, *21*, 73.

(66) Smith, G. F.; Getz, C. A. *Industrial & Engineering Chemistry Analytical Edition* **1938**, *10*, 191.

(67) Wangila, G. W.; Jordan, R. B. *Inorganica Chimica Acta* **2005**, *358*, 3753.

(68) Young, R. C.; Keene, F. R.; Meyer, T. J. *Journal of the American Chemical Society* **1977**, *99*, 2468.

(69) Brandt, W. W.; Gullstrom, D. K. *Journal of the American Chemical Society* **1952**, *74*, 3532.

(70) Doine, H.; Swaddle, T. W. *Canadian Journal of Chemistry* **1988**, *66*, 2763.

(71) Karpinska, J.; Starczweska, B.; Puzanowska-Tarasiewicz, H. *Analytical Sciences* **1996**, *12*, 10.

(72) Brunschwig, B. S.; Sutin, N. *Inorganic Chemistry* **1979**, *18*, 1731.

(73) Marcus, R. A. *Annual Review of Physical Chemistry* **1964**, *15*, 155.

(74) Poulsen, I. A.; Garner, C. S. *Journal of the American Chemical Society* **1962**, *84*, 2032.

(75) Fukuzumi, S.; Kotani, H.; Suenobu, T.; Hong, S.; Lee, Y.-M.; Nam, W. *Chemistry – A European Journal* **2010**, *16*, 354.

(76) Farhangrazi, Z. S.; Fossett, M. E.; Powers, L. S.; Ellis, W. R. *Biochemistry* **1995**, *34*, 2866.

(77) Sadeghi, S. J.; Gilardi, G.; Cass, A. E. G. *Biosensors and Bioelectronics* **1997**, *12*, 1191.

(78) Goral, V. N.; Ryabov, A. D. *Biochem Mol Biol Int* **1998**, *45*, 61.

(79) Ryabov, A. D.; Goral, V. N. *JBIC* **1997**, *2*, 182.

GENERAL CONCLUSIONS

The chemistry of iron(IV) complexes in the absence of stabilizing ligands is still not well-understood. Their high reactivity and short life time make it difficult to study their chemistry. In addition, the chemical environment is another factor that need to be taken into consideration when study these complexes. Our data and results have shown that a moderate change in the reaction conditions lead to a dramatic change in the chemistry and life time of these species.

Fe(IV) has always been invoked as in alternative intermediate to the hydroxyl radical in the reaction of Fe(II) and H_2O_2 (Fenton reaction).[1] The lack of the right substrate to distinguish between the two, OH radical and Fe(IV), in addition to the fact that different studies were done under different reaction conditions made it difficult to provide solid evidence on Fe(IV) formation. Now, we have shown that the intermediate in Fenton reaction changes form hydroxyl radical at pH $\leq$ 3 to Fe(IV) at near neutral pH. This was shown by the oxidation of $(CH_3)_2SO$ to $(CH_3)_2SO_2$, indicative of Fe(IV), and the regeneration of Fe(II) at pH 6-7. The OH radical reaction with $(CH_3)_2SO$ forms methylsulfinic acid, ethane and Fe(III) but only at pH $\leq$ 3.[2] However, large concentrations of $(CH_3)_2SO$ were needed to achieve significant turnover numbers at pH 6-7 owing to the rapid competing reaction between Fe(II) and Fe(IV) that leads to irreversible loss of the catalyst (Fe(II)).

When the reaction was run at pH 6-7 but in of phosphate buffer, instead of the used non-coordinating buffers. Products were changed to ethane and methylsulfinat, indicative of OH radicals, and strikingly showing how this reaction is sensitive to the chemical environment.

On the other hand, $(H_2O)_5FeO^{2+}$ generated in the reaction of $Fe(H_2O)_6^{2+}$ and O_3 reacts with alcohols, ethers and aldehydes through two parallel 1-e (H-atom transfer) and 2-e (hydride transfer) pathways.[3] The hydride path is catalytic as it generates $Fe(H_2O)_6^{2+}$ which can be reoxidized to $(H_2O)_5FeO^{2+}$. However, the catalytic efficiency is poor because of the loss of the catalyst ($Fe(H_2O)_6^{2+}$ as $(Fe(H_2O)_6^{3+}$ in the 1-e path. In this work we have shown that the reaction becomes catalytically efficient by changing the solvent to CH_3CN. Beside, greater selectivity toward the less oxidized product is observed and > 80% of the catalyst ($Fe(CH_3CN)_6^{2+}$) was regenerated even when only sub-millimolar concentrations of $Fe(CH_3CN)_6^{2+}$ were used. However, the catalyze oxidations of alcohols showed 70-85% products yields, unlike ethylether and $(CH_3)_2SO$ who showed 100% yields; This and the non-complete recovery of the catalyst indicate that the non-catalytic 1-e path is still involved. However, the 1-e path does not terminate the catalytic cycle as in water. This could be rationalized by the difference in the redox thermodynamics of iron in the two solvents and the acid-base chemistry of superoxide radical, $HO_2^{\bullet}/O_2^{\bullet-}$. The two-electron path is much more prominent in acetonitrile, presumably because it avoids the strongly oxidizing Fe(III) (E = 1.6 V vs. NHE)[4]. On the other hand, superoxide radical expected to form in the 1-e path is a key intermediate in the chain decomposition of O_3.[5-10] In acetonitrile $O_2^{\bullet-}$ is strong reductant (E^0 $(O_2/O_2^{\bullet-})$ = -0.80 V vs. NHE)[11] which rapidly reduces Fe(III) back to Fe(II). However, under acidic conditions the superoxide is protonated ($HO_2^{\bullet}$) and incapable of reducing $Fe(H_2O)_6^{3+}$. This proposal was tested by adding Fe(III) to the reaction mixture in acetonitrile. The presences of Fe(III) at the beginning of the reaction enhanced the alcohols yields and showed > 100% Fe(II) at the end of the reaction, proving that Fe(III) was reduced during the reactions and that the ozone decomposition was reduced.

Finally, the electron transfer reactivity of $Fe_{aq}^{IV}O^{2+}$ have been investigated with variuos inorganic and some organic substrates having reduction potentials ranging from 0.52 to 1.7 V vs. NHE. Most of the substrates have shown to react with $Fe_{aq}^{IV}O^{2+}$ quantitatively producing the 1-e oxidation product except for the phenothiazines who reacted by oxygen atom tranfer and produced the corresponding sulfoxide. Also, the reactions with the polypyridyl complexes of Fe(II) and Ru(II) did no oxidize the matal center.

The fact that $Os(phen)_3^{2+}$ rate constant was smaller than other substrates utilizing greater reduction potentials, and that $Fe_{aq}^{IV}O^{2+}$ failed to oxidize the metal center in other polypyridine complexes having reduction potentials greater than $Os(phen)_3^{2+}$ complex, strongly argues that $Os(phen)_3^{2+}$ reacts by outer-sphere ET mechanism. In addition, the no dependence of $Os(phen)_3^{2+}$ reactivity on acid concentration (0.05 – 0.2 M) indicates no prior protonation of the $Fe_{aq}^{IV}O^{2+}$, which is consistent with stepwise electron-transfer followed by proton transfer. Results suggest that the $Fe_{aq}^{IV}O^{2+}/Fe_{aq}^{III}O^{+}$ potential is not much lower than that for $Os(phen)_3^{3+}/Os(phen)_3^{2+}$ couple (0.84 V vs. NHE).

The fact that $Fe_{aq}^{IV}O^{2+}$ is capable of oxidizing wide range of metal compounds including Ce^{3+} (E^{o}_{red} = 1.7 V)[12] with ~ 10^4 M^{-1} s^{-1} and other metals with rate constant up to ~10^8 M^{-1} s^{-1} reveals its oxidation power.

References

(1) Bray, W. C.; Gorin, M. H. *Journal of the American Chemical Society* **1932**, *54*, 2124.

(2) Pestovsky, O.; Stoian, S.; Bominaar, E. L.; Shan, X.; Münck, E.; Que, L.; Bakac, A. *Angewandte Chemie International Edition* **2006**, *45*, 340.

(3) Pestovsky, O.; Bakac, A. *Journal of the American Chemical Society* **2004**, *126*, 13757.

(4) Sugimoto, H.; Sawyer, D. T. *J. Am. Chem. Soc.* **1985**, *107*, 5712-5716.

(5) Flyunt, R.; Leitzke, A.; Mark, G.; Mvula, E.; Reisz, E.; Schick, R.; von Sonntag, C. *The Journal of Physical Chemistry B* **2003**, *107*, 7242-7253.

(6) Langlais, B.; Reckhow, D. A.; Brink, D. R. In *Am Water Works Res*; CRC press: 1991.

(7) Gonzalez, M. C.; Mártire, D. O. *International Journal of Chemical Kinetics* **1997**, *29*, 589-597.

(8) Gonzalez, M. C.; Mártire, D. O. *Water Science and Technology* **1997**, *35*, 49-55.

(9) Naumov, S.; von Sonntag, C. *Environmental Science & Technology* **2011**, *45*, 9195-9204.

(10) Rush, J. D.; Bielski, B. H. J. *The Journal of Physical Chemistry* **1985**, *89*, 5062-5066.

(11) Sawyer, D. T.; Valentine, J. S. *Accounts of Chemical Research* **1981**, *14*, 393-400.

(12) Smith, G. F.; Getz, C. A. *Industrial & Engineering Chemistry Analytical Edition* **1938**, *10*, 191.

APPENDIX A

pH-INDUCED MECHANISTIC CHANGEOVER FROM HYDROXYL RADICALS TO IRON(IV) IN THE FENTON REACTION

Additional experimental detail

The following chemicals were obtained commercially and used as received: iron(II) perchlorate hydrate (98%), iron(III) perchlorate hydrate (low chloride < 0.005%), deuterio perchloric acid $DClO_4$ (68 wt% in D_2O, 99+ atom % D), titanium(IV) oxysulfate (99.99% purity, 15 wt% solution in dilute sulfuric acid), deuterium oxide (99.9 atom %D), (R)-(+)-methyl *p*-tolyl sulfoxide (99%), and 1,10-phenanthroline (99+ %) (all Aldrich), dimethyl sulfoxide (≥ 99.9%, A.C.S spectrophotometric grade, Sigma-Aldrich), sodium hydroxide (99.1%), hydrogen peroxide (30 wt%), perchloric acid (70 wt%), anhydrous dibasic sodium phosphate (all Fisher), monobasic sodium phosphate monohydrate (Baker) piperazine-N,N'-bis(4-butanesulfonic acid) (PIPBS), 4-(N-morpholino)butanesulfonic acid (MOBS), 3-(N-morpholino)-propanesulfonic acid (MOPS), and 2-(N-morpholino)ethanesulfonic acid (MES) (all GFS).

Stock solutions of iron(II) perchlorate in H_2O or D_2O were prepared freshly before each set of experiments and standardized with phenanthroline. Solutions of H_2O_2 were standardized with titanium oxysulfate[1] which places a reliable detection limit at 0.02 mM H_2O_2. Deionized water was further purified by passage through a Barnstead Easy Pure II -UV/UF water purifier.

UV-Vis absorbance measurements and kinetic studies used a Shimadzu UV-3101 PC spectrophotometer, Olis RSM-1000 stopped-flow instrument, and Applied Photophysics (APP) sequential stopped-flow DX-17MV at 25.0 ± 0.1 °C. Gaseous products were analyzed by an Agilent Technologies 7890A GC gas chromatograph equipped with a FID detector and a 15-m capillary column (GS-GASPRO), 0.320 mm I.D. Nitrogen flow rate was constant at 25 cm^3/s.

Both the split injector (1:40) and FID detector were held at 200^0 C. The initial oven temperature was 40^0 C, and was increased by 10^0 C/min. ^{1}H-NMR spectra were recorded with a 400 MHz Bruker DRX-400 spectrometer at room temperature. The pH was measured with an Accumet AP71 pH meter. Kinetic experiments were performed at 25.1 $\pm 0.1^0$ C.

Procedures All of the solutions were purged with argon before mixing and appeared clear to the eye in both tertiary amine and phosphate buffers prior to and during the reaction. The solvent was H_2O for kinetic studies, and D_2O for NMR product analysis. The pH (pD) was controlled with noncoordinating tertiary amine buffers MES (pK_a 6.06), MOPS (pK_a 7.09), MOBS (pK_a 7.48) and PIPBS (pK_{a1} 4.29, pK_{a2} 8.55)[2] or with phosphate buffers (pH 6-8). Buffer concentrations were typically 8-50 times greater than the concentration of the limiting reagents, i. e. at the level required to hold the pH at the desired value without interfering with the NMR spectra or altering the chemistry. The pH decrease in kinetics experiments was less than 0.2 units. In the NMR experiments, which typically used 1-2 mM of Fe(II) and H_2O_2, the pD decrease was typically 0.3-0.5 units. Solutions were acidified before the NMR spectra were recorded. Concentrations of Fe(II) in spent reaction solutions were determined with phenanthroline. A correction was applied for the absorbance of iron(III)-phenanthroline as previously described.[3]

The stoichiometry was determined from absorbance changes at 270 nm using $\Delta\varepsilon_{270}$ = 2650±50 M^{-1} cm^{-1} at pH 6-7. This value was determined by oxidizing a solution of Fe(II) (0.010 - 0.020 mM) with excess H_2O_2 (0.1 - 1.5 mM) in the stopped-flow and monitoring the absorbance for up to 30 seconds after the completion of the reaction. During this time, the reading remained constant and yielded ε_{270} = 2600±50 M^{-1} cm^{-1}. Several experiments were also performed on a longer time scale by mixing the reagents (0.02 mM Fe(II) and 0.2 mM H_2O_2 in

0.6 mM MES or MOPS buffer) in a spectrophotometric cell and monitoring the absorbance with a conventional spectrophotometer. The absorbance after the completion of the reaction remained constant for at least five minutes and yielded $\varepsilon_{270} = 2700 \pm 50\ M^{-1}\ cm^{-1}$. The constancy of ε_{270} on millisecond-to-minute time scale confirms that the turbidity or precipitation of iron(III) did not affect absorbance readings. This point is also illustrated in the kinetic plots in Figures S6-S8. The three experiments had identical initial concentrations of Fe(II) and H_2O_2 (in excess), while the concentration of $(CH_3)_2SO$ was varied. The reaction times varied over a factor of 14, but the overall absorbance change was the same within the experimental error, showing again that changes in the degree of hydrolysis or agglomeration of the Fe(III) product either did not take place or had no effect on the absorbance around 270 nm.

Product analysis by NMR. A solution of hydrogen peroxide was added to a magnetically stirred solution of $Fe(H_2O)_6^{2+}/Fe(H_2O)_5OH^+$ ($pK_a = 9.5$)[4] and substrate in D_2O buffered at the desired pD under argon. The pH was measured before and after the reaction, and converted to pD by adding 0.4 to the measured value. Immediately after the completion of the reaction, the solutions were acidified to pD 1 with perchloric acid to avoid agglomeration and precipitation of iron(III) hydroxide(s), and the NMR spectrum was run within minutes. Such solutions contained small amounts of unreacted Fe(II) or H_2O_2, but not both, so that no additional oxidation of the substrate could take place after the acidification. Acetonitrile (0.79 mM) was used as internal standard to quantify the products. No shift or broadening of the product resonances was observed in acidified solutions.

In phosphate buffer at pH 7, the products are ethane (60% yield by GC) and methylsulfinate (25% by NMR), indicative of $HO^{\bullet}$ radicals. The resonances were somewhat broadened, most likely because solutions of iron(III) became slightly inhomogeneous during the

time required to record the spectrum. The reasons for the lower yields of methylsulfinate are not fully understood, but a portion of the anion may be complexed to the Fe(III) product and thus not detectable by NMR. In acidic solutions, where the binding would be much weaker (pK_a for $CH_3S(O)OH$ is 2.35), the methyl signal for methylsulfinic acid is shifted to 2.50 ppm and appears on the side of the strong $(CH_3)_2SO$ signal (2.55 ppm) which makes the integration imprecise. Under these conditions, a signal for sulfonic acid (2.63 ppm) was also detected, but it was not well separated from DMSO. Control experiments with samples of genuine sulfinic acid confirmed that significant oxidation to sulfonic acid takes place in the time required for (aerobic) manipulation of the solutions and the recording of the spectrum. Despite the difficulties in detecting all of the expected sulfinic acid, the majority of the reaction in phosphate buffers appears to involve hydroxyl radicals based on the data and arguments in the main text, and on the finding that the yields of the accompanying product, ethane, were much higher, about 60% (Table 1).

$$HO^{\bullet} + (CH_3)_2SO \rightarrow CH_3SO_2H + CH_3^{\bullet} (\rightarrow 0.5\ C_2H_6)$$

Stopped-flow experiments. Aqueous solutions of iron(II) were mixed with the buffer and dmso immediately before the experiment and loaded into one of the stopped-flow syringes. The other syringe was filled with the H_2O_2 solution. The formation of Fe(III) was monitored either at 270 nm with the Applied Photophysics APP DX-17MV instrument or in the 260-320 nm range with an Olis RSM-1000 rapid scan instrument.

List of Figures

Figure S9. Plot of k_{obs} vs $[H_2O_2]$ for the Fe(II)/ H_2O_2 reaction at pH 6.1 (MES buffer). Conditions: $[Fe(ClO_4)_2]_0$ = 0.005 – 0.035 mM, [MES] = 0.25 – 0.55 mM, 25 °C. pH decreased during the reaction by 0.2 units, see text.

Figure S10. Plot of k_{obs} vs $[H_2O_2]$ for the Fe(II)/ H_2O_2 reaction at pH 7 in a MOPS buffer. Conditions: $[Fe(ClO_4)_2]_0$ = 0.008 – 0.015 mM, [MOPS] = 0.5 - 0.6 mM, 25 °C. pH decreased during the reaction by 0.2 units, see text.

Figure S11. Plot of k_{obs} vs [Fe(II)] for the Fe(II)/ H_2O_2 reaction at pH 6.1 in a MES buffer. Conditions: $[H_2O_2]_0$ = 0.005 - 0.02 mM, [MES] = 0.5-0.6 mM, 25 °C. pH decreased during the reaction by 0.2 units, see text.

Figure S12. Representative kinetic trace in phosphate buffer. Conditions: 0.031 mM Fe(II), 1.0 mM H_2O_2, pH 6.1 (0.6 mM phosphate buffer)

Figure S13. Plot of pseudo-first-order rate constants for the reaction of $Fe(ClO_4)_2$ with H_2O_2 against the concentration of H_2O_2 in phosphate buffer. Conditions: $[Fe(ClO_4)_2]$ = 0.018 – 0.030 mM, [phosphate] = 0.60 mM, pH = 6.2.

Figure S14. (a) ^1H NMR spectrum of the reaction mixture after the completion of the reaction between $Fe(ClO_4)_2$ (1.0 mM), H_2O_2 (1.0 mM), and $(CH_3)_2SO$ (5 mM) at pD 1 in the presence of 5 mM MES. The reaction generated CH_3SO_2H and C_2H_6 in amounts comparable to those obtained in the absence of MES. b) Mixture of MES (5 mM) and H_2O_2 (1 mM), pD 1. c) MES (5 mM), pD 1.

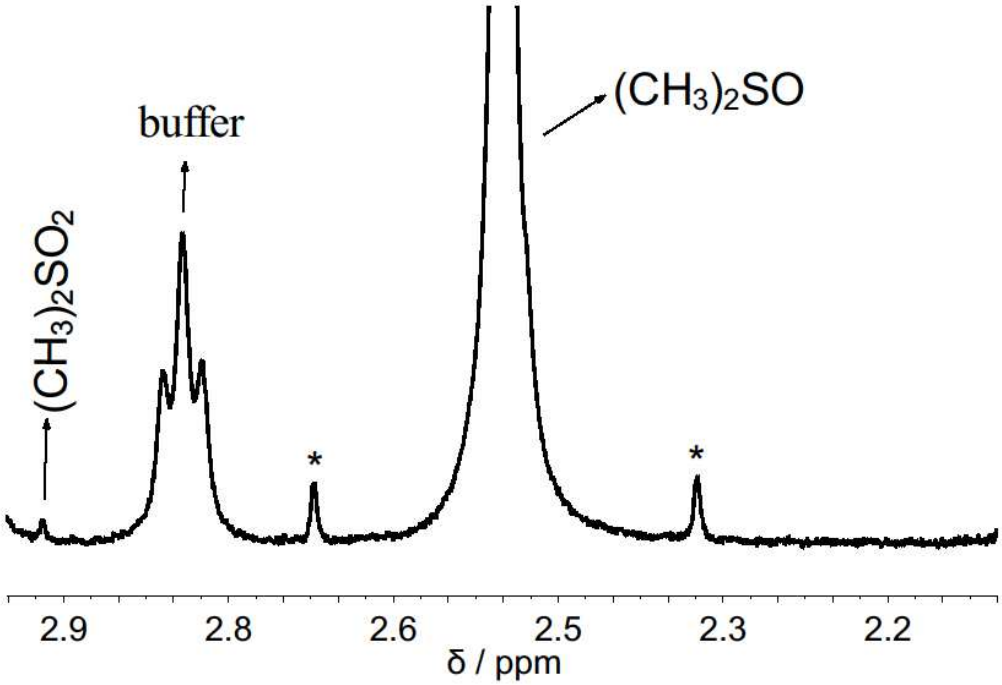

Figure S1. ^{1}H NMR spectrum of the products of the reaction of 1.2 mM $Fe(ClO_4)_2$, 1.1 mM H_2O_2 and 36 mM DMSO in MOPS buffer (11 mM). Initial pD 7.6, final pD 7.2. Spectrum was recorded after acidifying reaction mixture to 0.1 M $DClO_4$. The reaction generated (50 ± 5 μM) $DMSO_2$. ^{13}C satellites are denoted with an asterisk.

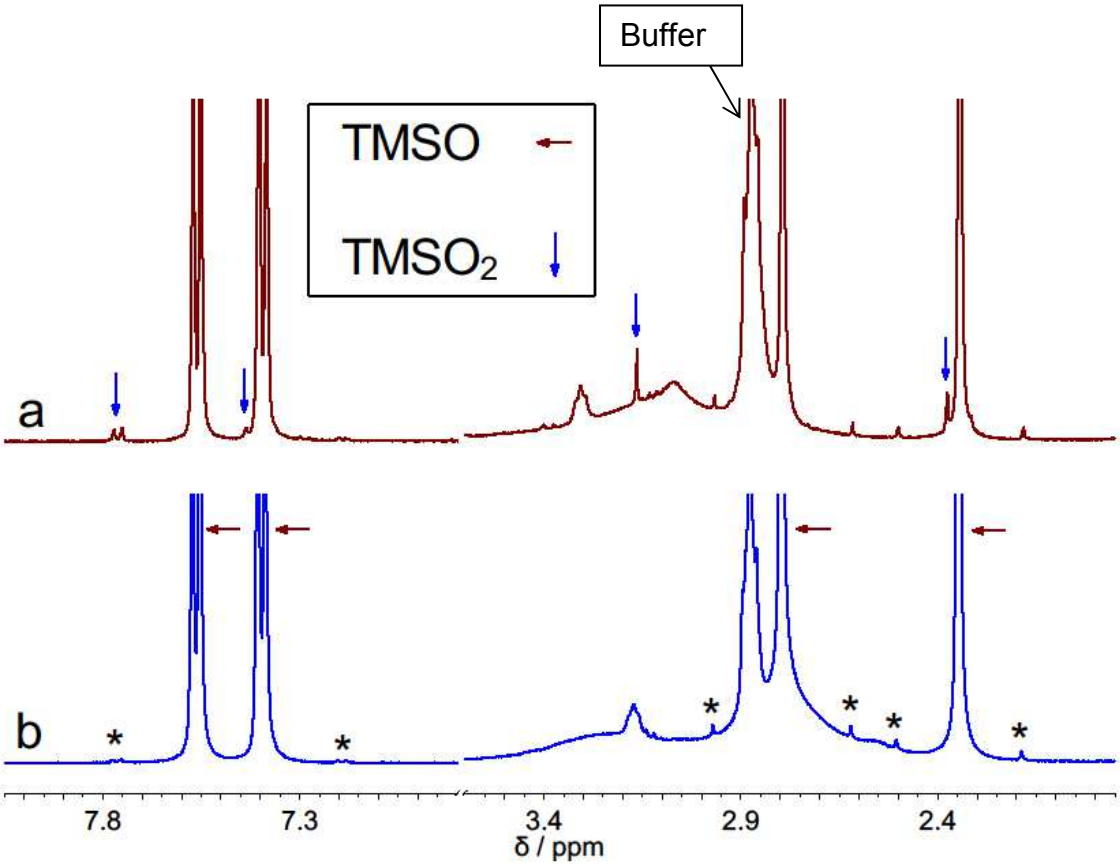

Figure S2. a) 1H NMR spectrum showing $TMSO_2$ (0.65 ± 0.05 mM) generated in the reaction of 1.8 mM $Fe(ClO_4)_2$, 2.4 mM H_2O_2 and 29 mM TMSO in PIPBS buffer (15 mM). Initial pD 7.1, final pD 5.7. **b)** Control experiment: ^1H NMR spectrum of a mixture of H_2O_2 (2.0 mM), TMSO (43 mM) and PIPBS buffer (22 mM) in D_2O, pD 7.1. The spectra were recorded without acidifying the reaction mixtures. ^{13}C satellite peaks are denoted with an asterisk.

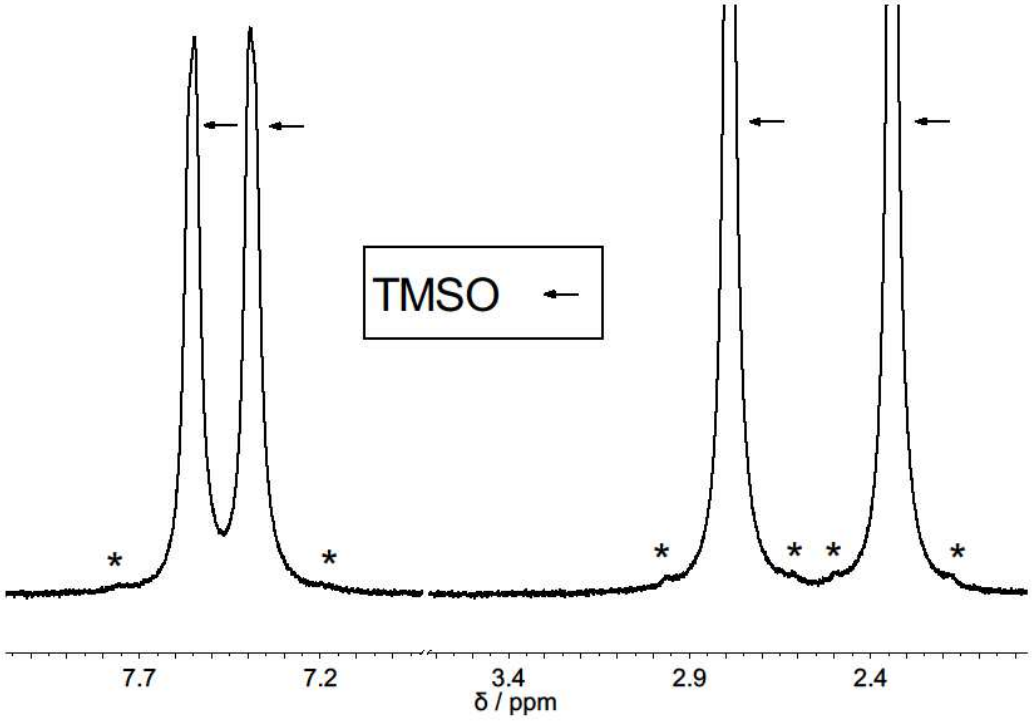

Figure S3. ^{1}H NMR spectrum after the completion of the reaction between 1.0 mM $Fe(ClO_4)_2$, 1.0 mM H_2O_2 and 50 mM TMSO in D_2O, phosphate buffer (20 mM). Initial pD 6.6, final pD 6.0. ^{13}C satellites are denoted with an asterisk.

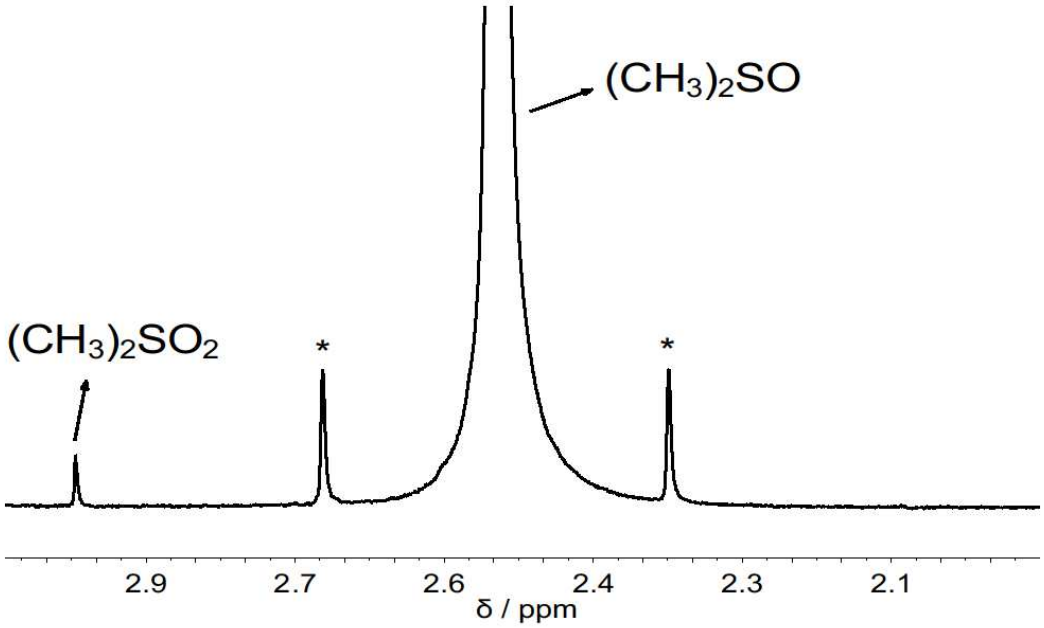

Figure S4. ^{1}H NMR spectrum showing $(CH_3)_2SO_2$ (0.26 mM) generated from the reaction of $Fe(ClO_4)_2$ (0.49 mM), H_2O_2 (0.49 mM) and $(CH_3)_2SO$ (190 mM) in D_2O, MES buffer (9.6 mM), pD 6.7. Spectrum was recorded after acidifying the reaction mixture to 0.1 M $DClO_4$. ^{13}C satellites are denoted with an asterisk.

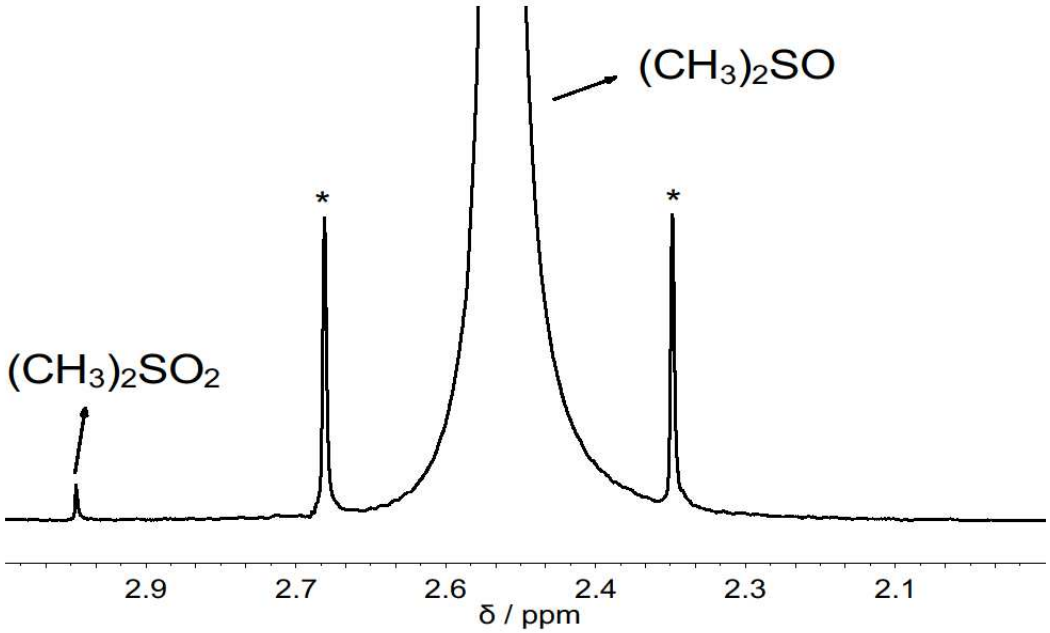

Figure S5 ^{1}H NMR spectrum showing $(CH_3)_2SO_2$ (0.49 mM) generated from the reaction of $Fe(ClO_4)_2$ (0.49 mM), H_2O_2 (0.49 mM) and $(CH_3)_2SO$ (950 mM) in MES buffer (9.6 mM), pD 6.70. Spectrum was recorded after acidifying the reaction mixture to 0.1 M $DClO_4$. ^{13}C satellite peaks are denoted with an asterisk.

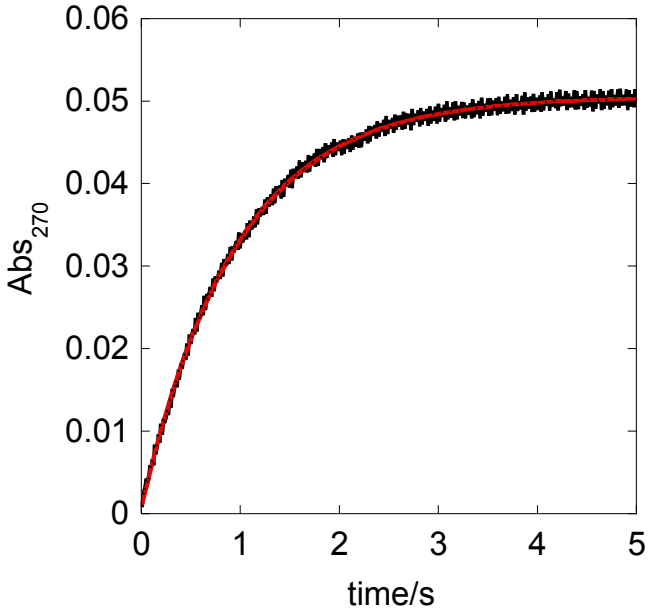

Figure S6. Kinetic (stopped flow) trace for a reaction between 0.020 mM Fe(II) and 0.78 mM H_2O_2 in the absence of DMSO, pH 6.2 (0.56 mM MES)

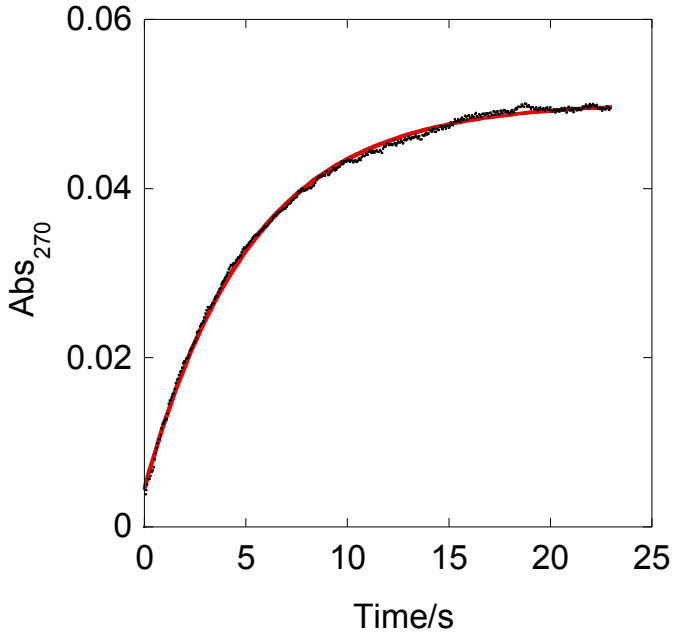

Figure S7. Kinetic (stopped flow) trace for a reaction between 0.020 mM Fe(II) and 0.78 mM H_2O_2 at 0.50 M DMSO, pH 6.2 (0.56 mM MES)

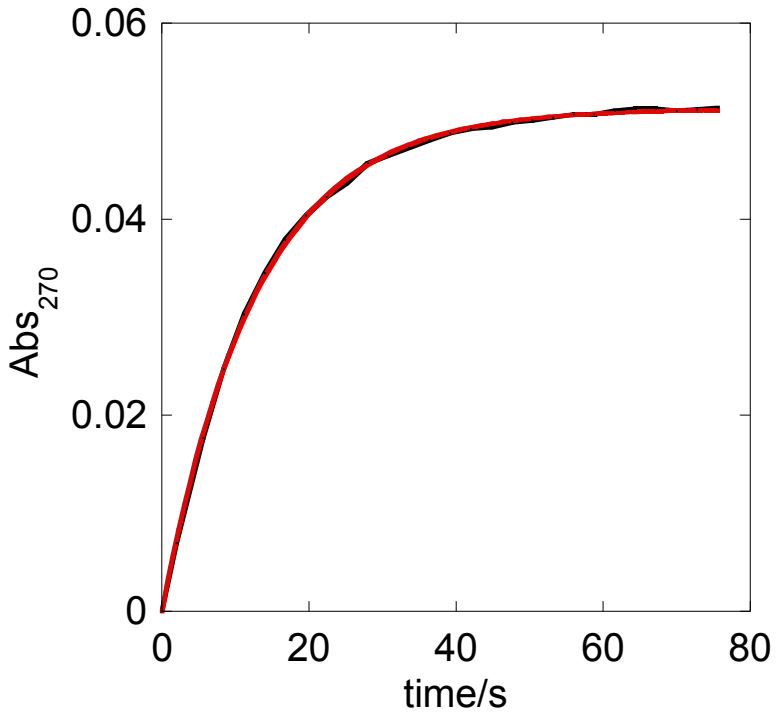

Figure S8. Kinetic (conventional spectrophotometer) trace for a reaction between 0.020 mM Fe(II) and 0.78 mM H_2O_2 at 0.98 M DMSO, pH 6.2 (0.6 mM MES)

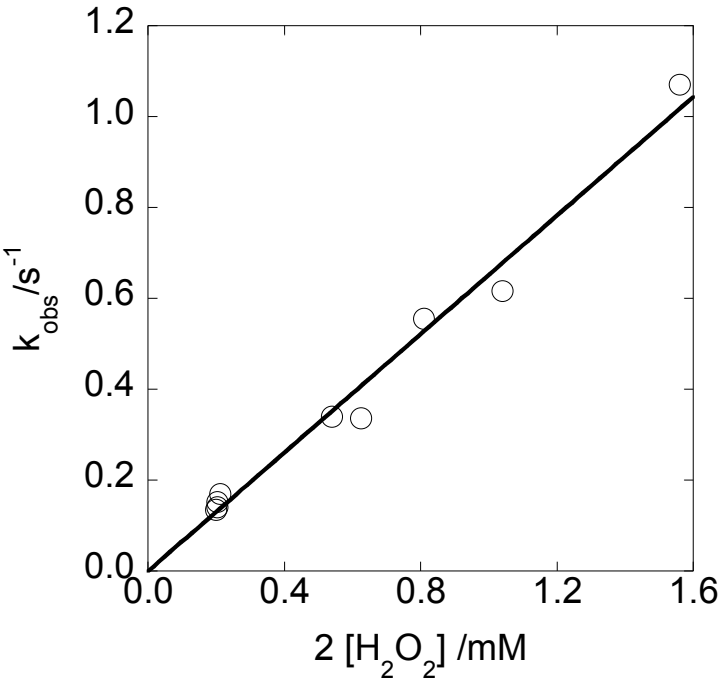

Figure S9. Plot of k_{obs} vs 2[H_2O_2] for the Fe(II)/ H_2O_2 reaction at pH 6.1 in MES buffer. Conditions: [$Fe(ClO_4)_2$]$_0$ = 0.005 – 0.035 mM, [MES] = 0.25 – 0.55 mM, 25 °C. The pH decreased during the reaction by 0.2 units, see text.

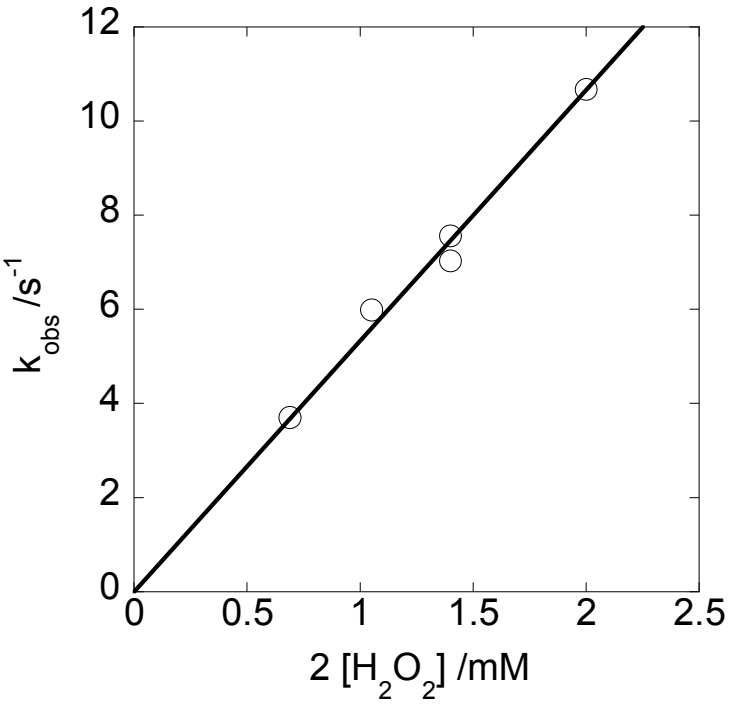

Figure S10. Plot of k_{obs} vs $[H_2O_2]$ for the Fe(II)/ H_2O_2 reaction at pH 7 in a MOPS buffer. Conditions: $[Fe(ClO_4)_2]_0$ = 0.008 – 0.015 mM, [MOPS] = 0.5 - 0.6 mM, 25 °C. pH decreased during the reaction by 0.2 units, see text.

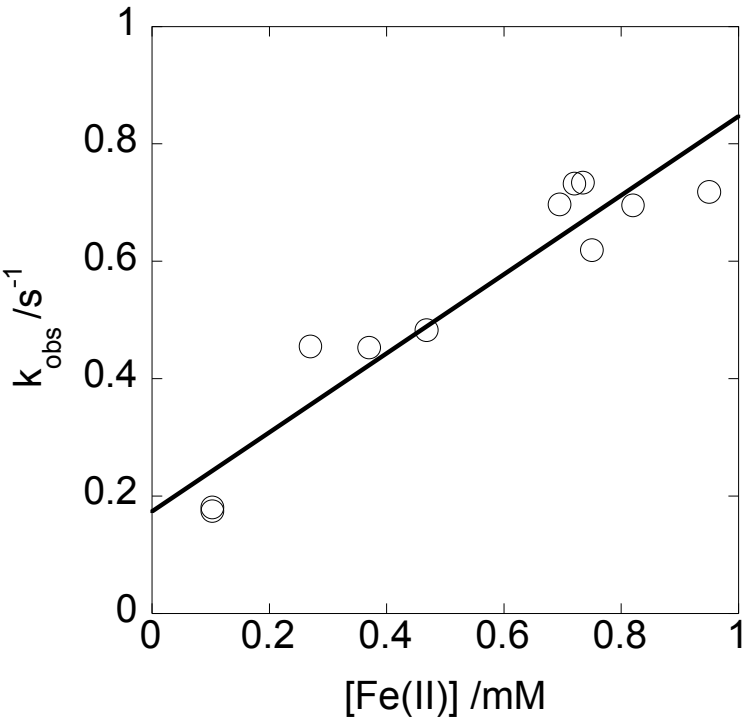

Figure S11. Plot of k_{obs} vs [Fe(II)] for the Fe(II)/ H_2O_2 reaction at pH 6.1 in a MES buffer. Conditions: $[H_2O_2]_0$ = 0.005 - 0.02 mM, [MES] = 0.5-0.6 mM, 25 °C. pH decreased during the reaction by 0.2 units, see text.

Comment on Figure S11. The scatter of the points in Figure S11 is larger than in experiments with excess H_2O_2 (Figs S9 - S10). The plot also exhibits an apparent intercept, but overall the data are in agreement with those obtained with excess H_2O_2 in that the slope of the line in Figure S11 (k_{Fe} = 670 ± 70) $M^{-1}s^{-1}$) is comparable to that obtained by plotting k_{obs} against 2[H_2O_2] in Figure S10 (k_{Fe} = 652 ± 19 $M^{-1}s^{-1}$) for experiments using excess H_2O_2. These results are as expected for the 2:1 [Fe(II)]/[H_2O_2] stoichiometry that was also calculated directly from the observed absorbance changes in these experiments. All of the experiments on catalytic oxidation of sulfoxides required (by definition) excess H_2O_2, conditions that exhibited clean kinetic behavior as shown in Figures S9 and S10.

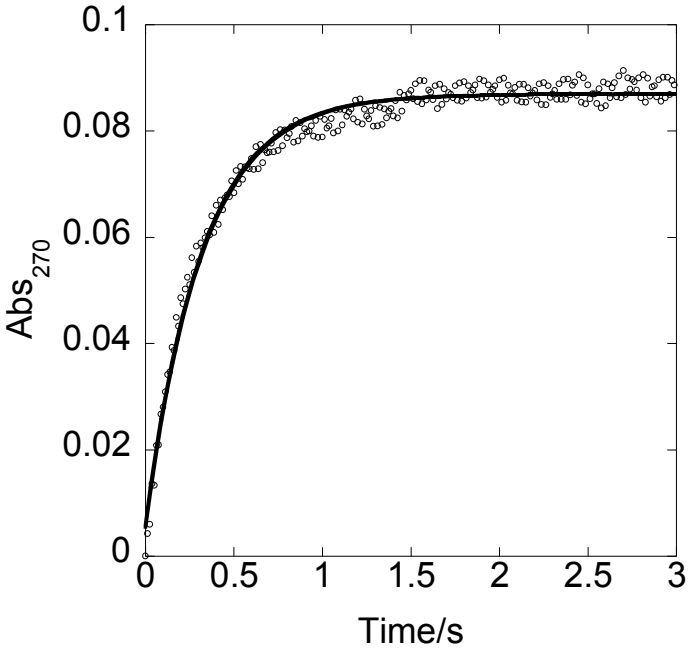

Figure S12. A representative kinetic trace in phosphate buffer. Conditions: 0.031 mM Fe(II), 1.0 mM H_2O_2, pH 6.1 (0.6 mM phosphate buffer)

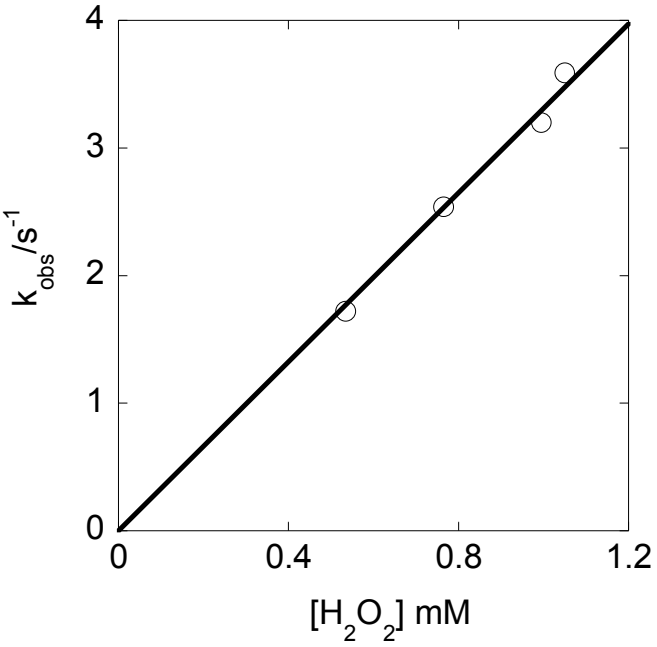

Figure S13. Plot of pseudo-first-order rate constants for the reaction of $Fe(ClO_4)_2$ with H_2O_2 against the concentration of H_2O_2 in phosphate buffer. Conditions: $[Fe(ClO_4)_2]$ = 0.018 – 0.030 mM, [phosphate] = 0.60 mM, pH = 6.1-6.2.

Comment on noninterference of buffers.

Despite the large rate constant reported for the reaction of HO• with tertiary amines k = (2-3) × 10^9 $M^{-1}s^{-1}$,[S5] this reaction cannot be important under our conditions even if HO• radicals were involved. This is so because the rate constant for the $(CH_3)_2SO$/HO• reaction is even larger, k_{DMSO} = 7 × 10^9 $M^{-1}s^{-1}$, and the concentration of $(CH_3)_2SO$ was also always much higher (and never less than four times higher) than the buffer concentration, so that inequality $k_{DMSO}[(CH_3)_2SO] >> k_{buffer}[buffer]$ held true in every experiment.

In acidic solutions, where the Fenton reaction generates HO•, we observed no change in the products of $Fe(H_2O)_6^{2+}/H_2O_2/(CH_3)_2SO$ reaction in the presence of added MES, as shown in Figure S14a [In addition to sulfinic acid and ethane, the reaction in acidic solutions also produces small amounts of the sulfone in a minor parallel path that does not involve Fe(IV)].[S6] The lack of reactivity at nitrogen in acidic solutions is caused by protonation, but the rate constants for hydrogen atom abstraction from C-H bonds are not expected to change significantly between pH 1 and pH 6. The addition of H_2O_2 to MES in the absence of $Fe(ClO_4)_2$ also had no effect on the NMR spectrum of MES (Figure S14b), as expected on the basis of literature data.[S7]

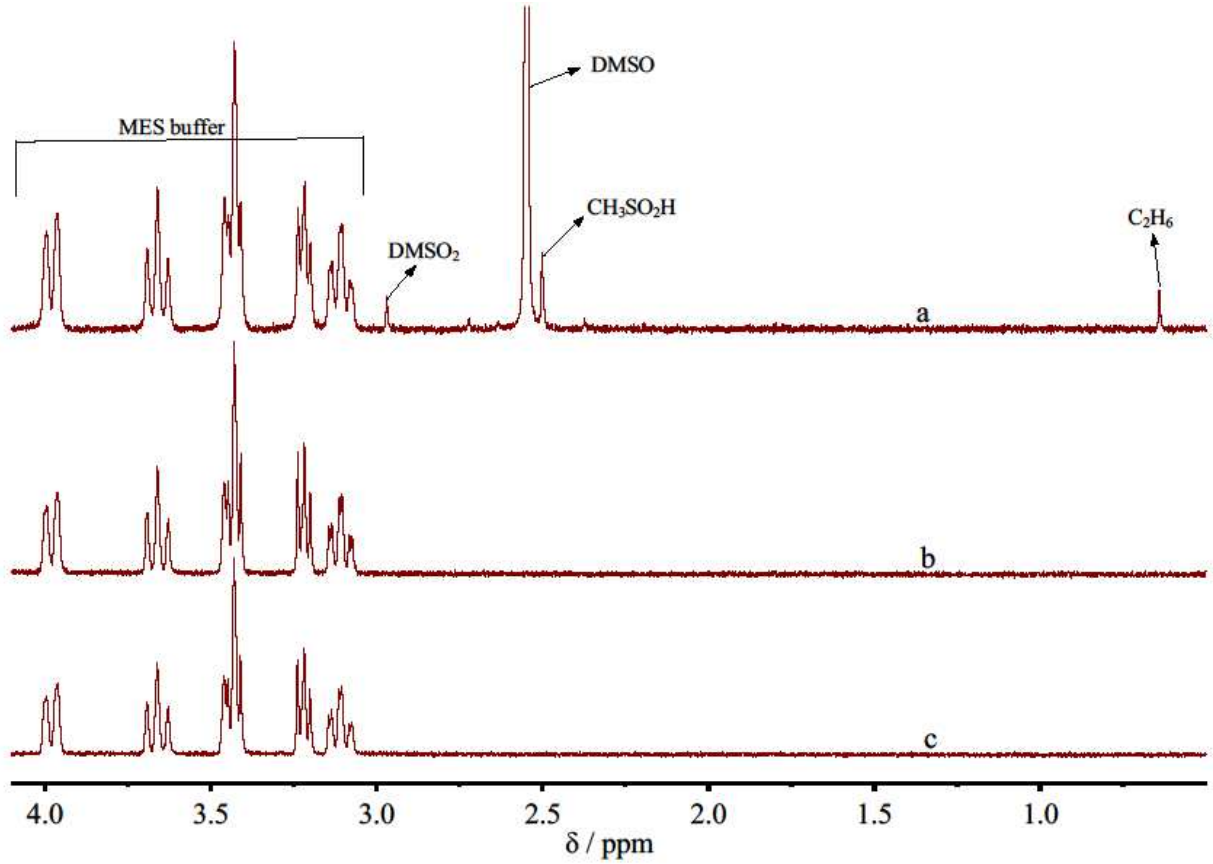

Figure S14. (a) ^{1}H NMR spectrum of the reaction mixture after the completion of the reaction between $Fe(ClO_4)_2$ (1.0 mM), H_2O_2 (1.0 mM), and $(CH_3)_2SO$ (5 mM) at pD 1 in the presence of 5 mM MES. The reaction generated CH_3SO_2H and C_2H_6 in amounts comparable to those obtained in the absence of MES. b) Mixture of MES (5 mM) and H_2O_2 (1 mM), pD 1. c) MES (5 mM), pD 1.

We also ruled out any reaction between the buffers and Fe(IV), the actual intermediate in the Fenton reaction at pH ≥6, by observing that the change in buffer concentration (MES, 10 mM - 24 mM, pD 6.7) under standard conditions (1.2 mM Fe(II), 1.1 mM H_2O_2, 36 mM $(CH_3)_2SO$) had no effect on the yield of sulfone.

References

(S1) Pestovsky, O.; Bakac , A. *J. Am. Chem. Soc.* **2004**, *126*, 13757-13764.

(S2) Kandegedara, A.; Rorabacher, D. B. *Anal Chem* **1999**, *71*, 3140-3144.

(S3) Pestovsky, O.; Bakac, A. *Inorg. Chem.* **2006**, *45*, 814-820.

(S4) Richens, D. T. *The Chemistry of Aqua Ions*; Wiley: Chichester, 1997.

(S5) Halliwell, B.; Gutteridge, J. M. C.; Aruoma, O. I. *Anal. Biochem.* **1987**, *165*, 215-219.

(S6) Pestovsky, O.; Stoian, S.; Bominaar, E. L.; Shan, X.; Münck, E.; Que, L. J.; Bakac, A. *Angew. Chem., Int. Ed.* **2005**, *44*, 6871-6874.

(S7) Zhao, G.; Chasteen, N. D. *Anal. Biochem.* **2006**, *349*, 262-267.

APPENDIX B

Fe(II) CATALYSIS IN OXIDATION OF HYDROCARBONS WITH OZONE IN ACETONITRILE

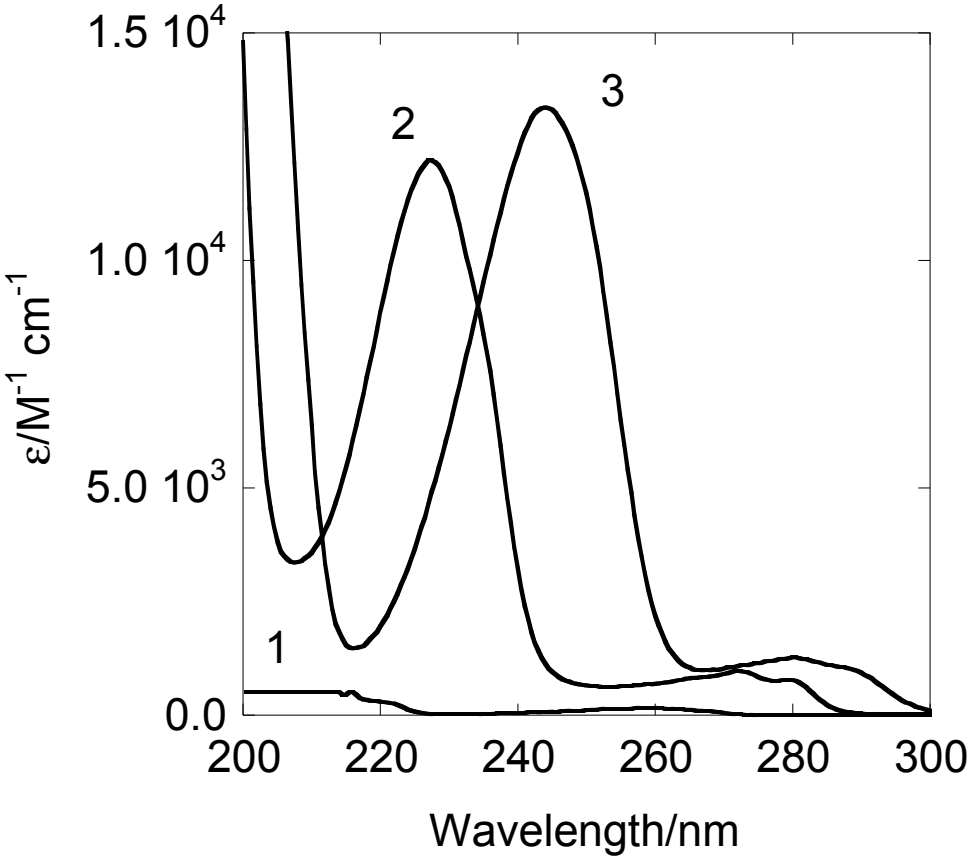

Figure S1. UV spectra of $PhCH_2OH$ (1), PhCOOH (2) and PhCHO (3).

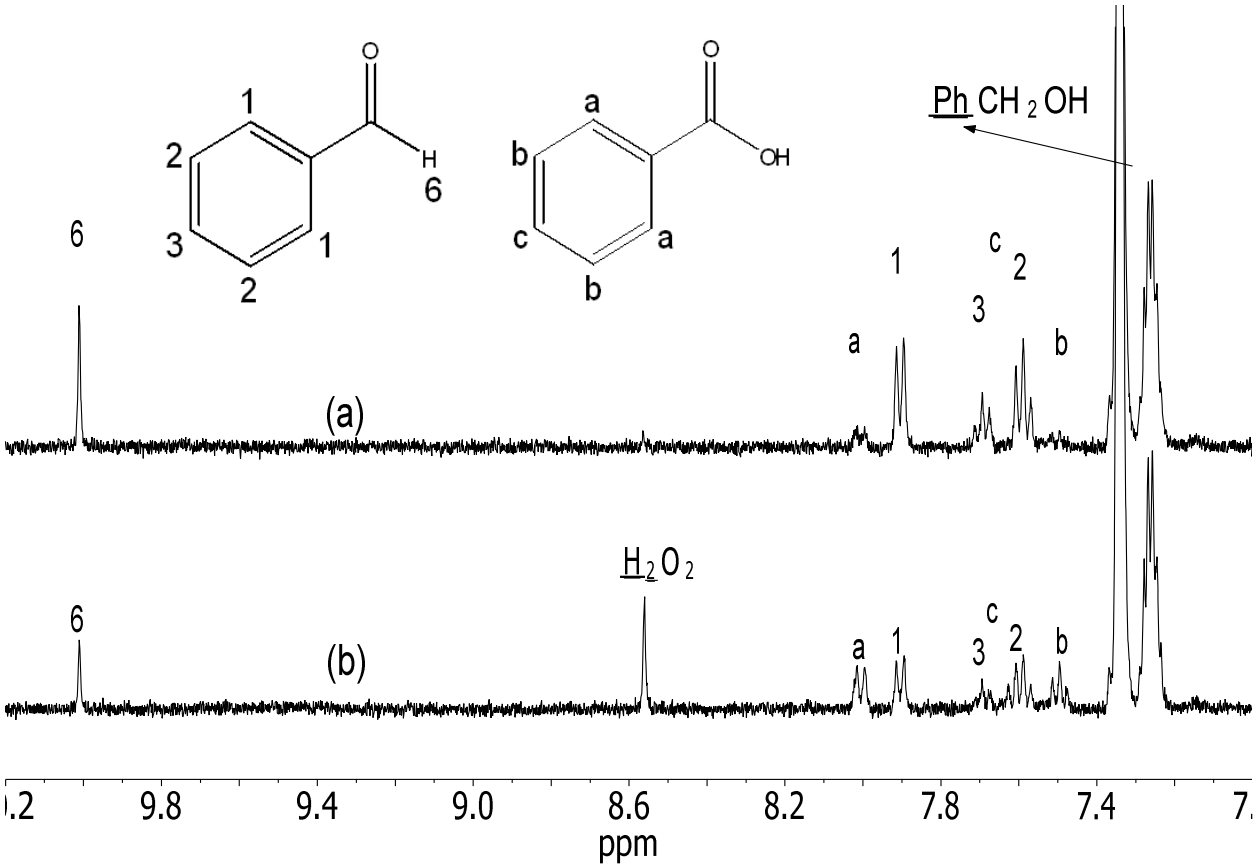

Figure S2. ^{1}H NMR of the products of reaction of (a) 0.048 mM Fe(II) / 1.8 mM O_3 and 10 mM $PhCH_2OH$, and (b) 2.1 mM O_3 and 9.5 mM $PhCH_2OH$. Products are: (a) 1.2 mM PhCHO + 0.17 mM PhCOOH; (b) 0.53 mM PhCHO + 0.53 mM PhCOOH + 0.48 mM H_2O_2.

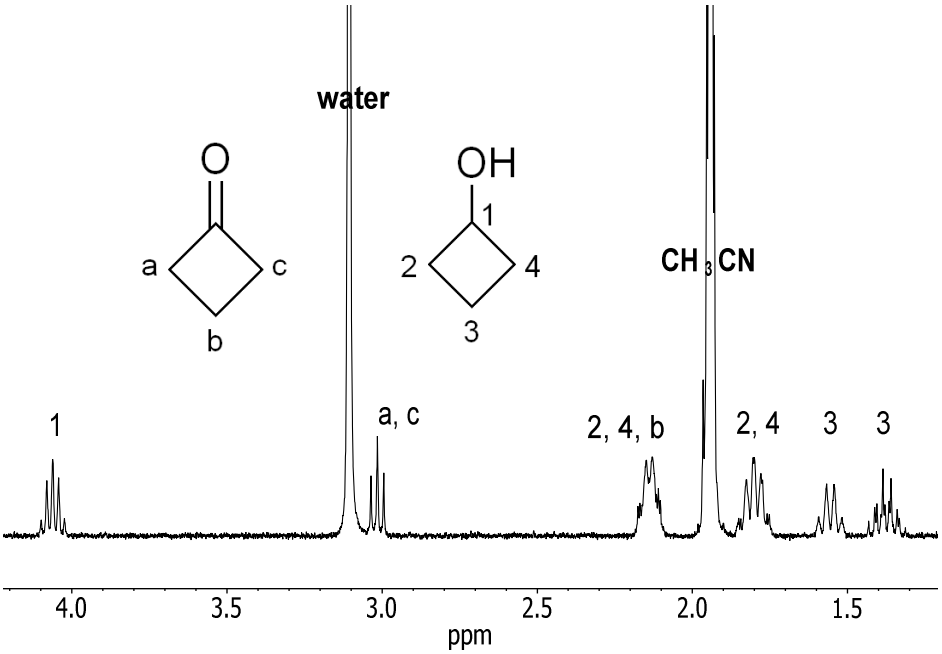

Figure S3. ^{1}H NMR of the products of reaction of 1.8 mM O_3 + 9.6 mM cyclobutanol, catalyzed by 0.025 mM Fe(II).

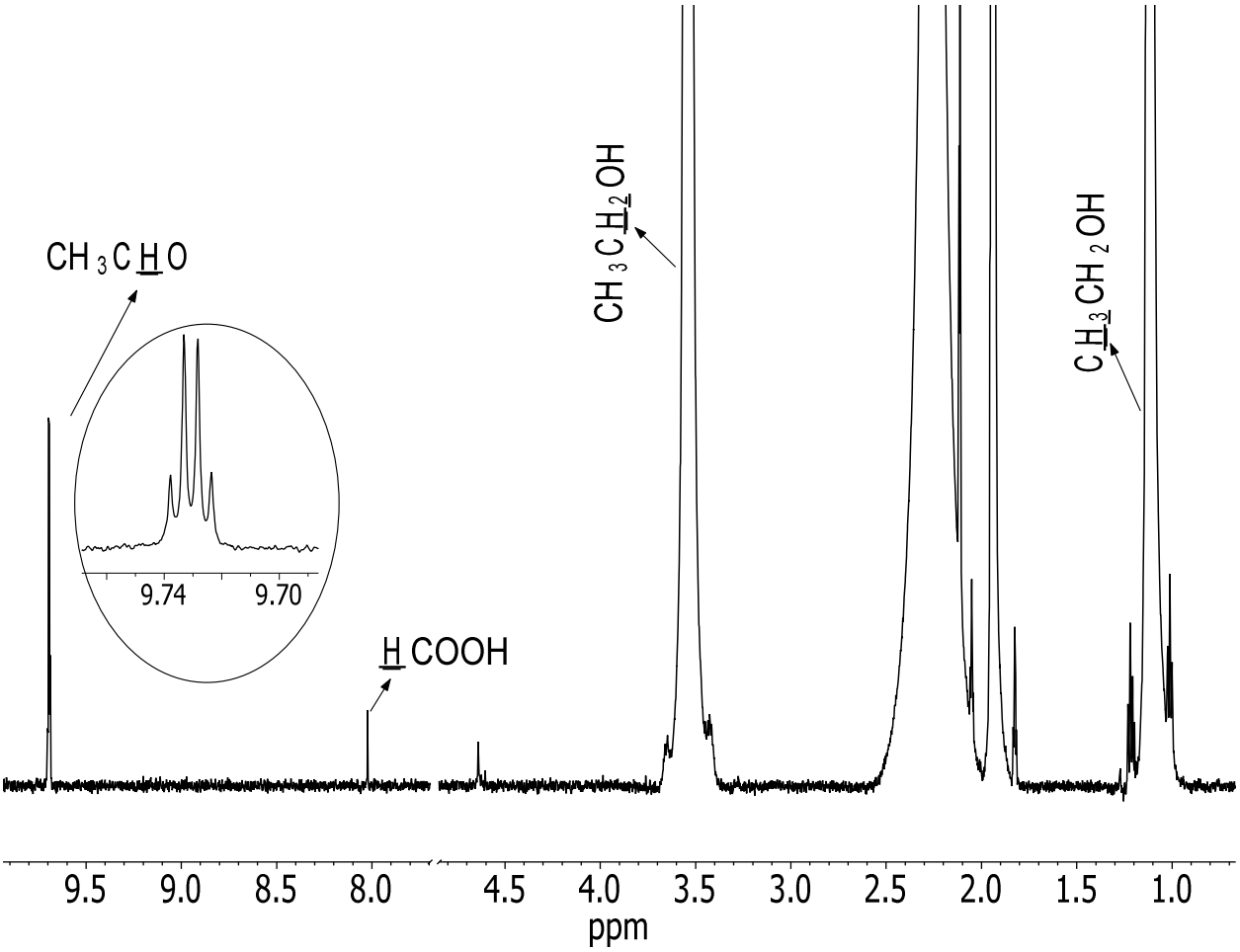

Figure S4. ^{1}H NMR of the products of reaction of 49 mM EtOH + 1.0 mM O_3/0.06 mM Fe(II).

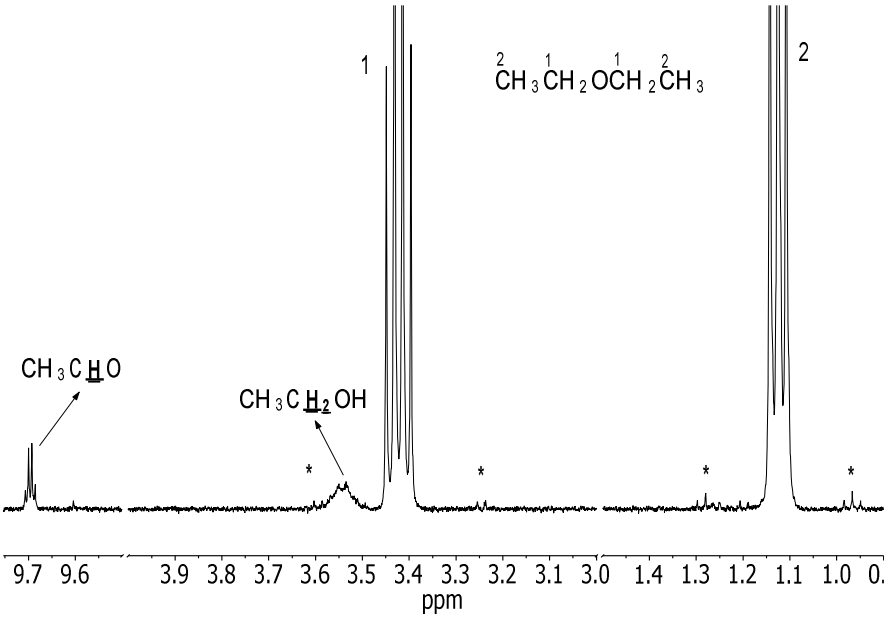

Figure S5. ^{1}H NMR of the products of reaction of 8.5 mM Et_2O + 1.2 mM O_3/0.052 mM Fe(II).

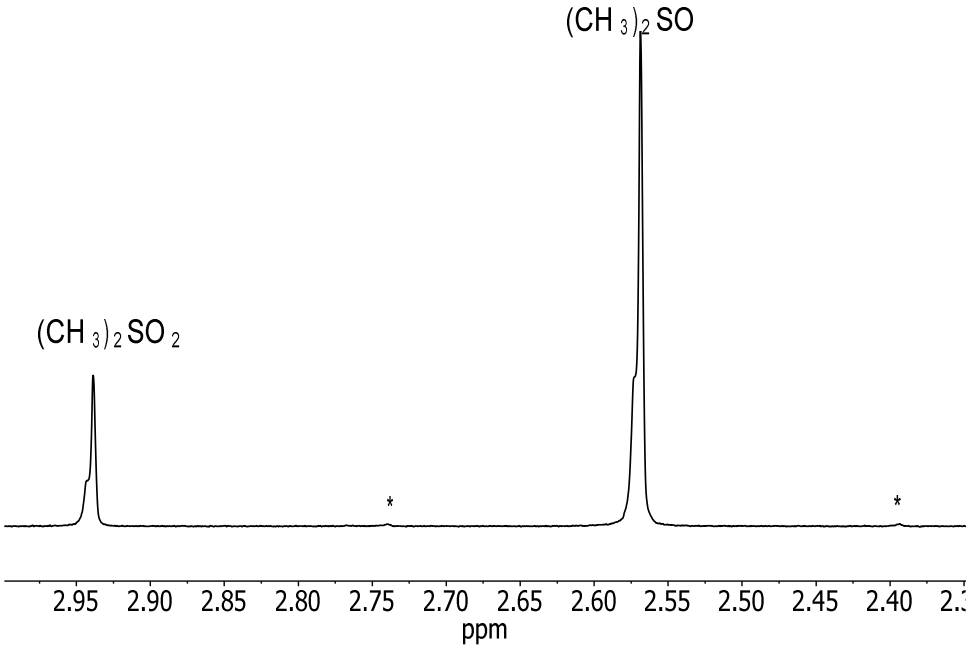

Figure S6. ^{1}H NMR of the products of reaction of 9.6 mM DMSO + 1.9 mM O_3/ 0.028 mM Fe(II).

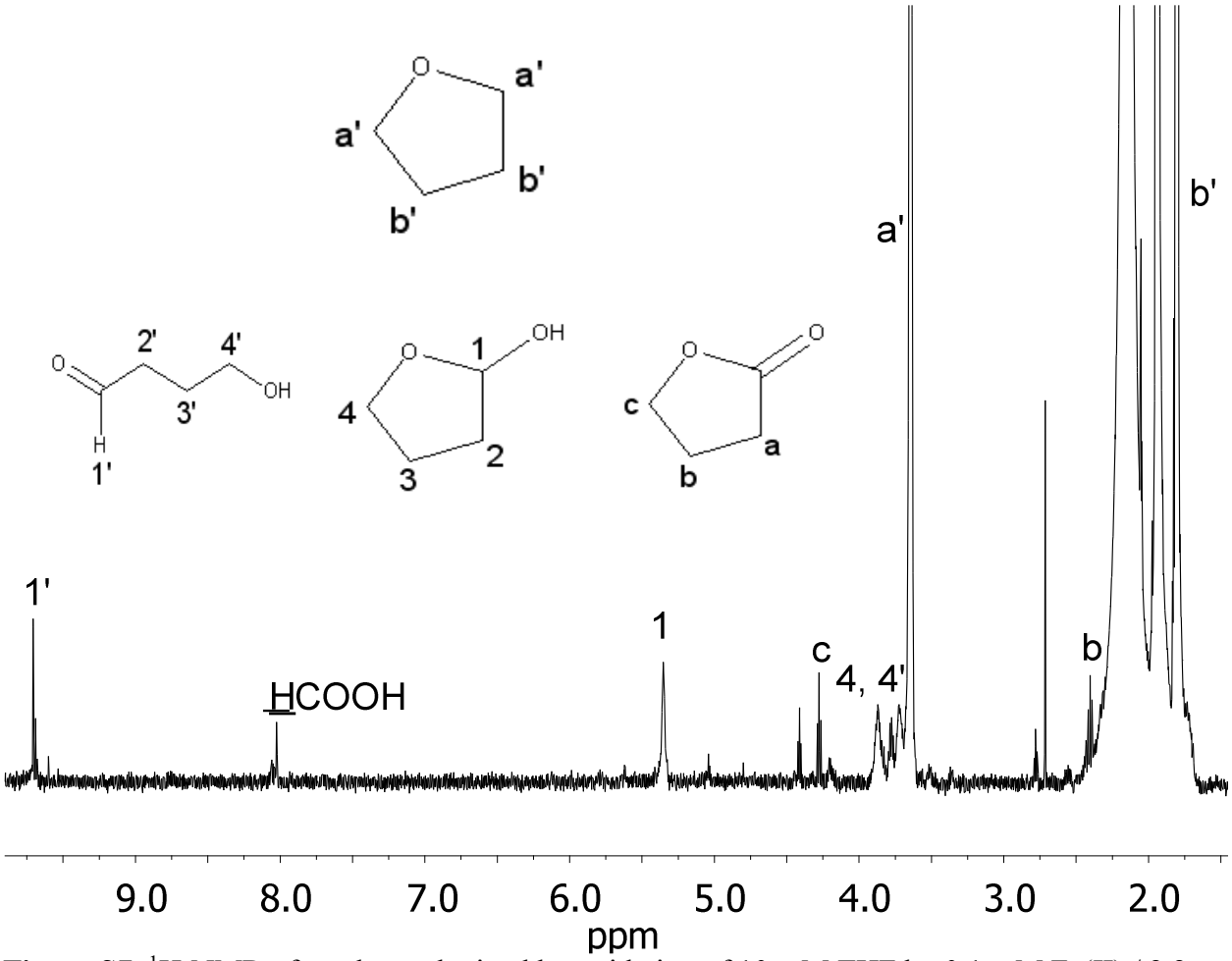

Figure S7. ^{1}H-NMR of products obtained by oxidation of 10 mM THF by 0.1 mM Fe(II) / 2.2 mM O_3.

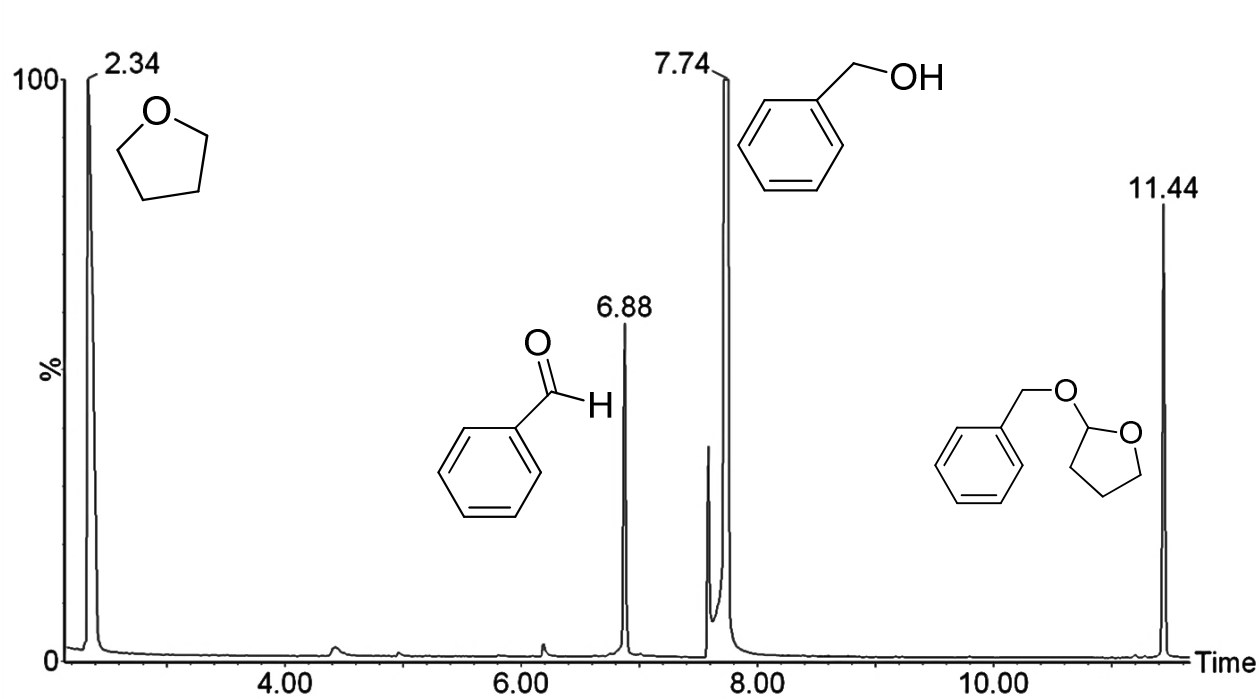

Figure S8. Gas chromatogram of products obtained by oxidation of a mixture of $PhCH_2OH$ (5.6 mM) and THF (7.7 mM) by 0.05 mM Fe(II) / 1.0 mM O_3.

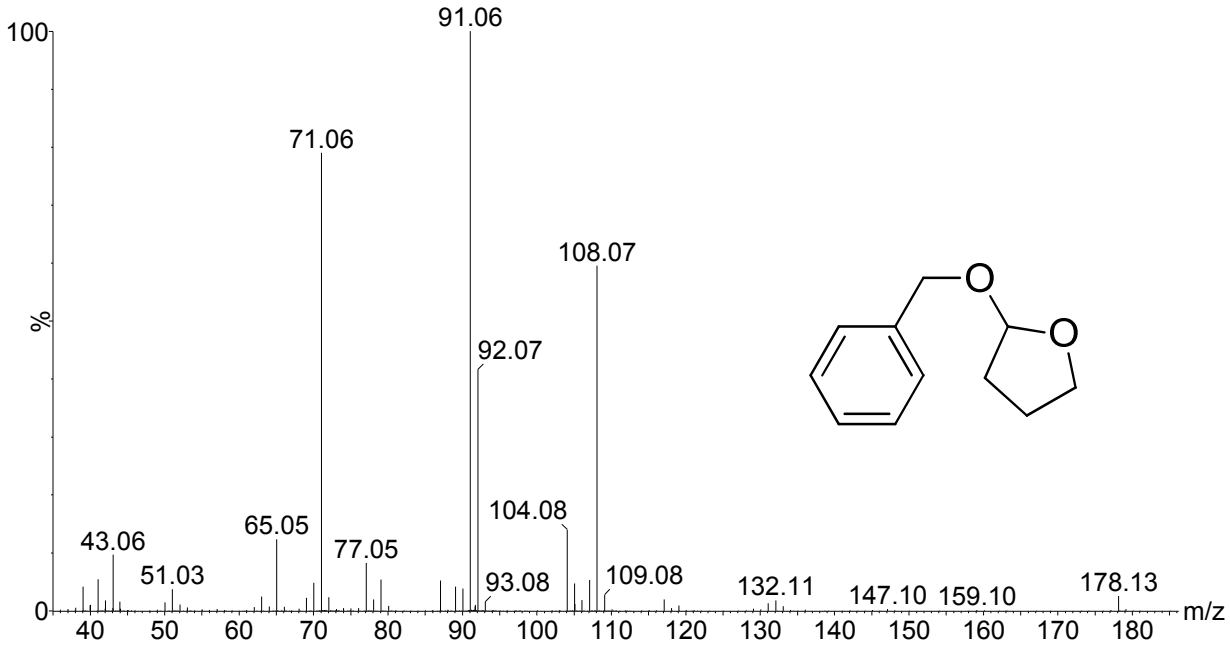

Figure S9. Mass spectra of the product eluted at 11.44 min for the oxidation of a mixture of $PhCH_2OH$ (5.6 mM) and THF (7.7 mM) with 0.05 mM Fe(II) / 1.0 mM O_3.

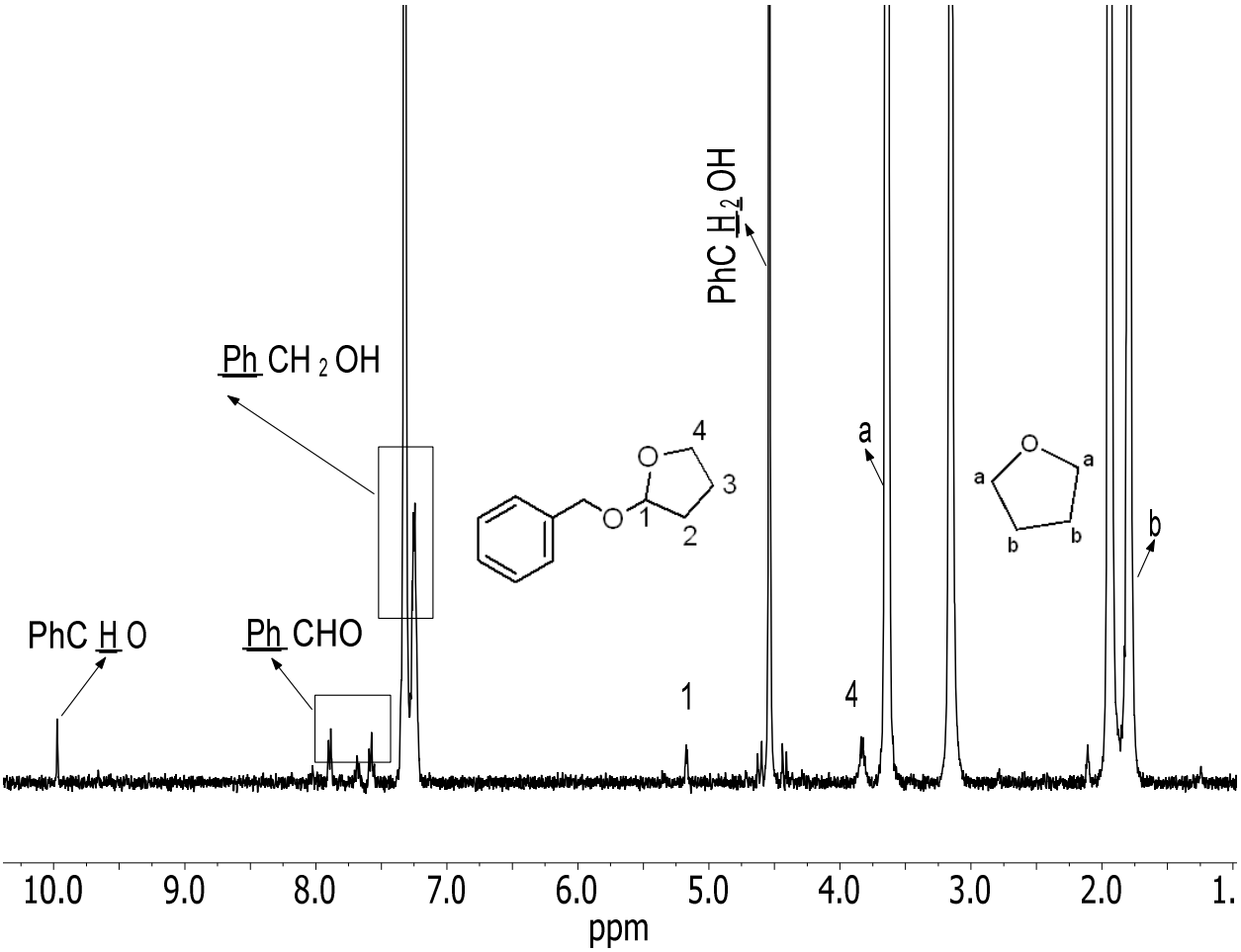

Figure S10. ^{1}H NMR of products obtained by oxidation of a mixture of $PhCH_2OH$ (5.6 mM) and THF (7.7 mM) by 0.05 mM Fe(II) / 1.0 mM O_3. Products are 0.54 mM $PhCH_2O$-THFand 0.41 mM PhCHO.

Table S1. Rate Constants for O_3/Substrate Reactions in the Absence of Fe(II) in MeCN

Substrate	$k_{O3}/M^{-1}s^{-1}$
MeOH	0.24
EtOH	3.2
2-PrOH	13.4
cyclobutanol	10.2
$PhCH_2OH$	22.1
THF	55.3
DMSO	118

Table S2. Kinetic Data for $Fe(CH_3CN)_6^{2+}$-Catalyzed Oxidations with Ozone[a]

$[Fe(II)]_{initial}$ / μM	**[2-PrOH]** /mM	k_{obs} /s^{-1}	k_{corr} /s^{-1}	$[Fe(II)]_{final}$/ μM
24	1	1	0.99	13
26	4.2	1.35	1.29	19
26	7	1.5	1.41	22
27	30	2.2	1.8	23
26	51	2.6	1.94	19
	[EtOH]/ mM			
25	6	1.09	1.07	17
26	15	1.45	1.41	18
25	50	1.6	1.45	18
	[THF] /mM			
26	4.4	1.71	1.48	19
26	8.8	2.05	1.58	21
	[cyclo-BuOH]/ mM			
25	4.7	1.73	1.68	18
25	10	1.86	1.76	20
23	30	2.07	1.77	15
	[Et_2O]/ mM			
26	5	1.15	1.1	21
25	11	1.21	1.1	20
25	21	1.37	1.15	21
25	35	1.49	1.13	20

[a] $[O_3]$ = 0.085-0.12 mM. For definition of k_{obs} and k_{corr} see eq 1-3

Table S3 Net increase in $[O_2]$ in the $Fe(CH_3CN)_6^{2+}/O_3$/Substrate Reactions

Substrate /(mM)	$[Fe(II)]_o$/mM	$[O_3]_o$/mM	Measured $[O_2]$ /mM
-	0.06	0.59	0.12
-	0.58	0.62	0.14
EtOH /(20)	0.057	0.58	0.35
DMSO /(15)	0.057	0.6	0.53

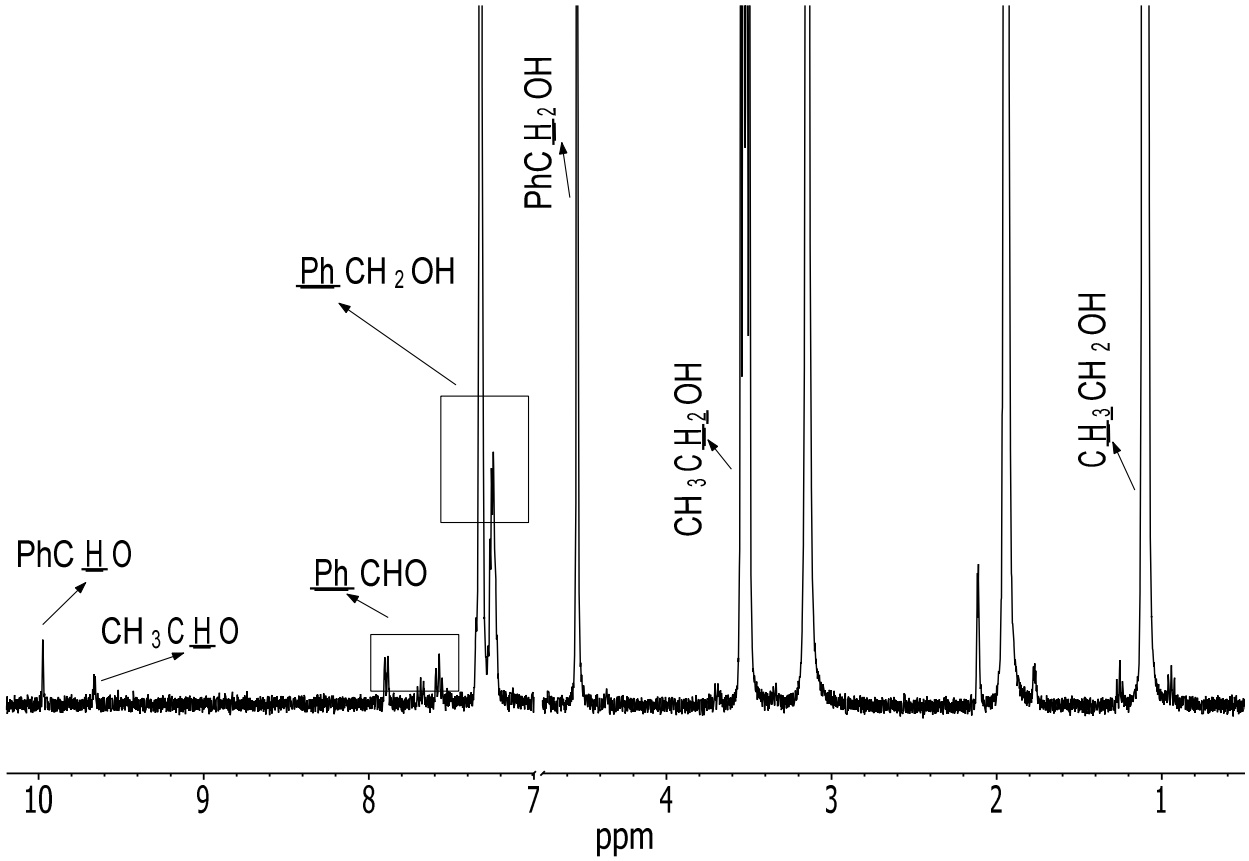

Figure S11. ^1H NMR of the products of oxidation of C_2H_5OH (19 mM) and $PhCH_2OH$ (4.9 mM) by O_3 (0.66 mM)/$Fe(CH_3CN)_6^{2+}$ (0.05 mM)

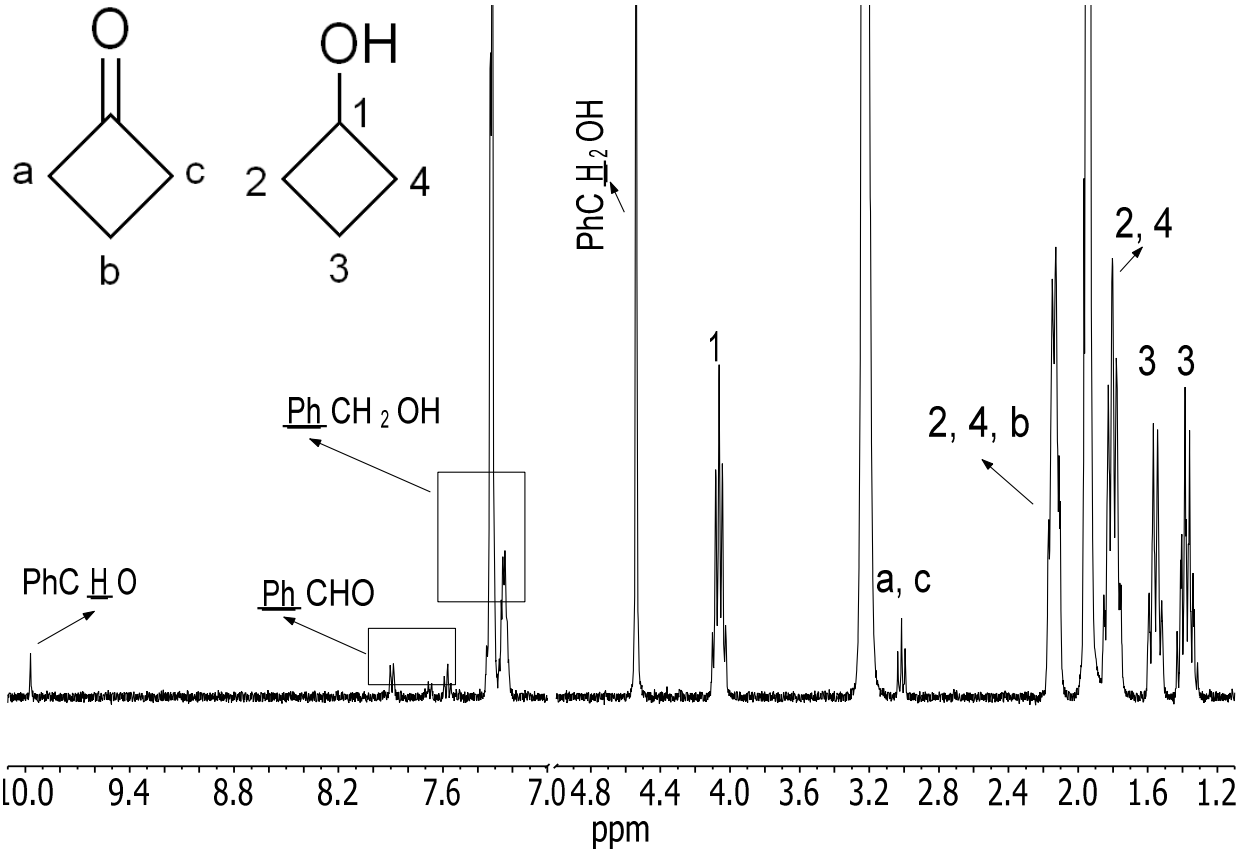

Figure S12. ^{1}H NMR of the products of oxidation of cyclo-C_4H_7OH (10 mM) + $PhCH_2OH$ (4.9mM) by O_3 (0.73 mM)/$Fe(CH_3CN)_6^{2+}$ (0.05 mM)

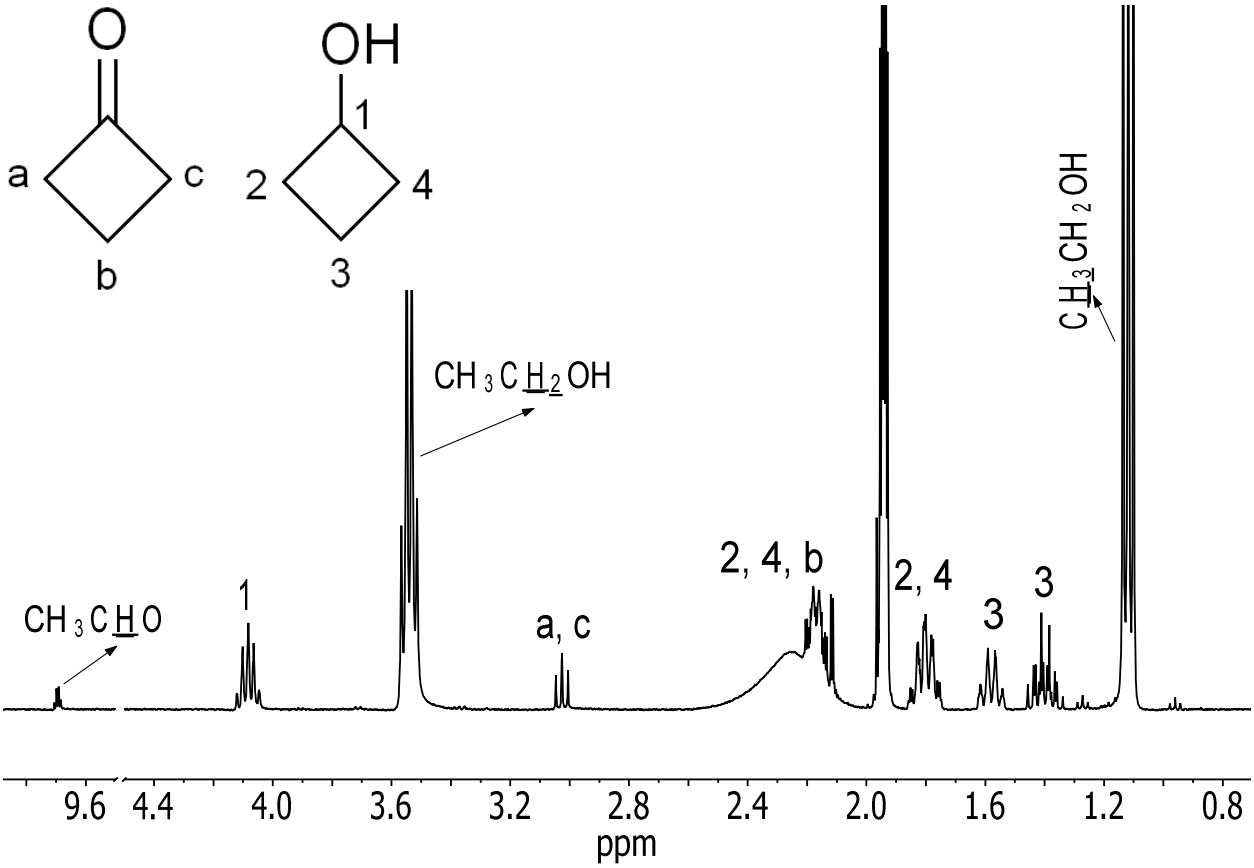

Figure S13. ^{1}H NMR of the products of oxidation of ethanol (30 mM) and cyclo-C_4H_7OH (10 mM) by O_3 (1.7 mM)/$Fe(CH_3CN)_6^{2+}$ (0.025 mM)

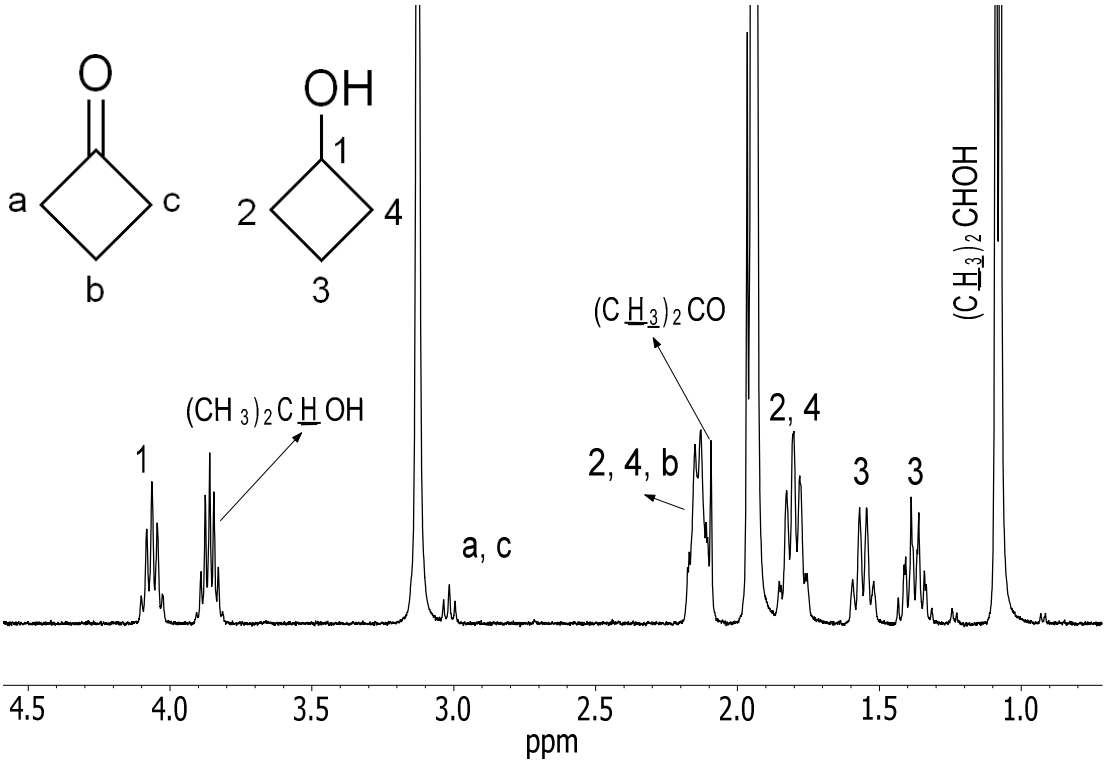

Figure S14. ^{1}H NMR of the products of oxidation of 2-propanol (11 mM) and cyclo-C_4H_7OH (10 mM) by O_3 (0.86 mM)/$Fe(CH_3CN)_6^{2+}$ (0.05 mM)

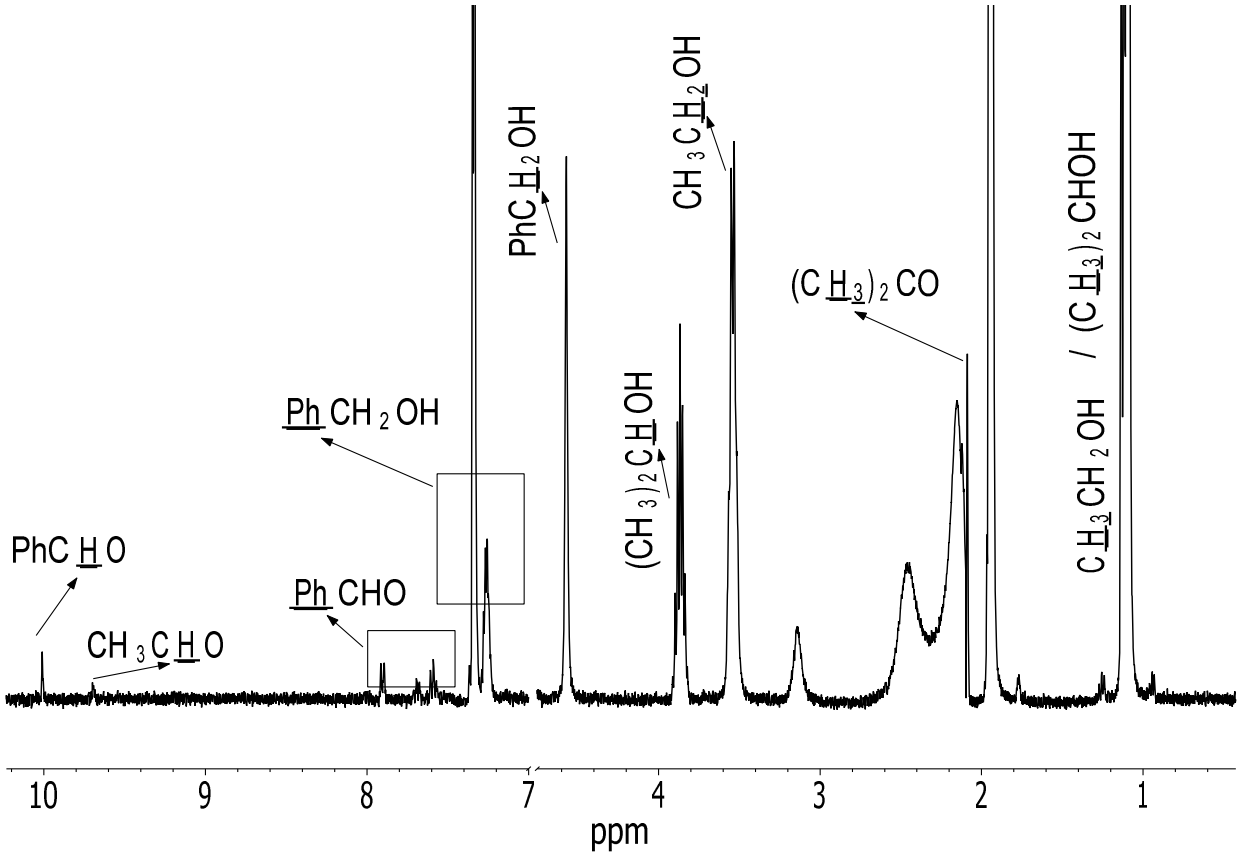

Figure S15. ^{1}H NMR of the products of oxidation of C_2H_5OH (10 mM), $PhCH_2OH$ (4.7 mM) and $(CH_3)_2CHOH$ (9.6 mM) by O_3 (1.0 mM)/$Fe(CH_3CN)_6^{2+}$ (0.052 mM)

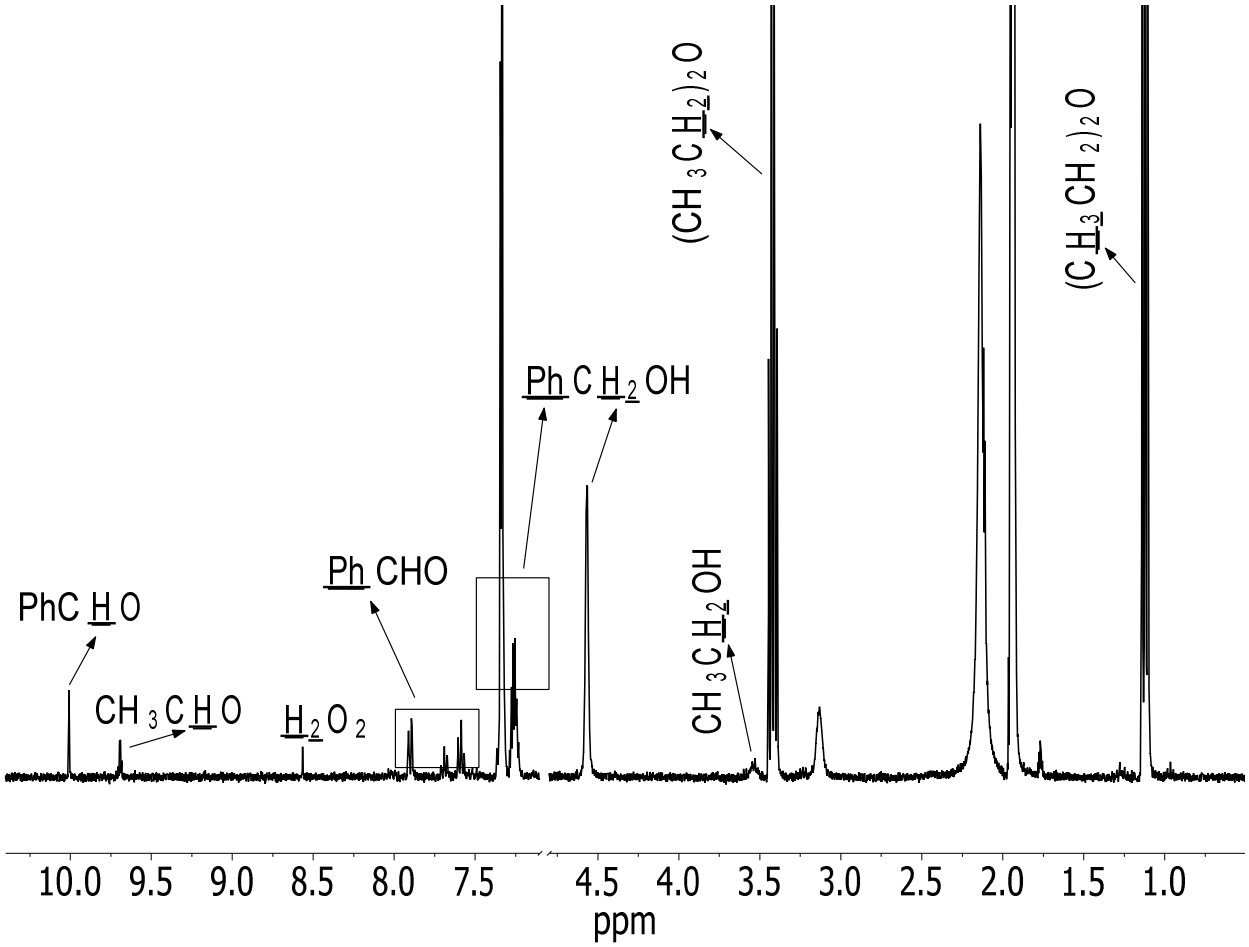

Figure S16. ^{1}H NMR of the products of oxidation of $C_2H_5OC_2H_5$ (4.7) and $PhCH_2OH$ (4.8 mM) by O_3 (1.15 mM)/$Fe(CH_3CN)_6^{2+}$ (0.048 mM)

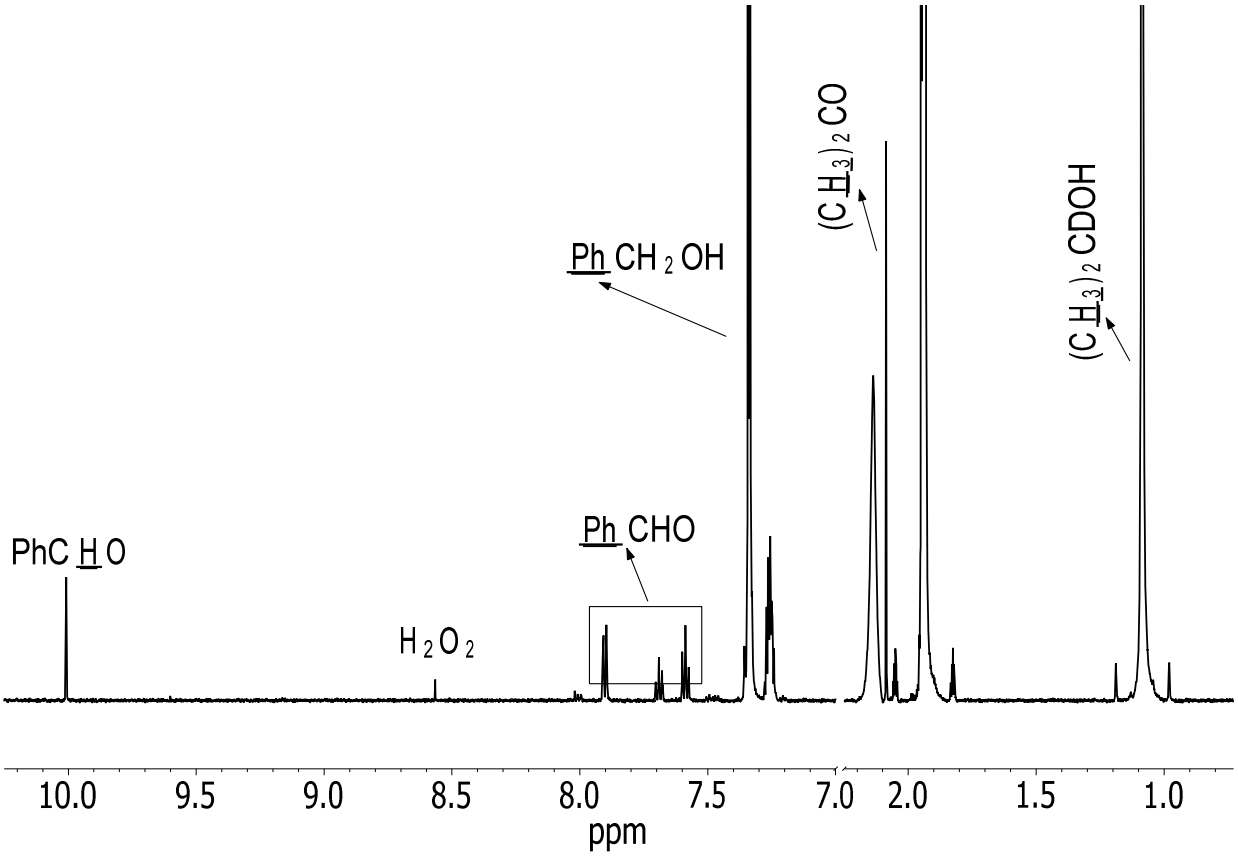

Figure S17. ^{1}H NMR of the products of oxidation of 2-propanol-d1 (10 mM) and $PhCH_2OH$ (4.8 mM) by O_3 (0.85 mM)/$Fe(CH_3CN)_6^{2+}$ (0.05 mM)

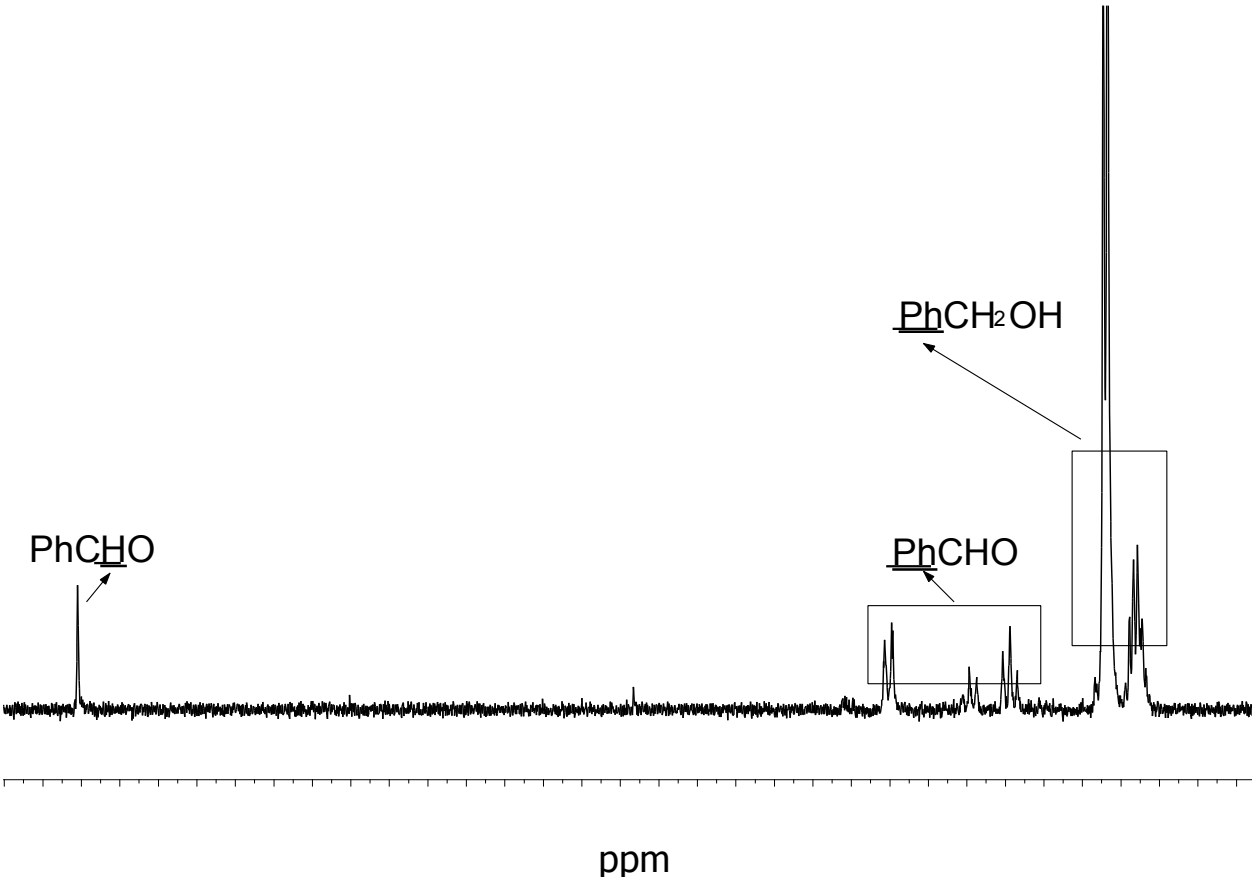

Figure S18. ^{1}H NMR of the products of oxidation of ethyl ether-d10 (5.6 mM) and $PhCH_2OH$ (4.8 mM) by O_3 (1.15 mM)/$Fe(CH_3CN)_6^{2+}$ (0.048 mM)

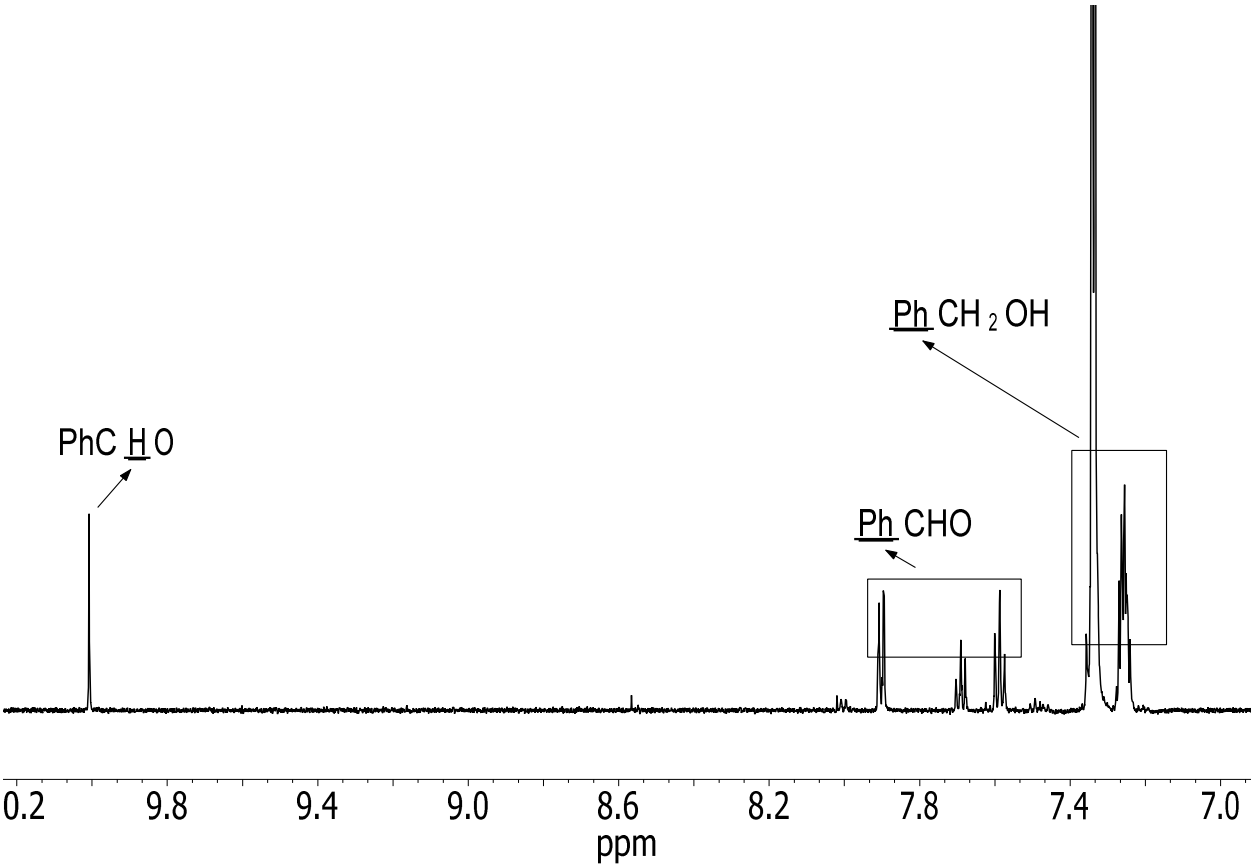

Figure S19. ^{1}H NMR of the products of oxidation of 2-propanol-d8 (10 mM) and $PhCH_2OH$ (4.8 mM) by O_3 (1.0 mM)/$Fe(CH_3CN)_6^{2+}$ (0.05 mM)

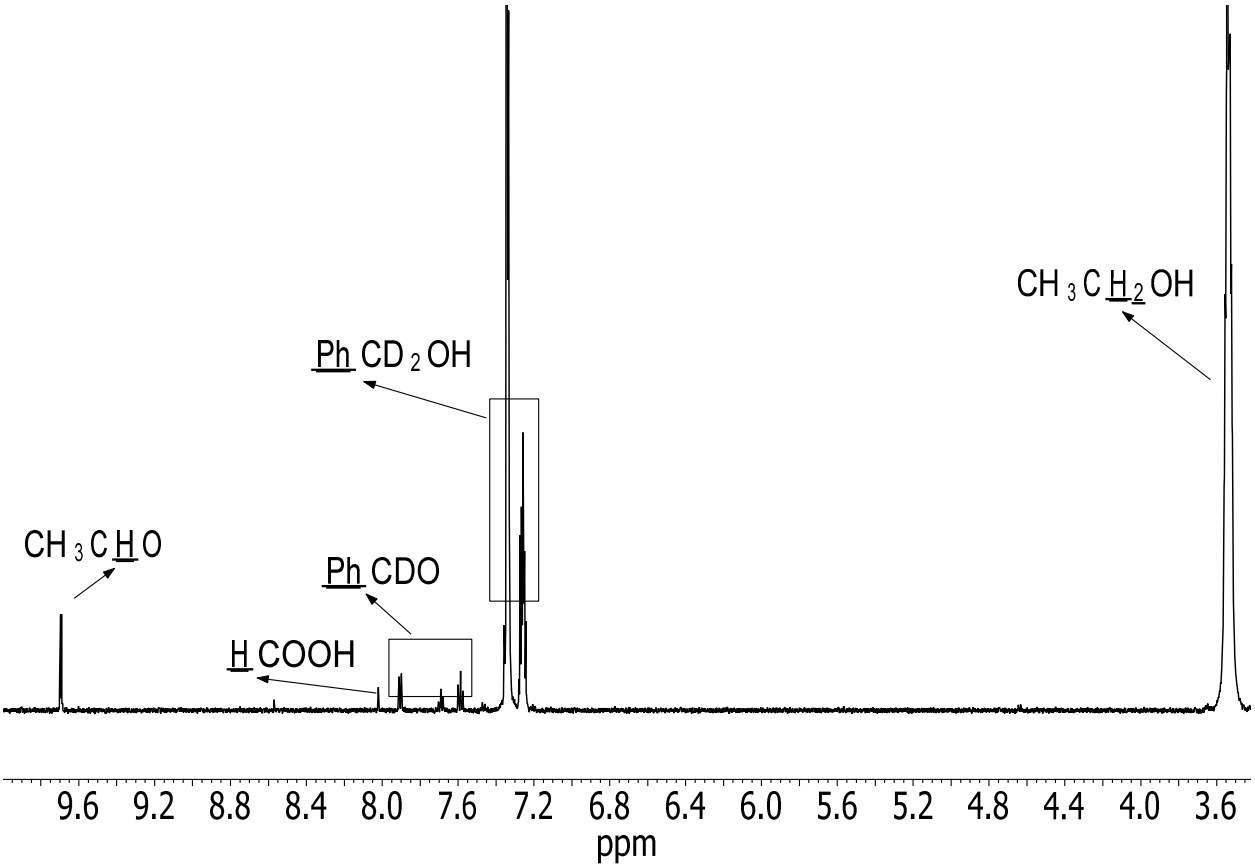

Figure S20. ^{1}H NMR of the products of oxidation of C_2H_5OH (17 mM) and $PhCD_2OH$ (4.7 mM) by O_3 (1.1 mM)/$Fe(CH_3CN)_6^{2+}$ (0.048 mM)

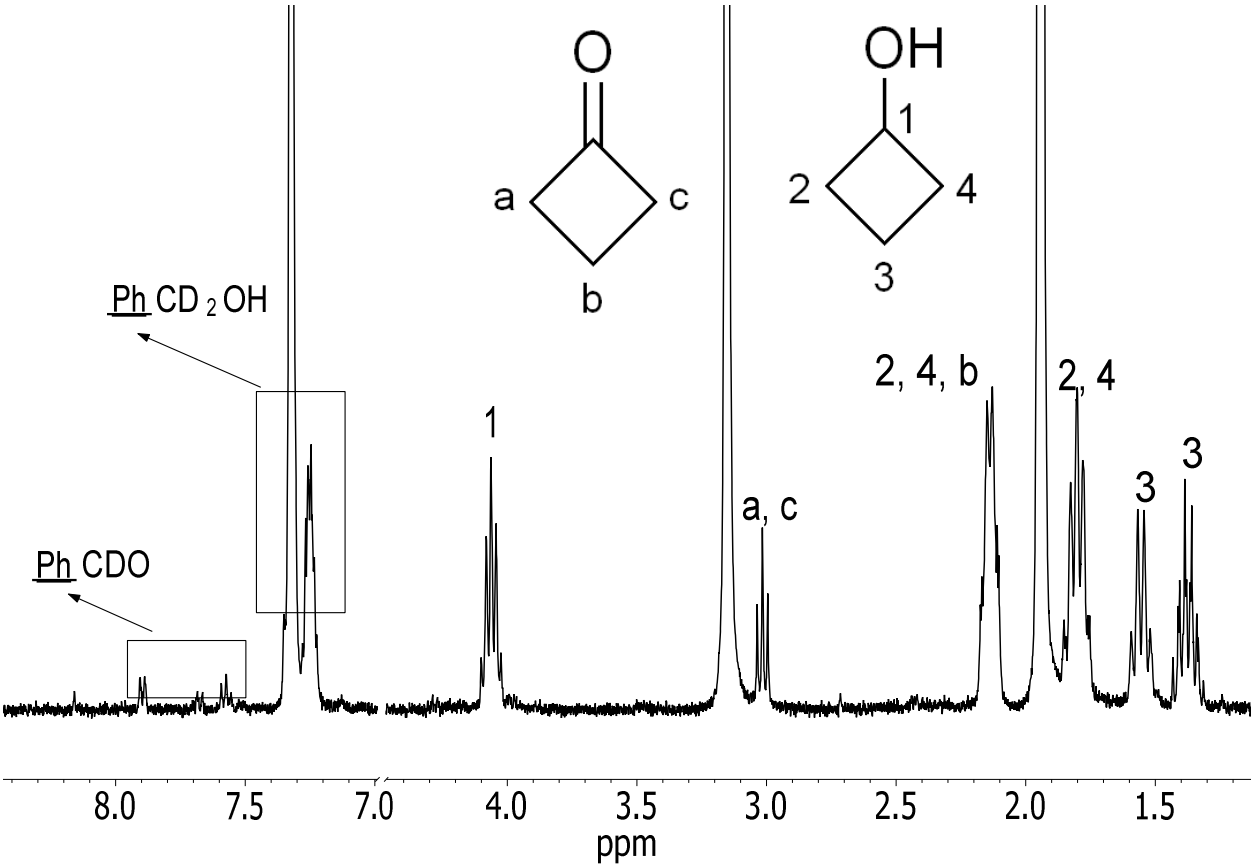

Figure S21. ^{1}H NMR of the products of oxidation of cyclobutanol (9.7 mM) and $PhCD_2OH$ (9.1 mM) by O_3 (1.39 mM)/$Fe(CH_3CN)_6^{2+}$ (0.049 mM)

APPENDIX C

ELECTRON TRANSFER REACTIVITY OF AQUEOUS IRON(IV) OXO COMPLEX

Table S1. Measured Rate Constants for Oxidations with $Fe_{aq}O^{2+}$ Under Different Experimental Conditions.

Substrate	Exp #	Reagents concentrations /mM		k_{Fe} /M^{-1} s^{-1}	Avg. k_{Fe} /M^{-1} s^{-1}
		[$Fe_{aq}^{IV}O^{2+}$]	[substrate]		
Fe(Cp)($C_5H_4CH_2OH$)	1	0.1	0.1	6.2×10^7	6.4×10^7
	2	0.019	0.02	6.5×10^7	
Fe(Cp)(C_5H_4COOH)	1	0.09	0.09	1.2×10^7	1.2×10^7
	2	0.05	0.05	1.2×10^7	
Fe(C_5H_4COOH)$_2$	1	0.02	0.08	9.3×10^5	1.0×10^6
	2	0.026	0.07	1.1×10^6	
Ni(cyclam)$^{2+}$	1	0.005	0.005	5.0×10^7	4.9×10^7
	2	0.05	0.05	4.7×10^7	
Ni(hmc)$^{2+}$	1	0.005	0.005	1.0×10^7	1.2×10^7
	2	0.01	0.01	1.3×10^7	
Co($dmgBF_2$)$_2$	1	0.014	0.008	2.3×10^6	2.2×10^6
	2	0.016	0.016	2.2×10^6	
	3	0.027	0.03	2.1×10^6	
Na_3IrCl_6	1	0.034	0.012	1.1×10^6	1.3×10^6
	2	0.012	0.06	1.5×10^6	
Os(phen)$_3^{2+}$	1	0.05	0.01	2.3×10^5	2.5×10^5
	2	0.033	0.0045	2.2×10^5	
	3	0.028	0.0053	2.1×10^5	
	4	0.012	0.0108	2.9×10^5	
	5	0.018	0.019	2.8×10^5	
Ce(ClO_4)$_3$	1	0.1	0.44	1.5×10^4	1.5×10^4
	2	0.10	1.8	1.4×10^4	
$HABTS^-$	1	0.005	0.005	4.8×10^6	4.6×10^6
	2	0.034	0.084	4.3×10^6	
TFP	1	0.02	0.02	5.3×10^6	5.3×10^6
CPZ	1	0.0045	0.0095	9.2×10^6	1.2×10^7
	2	0.0045	0.005	1.3×10^7	
	3	0.019	0.021	1.3×10^7	

TFP = trifluoperazine, CPZ = chlorpromazine, $HABTS^-$ = 2,2'-azino-bis(3-ethylbenzothiazoline-6-sulphonic acid), Cp = cyclopentadienyl, cyclam = 1,4,8,11-tetraazacyclotetradecane, hmc = 5,7,7,12,14,14-hexamethyl-1,4,8,11-tetraazacyclotetradecane.

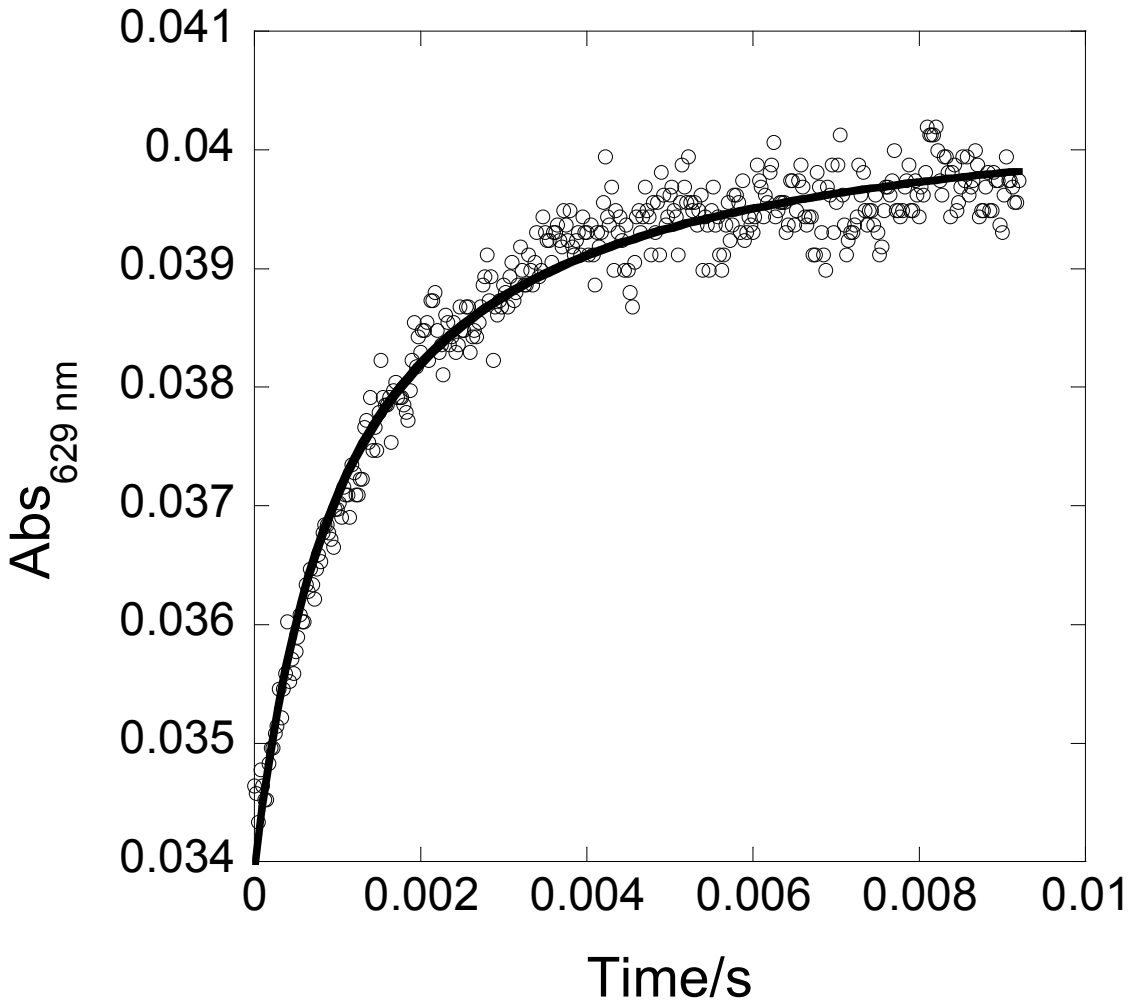

Figure S1. Kinetic trace for a reaction between 0.10 mM $Fe_{aq}^{IV}O^{2+}$ and 0.10 mM $Fe(Cp)(C_5H_4CH_2OH)$.

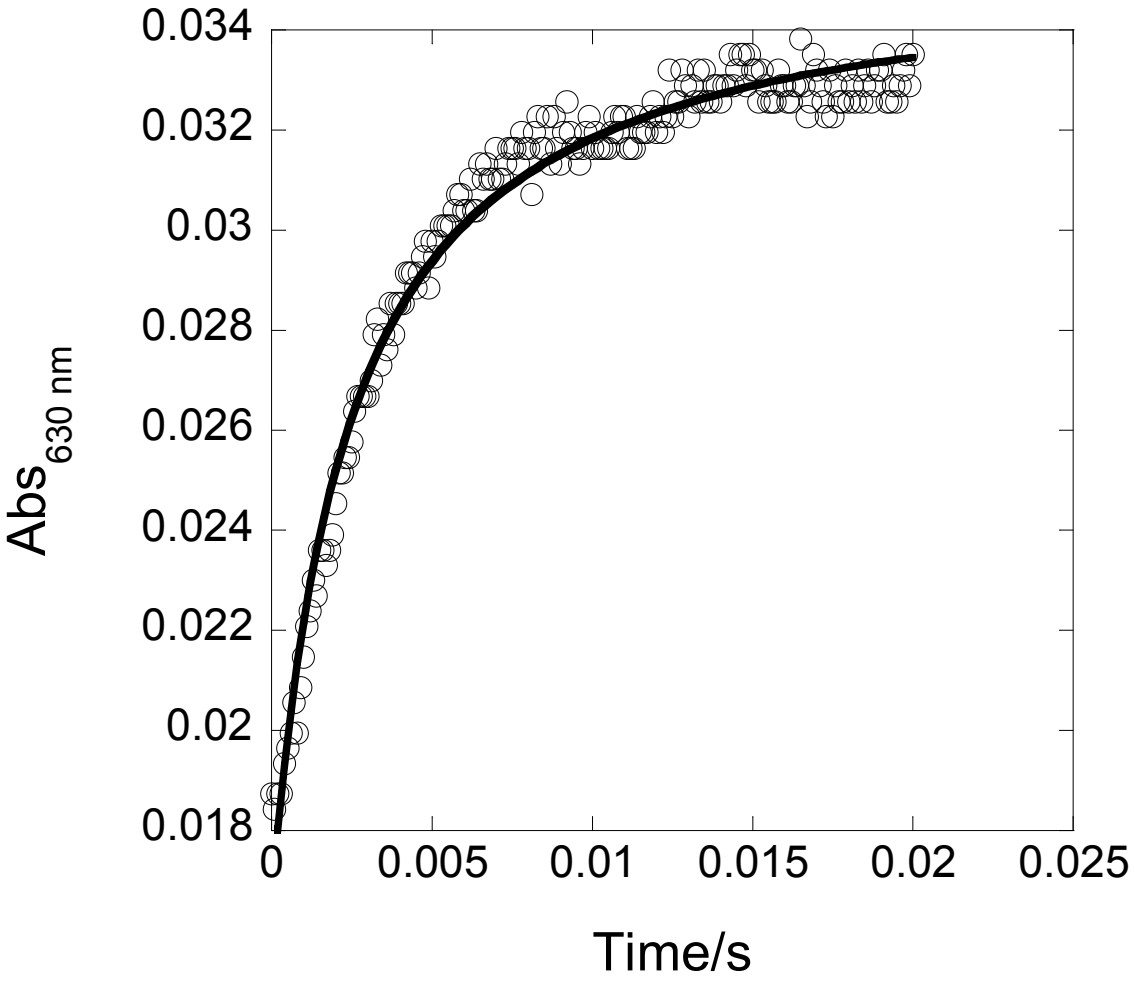

Figure S2. Kinetic trace for a reaction between 0.09 mM $Fe_{aq}^{IV}O^{2+}$ and 0.09 mM $Fe(Cp)(C_5H_4COOH)$.

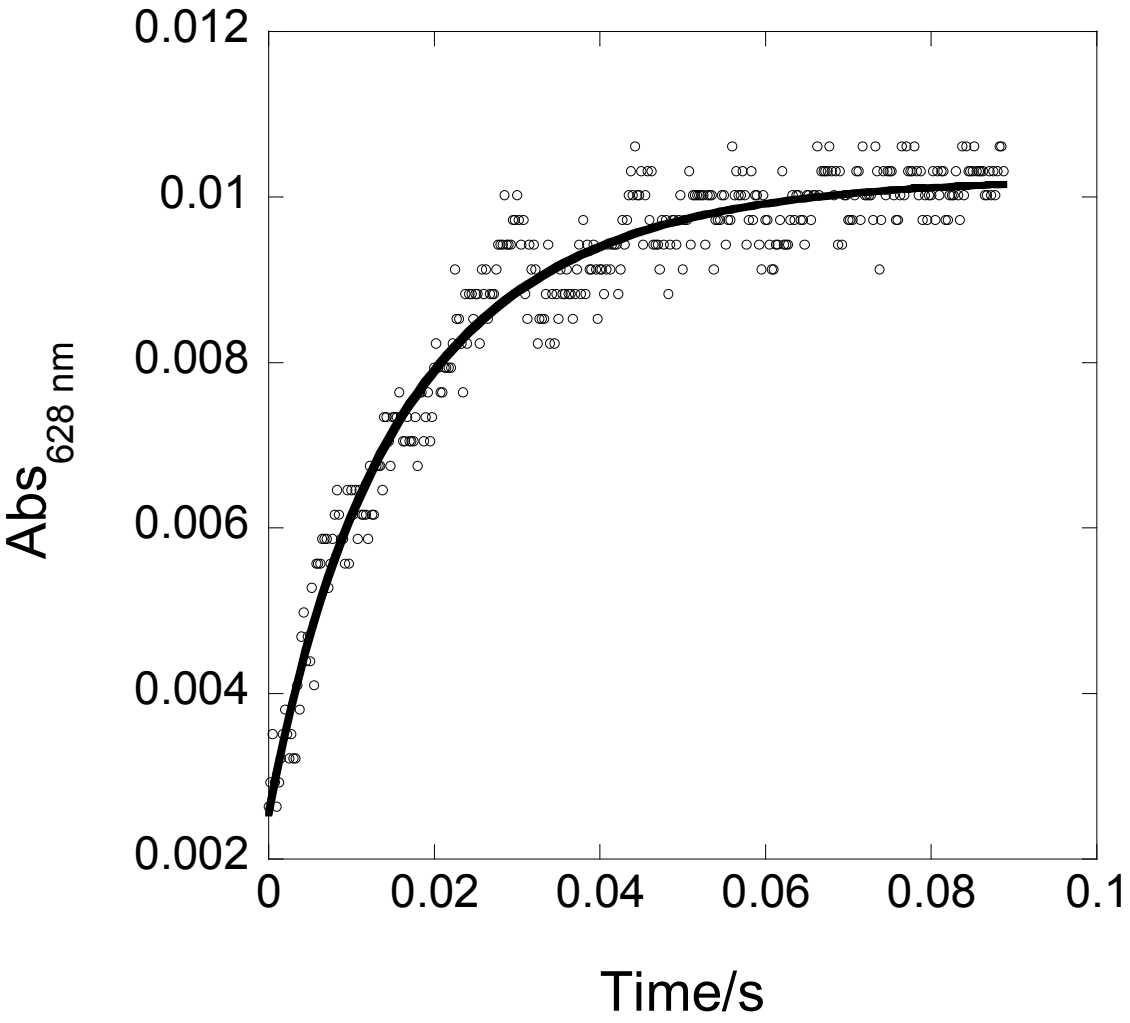

Figure S3. Kinetic trace for a reaction between 0.026 mM $Fe_{aq}^{IV}O^{2+}$ and 0.70 mM $Fe(C_5H_4COOH)_2$.

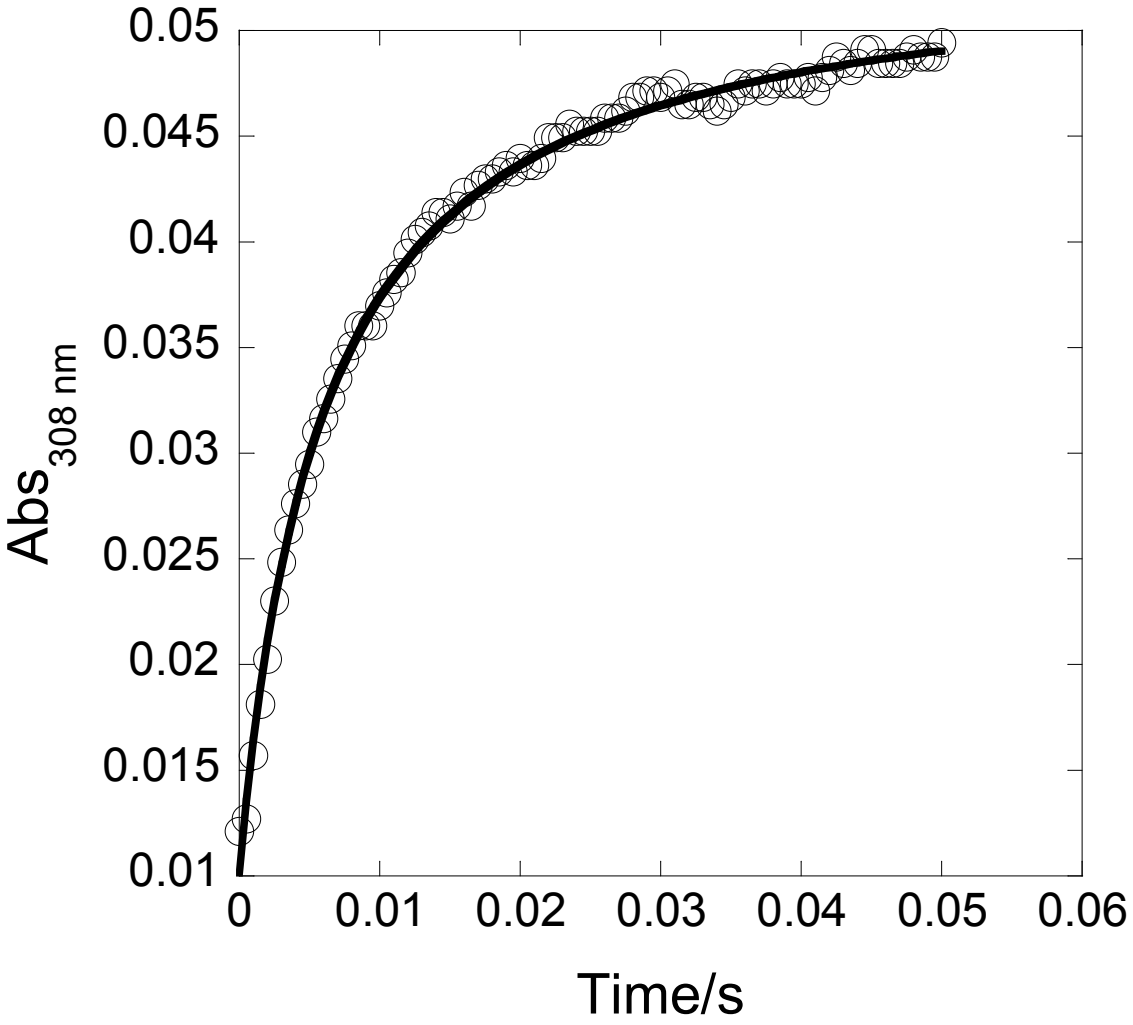

Figure S4. Kinetic trace for a reaction between 0.005 mM $Fe_{aq}^{IV}O^{2+}$ and 0.005 mM $Ni(cyclam)^{2+}$.

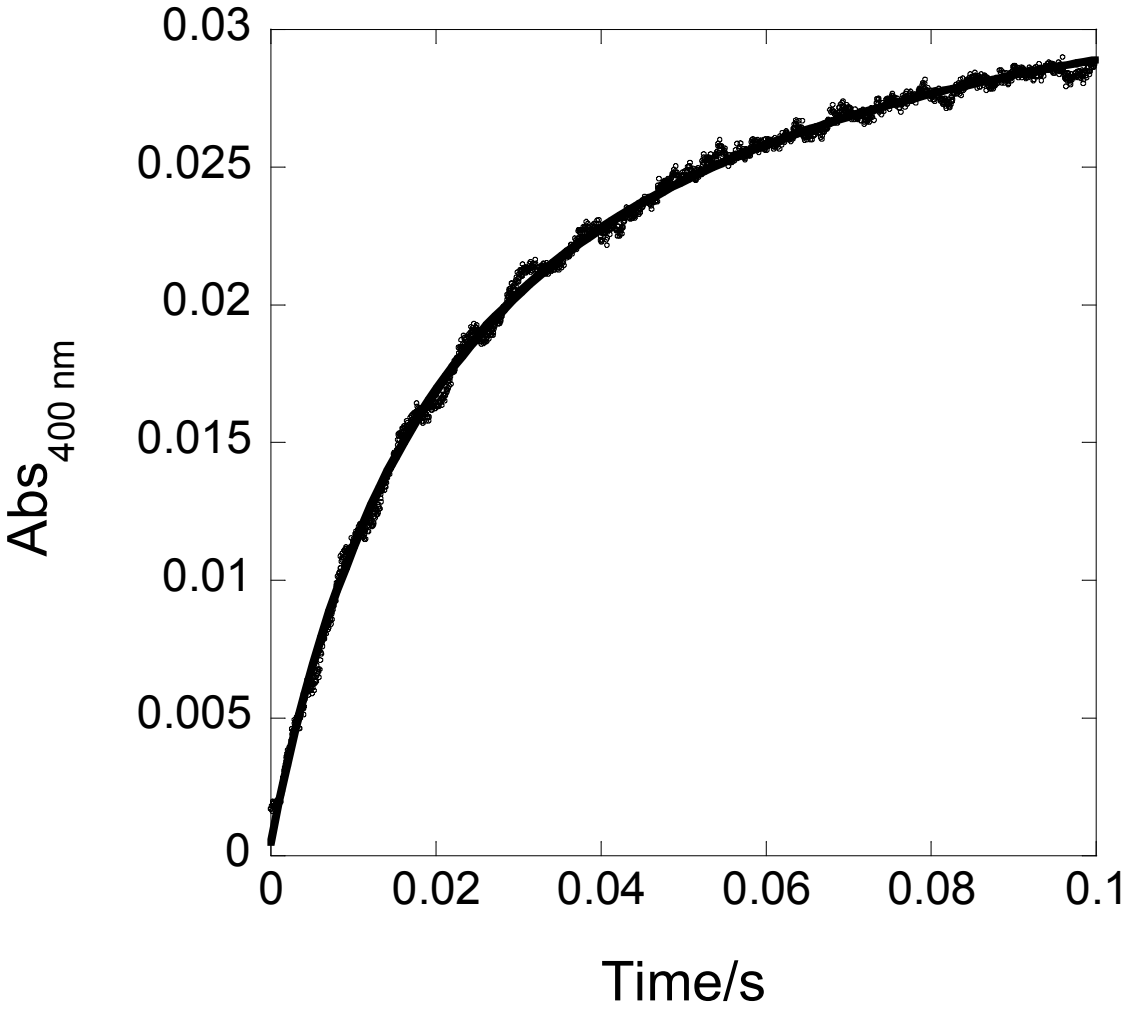

Figure S5. Kinetic trace for a reaction between 0.005 mM $Fe_{aq}^{IV}O^{2+}$ and 0.005 mM $Ni(hmc)^{2+}$.

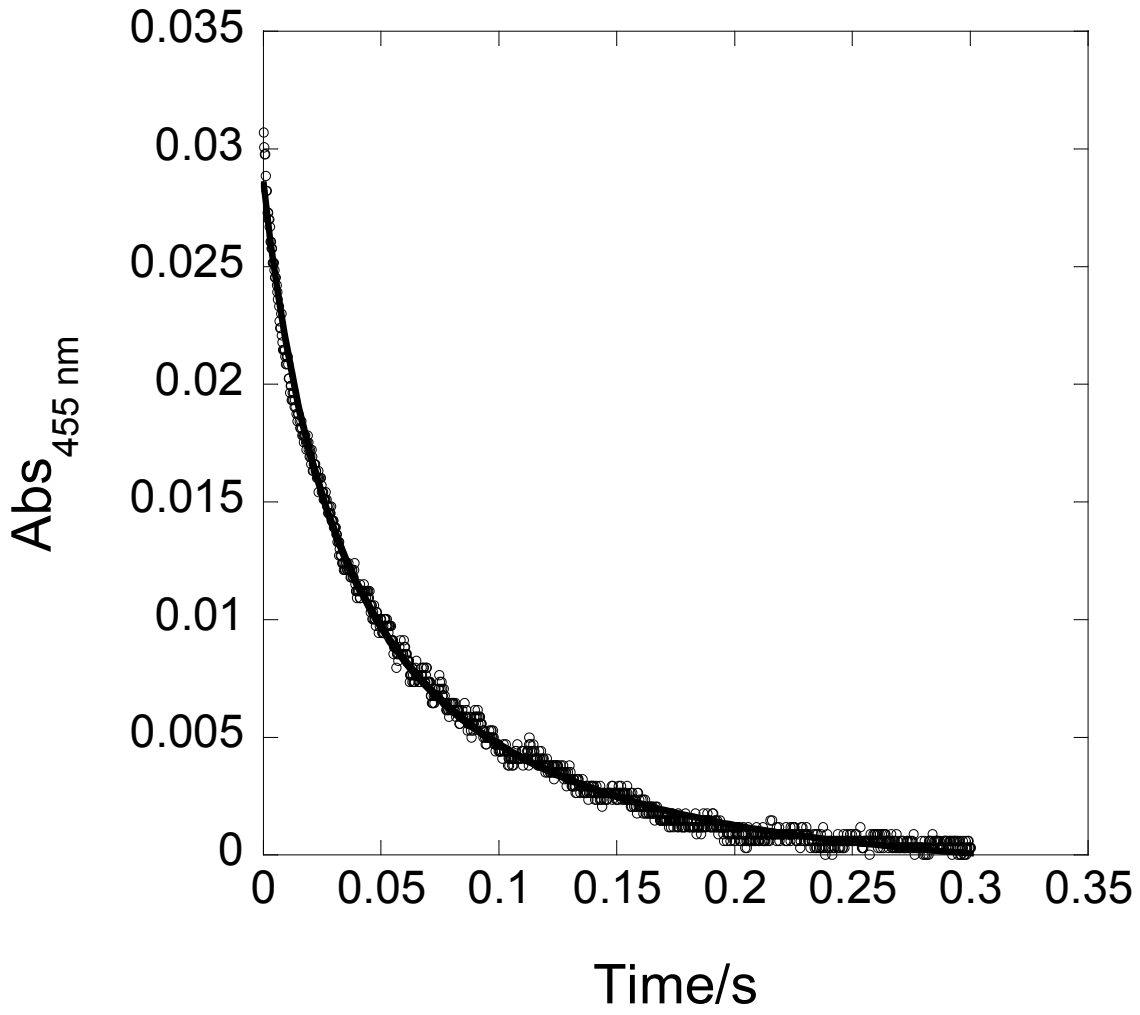

Figure S6. Kinetic trace for a reaction between 0.014 mM $Fe_{aq}^{IV}O^{2+}$ and 0.008 mM $Co(dmgBF_2)_2$.

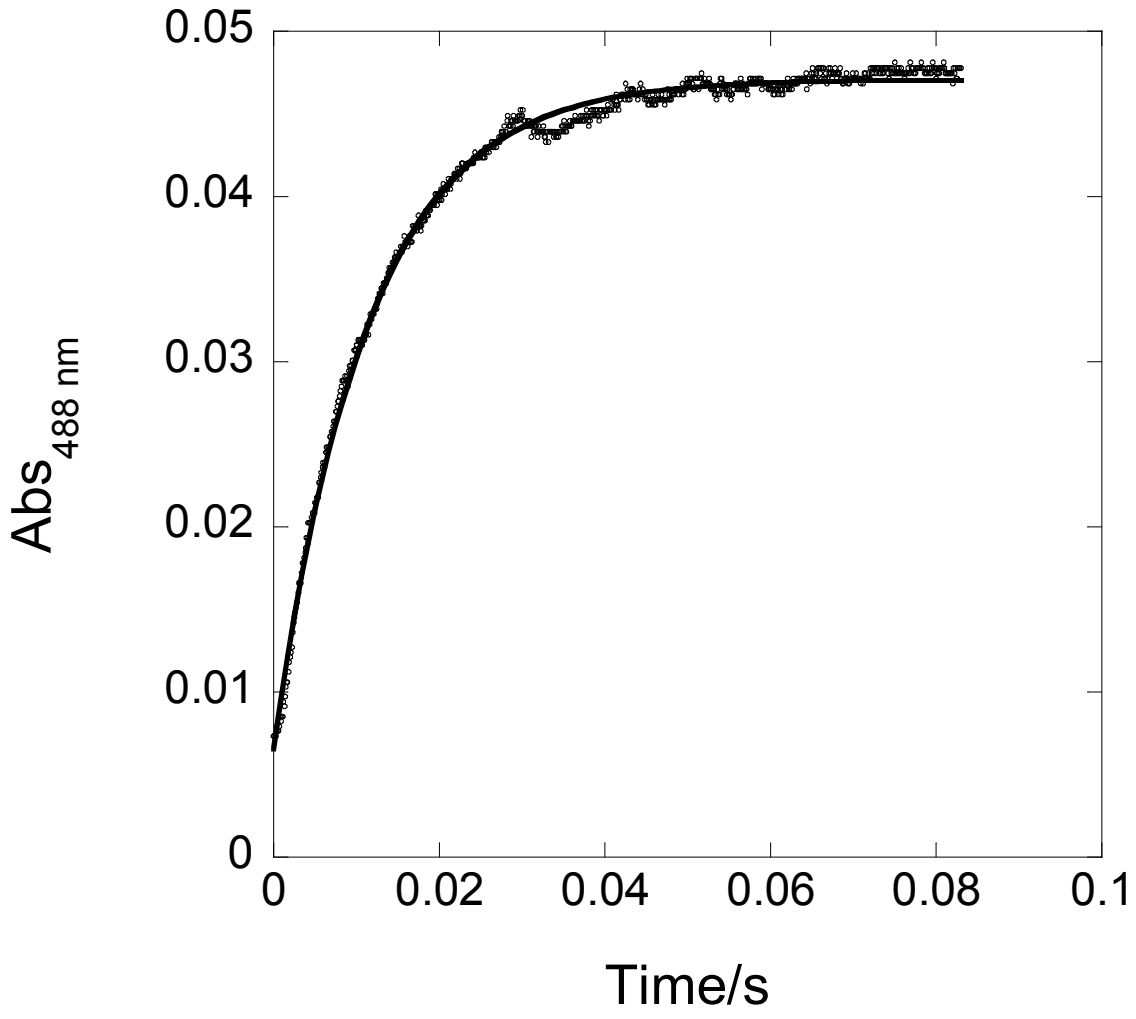

Figure S7. Kinetic trace for a reaction between 0.012 mM $Fe_{aq}^{IV}O^{2+}$ and 0.06 mM Na_3IrCl_6.

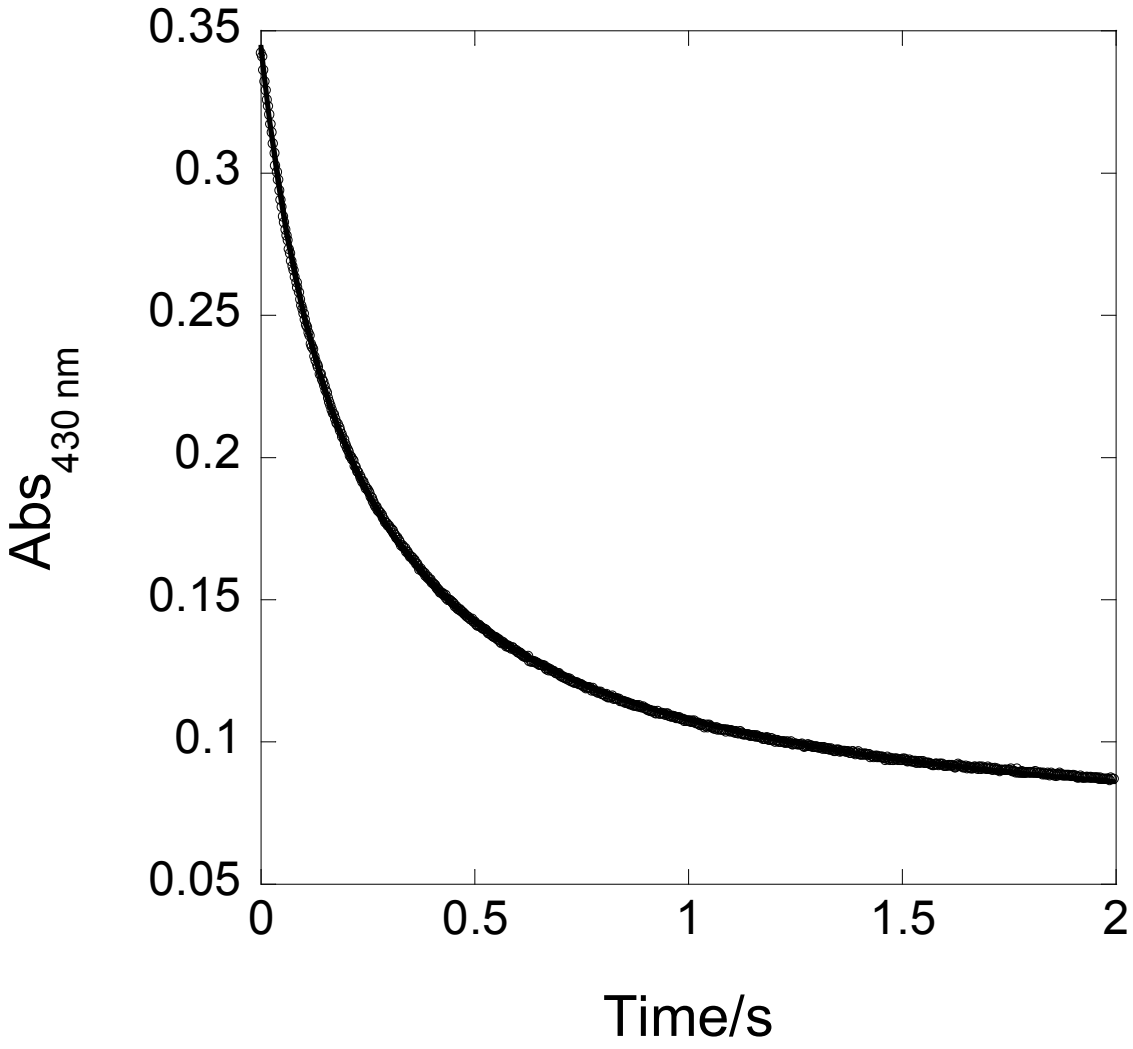

Figure S8. Kinetic trace for a reaction between 0.018 mM $Fe_{aq}^{IV}O^{2+}$ and 0.019 mM $Os(phen)_3^{2+}$.

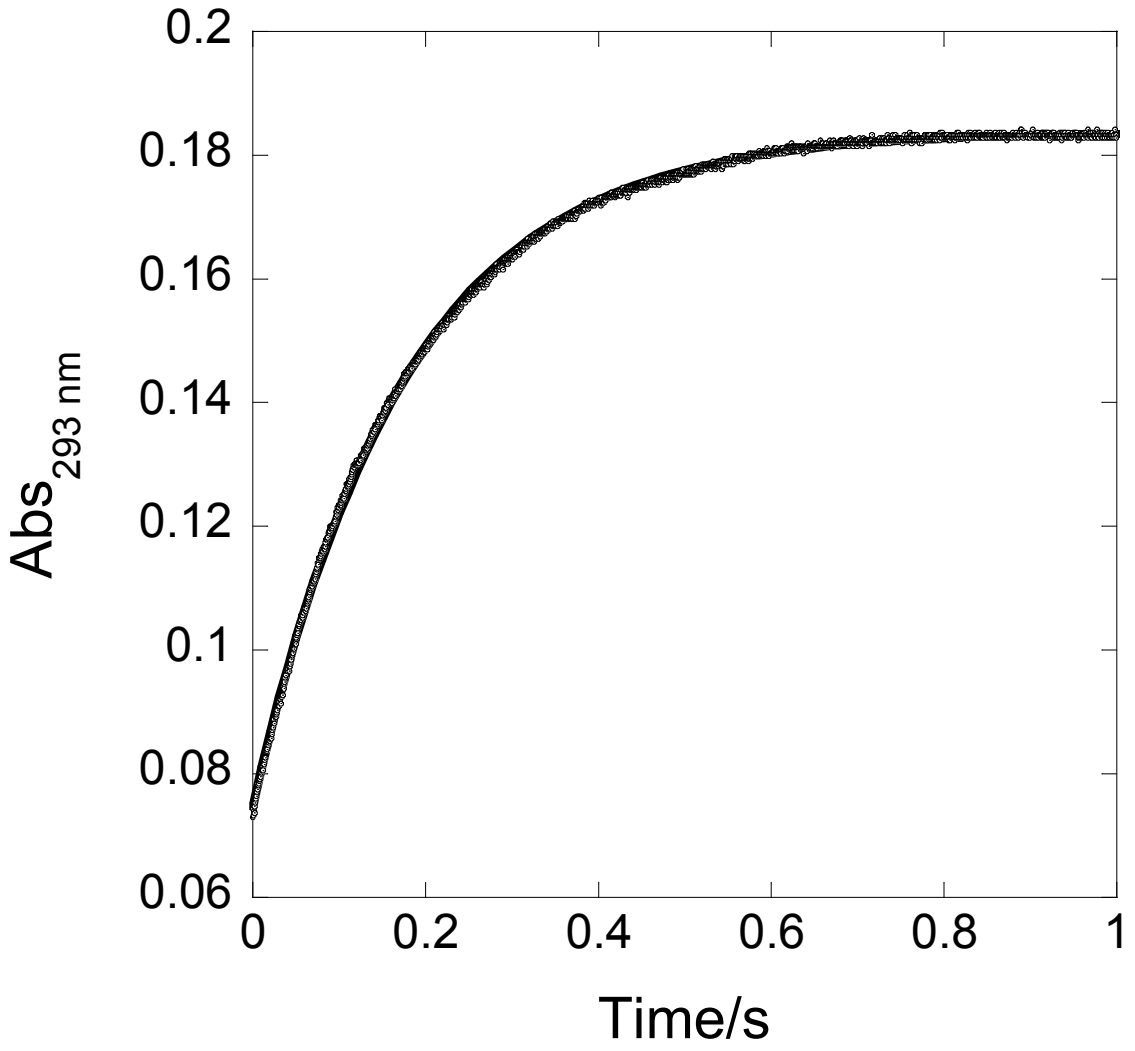

Figure S9. Kinetic trace for a reaction between 0.10 mM $Fe_{aq}^{IV}O^{2+}$ and 0.44 mM $Ce(ClO_4)_3$.

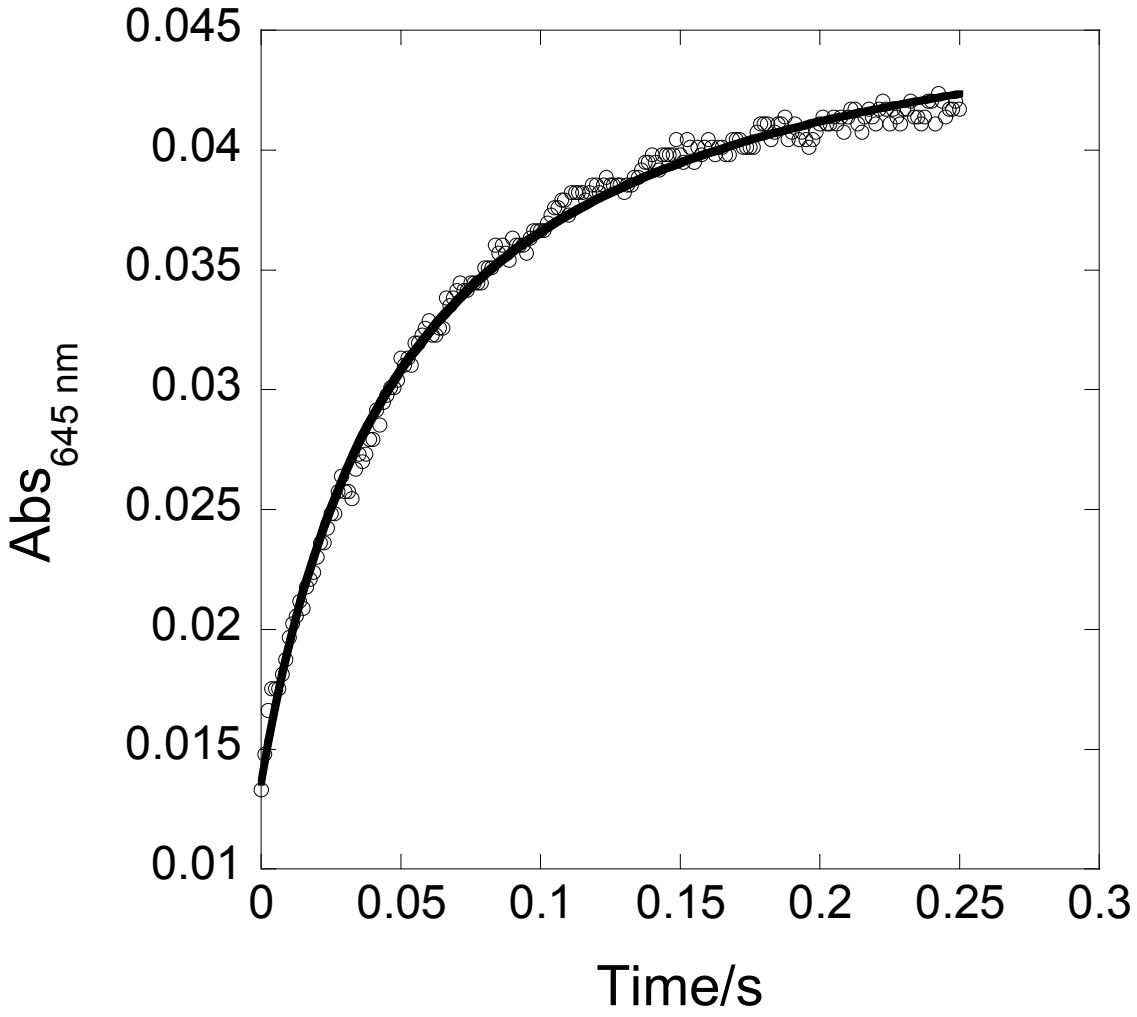

Figure S10. Kinetic trace for a reaction between 0.005 mM $Fe_{aq}^{IV}O^{2+}$ and 0.005 mM $HABTS^{-}$.

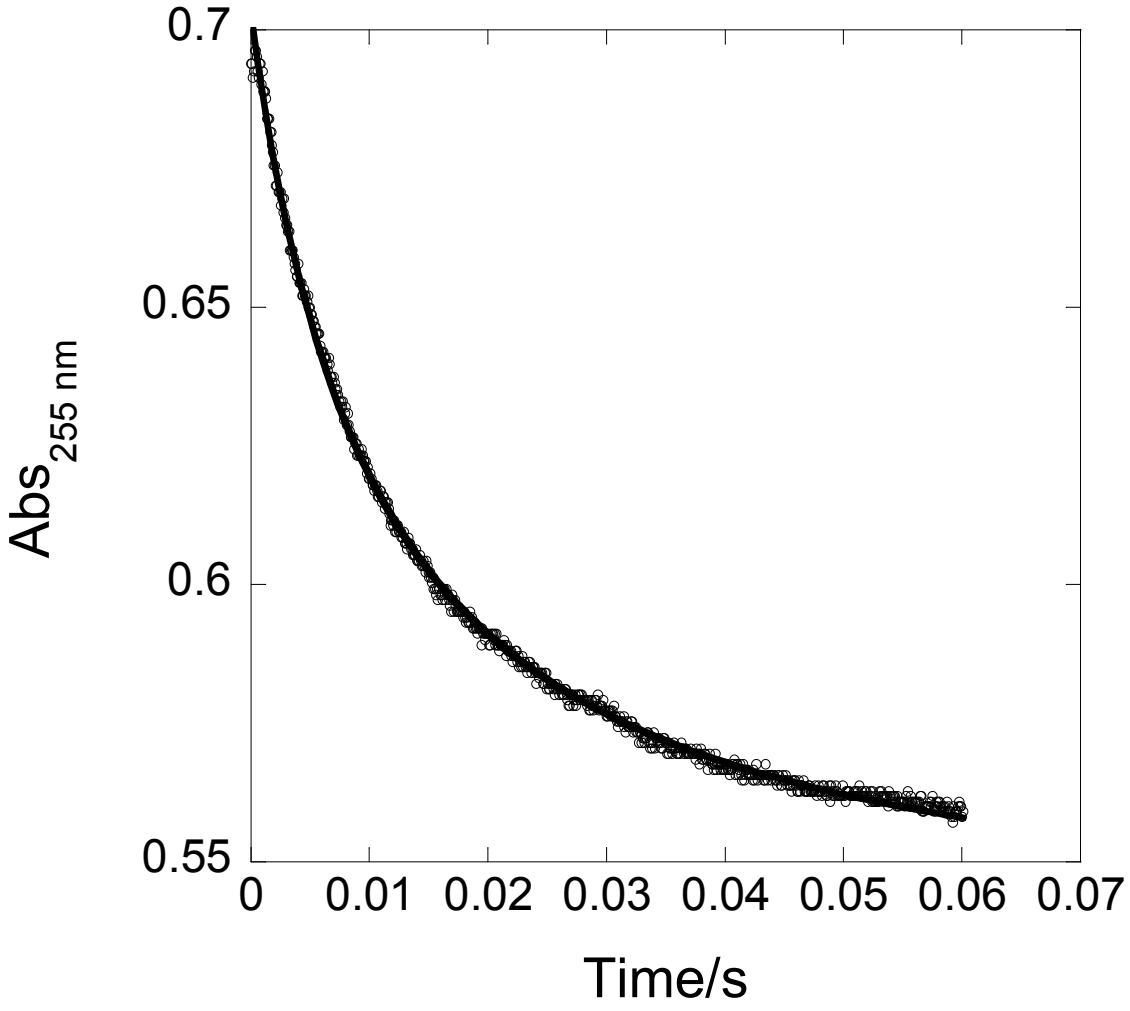

Figure S11. Kinetic trace for a reaction between 0.02 mM $Fe_{aq}^{IV}O^{2+}$ and 0.02 mM TFP.

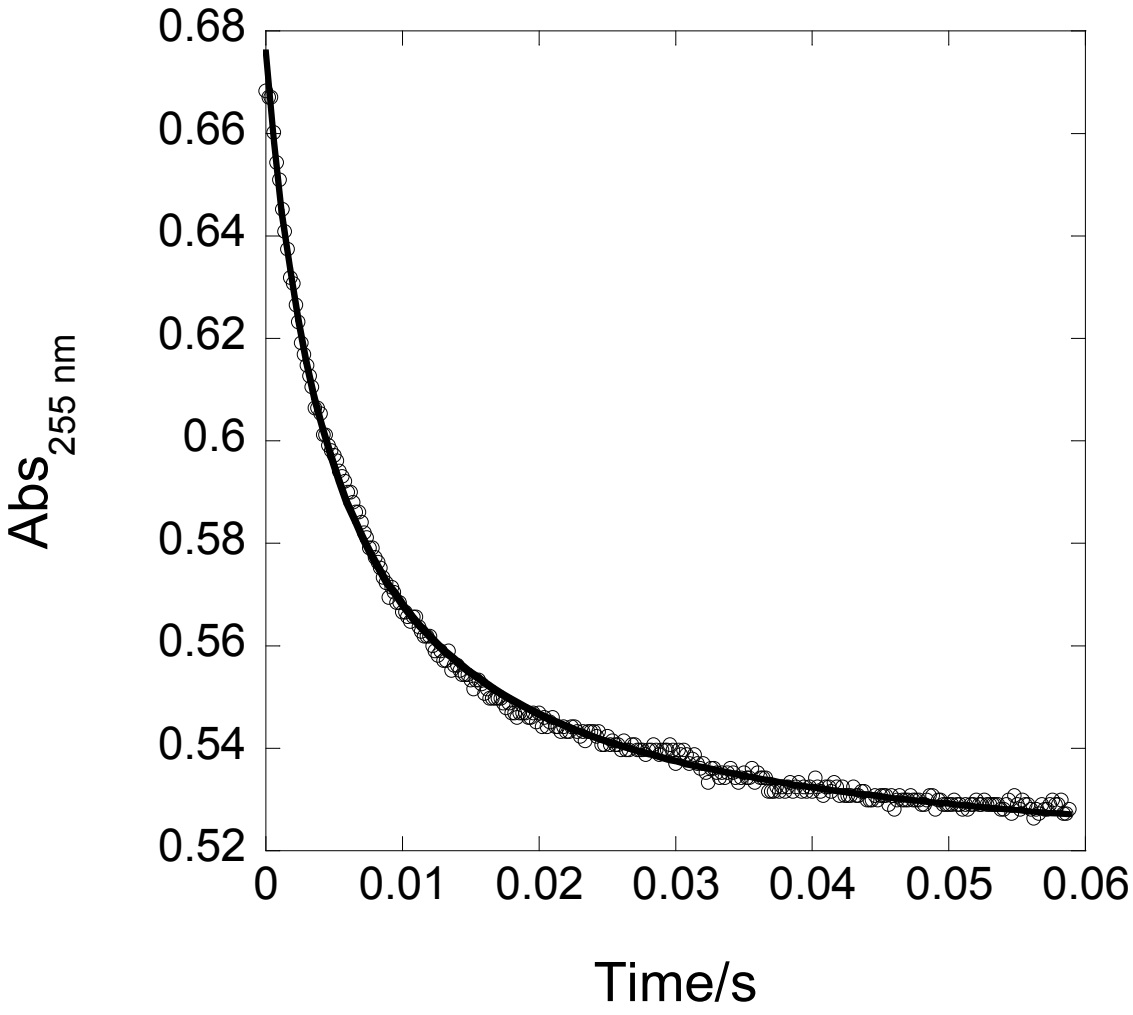

Figure S12. Kinetic trace for a reaction between 0.019 mM $Fe_{aq}^{IV}O^{2+}$ and 0.021 mM CPZ.